# UNCERTAINTY QUANTIFICATION IN CRACK GROWTH MODELING UNDER MULTI-AXIAL VARIABLE AMPLITUDE LOADING

By

Christopher R. Shantz

Dissertation

Submitted to the Faculty of the

Graduate School of Vanderbilt University

in partial fulfillment of the requirements

for the degree of

DOCTOR OF PHILOSOPHY

in

Civil Engineering

August, 2010

Nashville, Tennessee

Approved:

Professor Sankaran Mahadevan

Professor Prodyot K. Basu

Professor Caglar Oskay

Professor Carol Rubin

To my wife and family

ACKNOWLEDGEMENTS

I would like to acknowledge several people and organizations which have enabled the completion of this research. This work would not have been possible without the financial support provided by the National Science Foundation's IGERT fellowship and the Federal Aviation Administration's (FAA) Rotorcraft Damage Tolerance (RCDT) program. I am especially thankful to the FAA program directors Dr. John Bakuckas and Dr. Dy Le, as well as Mrs. Traci Stadtmueller for their support of this work. I am grateful to many other members of the RCDT program with whom I have had the privilege to work with and learn from, especially Dr. Xiaoming Li at Bell Helicopters Inc.

I would like to thank my committee members, Dr. Mahadevan, Dr. Basu, Dr. Oskay, and Dr. Rubin, for their consistent guidance, wisdom, and passion for scientific research within this field. I am especially honored to have had Dr. Mahadevan as my advisor throughout my time at Vanderbilt. His unparalleled depth of knowledge, generosity, patience, and vision has helped me develop as a person, professional, and researcher, and has taught me more than I could ever give him credit for here.

Nobody has been more important to me than the members of my family. Most importantly, I wish to thank my amazing wife, Bethany, for her unwavering love and support throughout this time in my life. She has been my light, my love, and my inspiration. I would also like to thank my parents who have helped instill in me the work ethic and dedication that was necessary to complete this work, as well as my siblings and in-laws whose encouragement is with me in whatever I pursue.

Finally, I am grateful to all of those students in the Reliability and Risk engineering program at Vanderbilt with which I have had the opportunity to work with. I have learned much from our meetings and discussions and value the professional relationships and personal friendships that we have developed.

TABLE OF CONTENTS

Page

LIST OF TABLES

LIST OF FIGURES

# CHAPTER I

# INTRODUCTION

## 1.1 Introduction

Mechanical components in engineering systems are often subjected to cyclic loads leading to fatigue and progressive crack growth. It is essential to predict the performance of such components to facilitate risk assessment and management, inspection and maintenance scheduling, and operational decision-making. In 1978, the National Bureau of Standards and Battelle Laboratories completed an exhaustive study that estimated the total cost associated with material fracture and failure in the United States to be over $88 billion dollars per year (corresponding to almost 4% of the national GDP at the time) [1]. The study concluded that substantial material, transportation, and capital investment costs could be saved if technology transfer, combined with research and development, succeeded in reducing the factors of uncertainty related to structural reliability. Emphasis on fracture mechanics, material properties, and improved inspection schedules/techniques were identified as potential methods of improving structural reliability while reducing material usage and replacement of critical components. Among the major industry sectors where fatigue and fracture of structural components are of critical concern is that of the aeronautical and aerospace industry.

Originally, the aeronautical community adopted the safe life design approach in order to increase structural integrity throughout the design life of a component. Within the safe life design method, components are assumed to be flaw free and are designed and

tested to withstand a pre-determined design life. The mean fatigue life of the structure is estimated and then divided by a subjective safety factor in order to assure a safe operation life of the component. Under this design philosophy, components are retired from service following this safe life time period, regardless of their current condition. The disadvantages of this approach are that components tend to be over-engineered, a large percentage of components are retired long before their actual useful lives have been reached, safety factors are not statistically evaluated, and the method does not account for single "rogue" defects that could grow to a critical size during the design life. The damage tolerance approach was later adopted in order to overcome some of these limitations.

The U.S. Air Force became the first organization in the United States to formally require damage tolerance design with the issuance of MIL-A-83444 Airplane Damage Tolerance Requirements in 1974, which specifies that cracks shall be assumed to exist in all primary aircraft structures [2]. Damage tolerance design is based on the assumption that initial flaws (cracks, scratches, inclusions, etc) exist in any structure and such flaws will propagate under repeated cyclic loading conditions which are substantially less than the yield strength of the material, ultimately causing structural failure. Damage tolerance concepts are based on fracture mechanics principles and have been pursued for fixed-wing aircraft structures since mid 1970's [3]. This approach to structural analysis has forced engineers to develop a more thorough understanding of relevant component service loads and stress spectrums, material properties, and crack growth mechanisms.

Although significant work has been pursued for fixed wing aircraft over the past few decades, relatively little work has been completed on its application to rotorcraft due

to complex component geometries, high cycle, low stress dynamic loading conditions, and the necessity for accurate small crack, near threshold crack growth modeling. Following a detailed assessment in 1999 by the Federal Aviation Administration (FAA) and the Technical Oversight Group for Aging Aircraft (TOGAA) on the current approaches to rotorcraft design for fatigue, the TOGAA recommended that a damage tolerance philosophy should be used to supplement the existing safe-life methodology for rotorcraft design and certification. In response to the assessment and recommendation, the FAA initiated the process to revise FAR 29.571, Fatigue evaluation to include damage tolerance requirements and developed a rotorcraft damage tolerance (RCDT) R&D roadmap identifying multiple areas of research instrumental to development of rotorcraft specific damage tolerance techniques and tools [4]. Much of the research contained within this dissertation is motivated by the updated FAA RCDT initiative and directly supports the critical research areas identified within the RCDT R&D roadmap including, but not limited to, initial flaw state determination, fatigue crack growth analysis, and risk assessment - probabilistic modeling.

The traditional damage tolerance (DT) approach to aircraft structures has assumed a deterministic damage accumulation process where deterministic crack growth curves, constant material properties, and specific initial flaw sizes are used. For DT-based design, a safety factor is commonly used to ensure structural integrity. However, fatigue crack growth is a stochastic process and there are different kinds of uncertainty – physical variability, data uncertainty and modeling errors – that should be included within the analysis to more accurately represent the fatigue life of the component. In order to accurately assess the risk of failure of structural components, these sources of uncertainty

need to be identified and their statistical characteristics quantified. The probabilistic method is more appropriate for damage tolerance analysis since it can properly account for various uncertainties and assist the decision-making process with respect to design and maintenance scheduling. Uncertainty appears at different stages of analysis and the interaction between these sources of uncertainty cannot be modeled easily. Additionally, the uncertainty quantification and propagation methodology must be developed to be computationally efficient since the reliability assessment may require repeated evaluation for accurate predictions.

The remaining sections within this chapter provide an overview of relevant topics to fatigue crack growth analysis and will detail the research objectives and contributions of this work. In order to provide a baseline level of understanding which is necessary for later development and discussion, Section 1.2 reviews some of the major topics that are relevant to crack growth analysis. Section 1.3 discusses some of limitations that exist in the previous methodology and clearly states the main objectives of this research. A brief summary of the major contributions contained in the subsequent chapters of this work within the areas of uncertainty quantification and fatigue crack growth analysis is also provided. Additionally, the demonstration problem to which the methods developed within this work are applied is given within this section. The final section within this chapter provides details on the overall organization of the subject material contained within the remaining chapters of the dissertation.

## 1.2 Fatigue Crack Modeling Background

As mentioned previously, the damage tolerance approach can be utilized to ensure that structural components have the capacity to withstand environmental loading even under the presence of cracks or other defects. Inherent to this philosophy is the underlying assumption that all structures have some initial flaws, which will propagate under fatigue loading conditions. Linear elastic fracture mechanics (LEFM) based methodologies have been used extensively to better characterize the fatigue crack growth process in metals and are based on the application of classical linear elasticity to cracked bodies. Linear elastic fracture mechanics theory is applicable for analysis of stable crack growth resulting from repeated fluctuating loading conditions and can be used within the damage tolerance approach to address structural integrity concerns by considering both the damage propagation (growth) and the residual strength of the flawed component.

Residual strength is the amount of static strength of the structure available at any time during a component's service life. The residual strength is expected to decrease with increasing severity of damage. Plane strain fracture toughness is a material property which describes the ability of a material containing a crack to resist fracture (rapid, unstable crack growth), and is denoted by the parameter $K_{IC}$. The structural safety of the system of interest is maintained by ensuring that damage is never allowed to grow to a sufficient size such that the stress intensity factor at the damage location exceeds $K_{IC}$ and the residual strength of the system does not drop below the maximum in-service load value. By enforcing these two conditions, it is possible to identify a critical crack size over which the structural integrity of the system is insufficient. A schematic of the

relationship between residual strength and crack size is shown in *Figure 1* and that of stress intensity to crack size is shown in *Figure 2*.

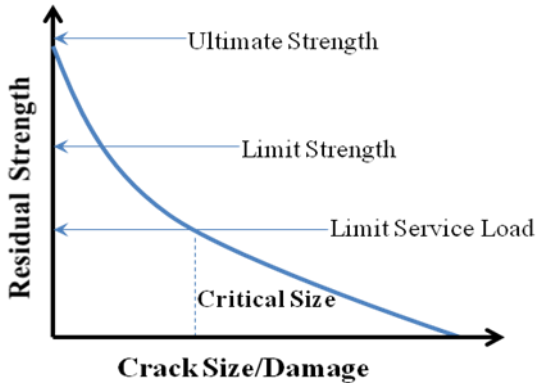


***Figure 1:*** *Schematic of structural residual strength with respect to crack size*

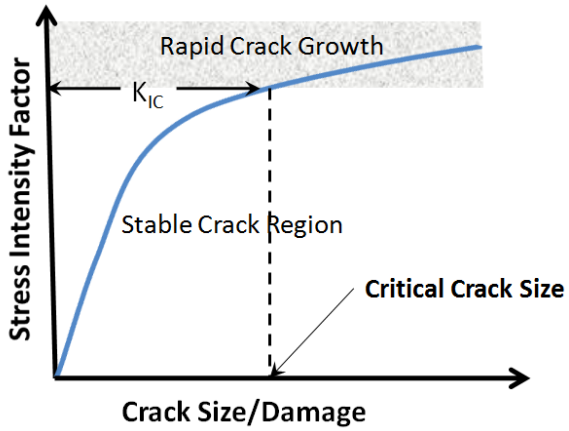


***Figure 2:*** *Schematic of relationship between stress intensity factor and crack size*

Fatigue crack propagation occurs as a result of cyclic loading conditions with cracks growing a given increment ($\Delta a$) in a given number of loading cycles ($\Delta N$). When the crack size reaches a critical level, crack growth becomes unstable and failure occurs. According to linear elastic fracture mechanics (LEFM), the plastic deformation near the

crack tip is controlled by the stress intensity factor range ($\Delta K$), and is applicable provided the small scale yielding (SSY) condition is satisfied. The fatigue crack growth rate is typically represented with the nonlinear functional relationship

$$\frac{da}{dN} = \frac{\Delta a}{\Delta N} = f\left(\Delta K, R, K_{Ic}, K_{th}, a, ...\right) \tag{1}$$

where $da/dN$ is the crack growth rate per cycle, $f$ is a non-negative function, $\Delta K$ is the range of the stress intensity factor, $R$ is the ratio between the minimum and maximum applied loading, $K_{Ic}$ is the plane strain fracture toughness, $K_{th}$ is the threshold stress intensity factor, and $a$ is the crack length. $K_{Ic}$ and $K_{th}$ are both material properties and are depicted within the schematic in *Figure 3*. The stress intensity factor ($\Delta K$) is viewed as the primary parameter, and is related to the applied loading, crack length, and geometry of the component. Different empirical formulas have been proposed to represent some portion(s) of the fatigue crack growth rate curve, with the Paris [5], Forman [6], and Walker [7] laws given in Eqns. (2), (3), and (4) respectively.

$$\frac{da}{dN} = C\left(\Delta K\right)^m \tag{2}$$

$$\frac{da}{dN} = f\,\frac{C\left(\Delta K\right)^m}{\left(1-R\right)K_c - \Delta K} \tag{3}$$

$$\frac{da}{dN} = C\left(\frac{\Delta K}{\left(1-R\right)^{1-p}}\right)^m \tag{4}$$

The traditional fatigue crack growth rate curve is based on long crack behavior and generally is sigmoidial in shape with three distinct regions; the near threshold, linear

(Paris), and the near critical regions. A representative plot of the fatigue crack growth rate curve is shown in *Figure 3*.

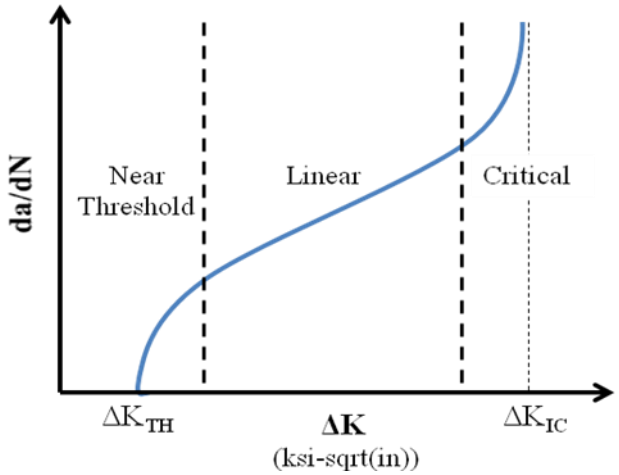


***Figure 3:*** *Idealized fatigue crack growth rate curve for metals.*

The near threshold region (Region I) is that part of the curve generally below $10^{-8}$ in/cycle ($10^{-10}$ m/cycle) and is characterized by the stress intensity factor range ($\Delta K$) too low to effectively propagate a crack. The linear/Paris region (Region II) encompasses data where the crack growth rate has a linear relation with the stress intensity factor range and is commonly modeled by the Paris law [5]. The final region of the crack growth rate curve is related to the fracture toughness of the material, where a small increase in the stress intensity amplitude produces a large increase in crack growth rate as the material approaches unstable fracture. For the high cycle fatigue crack growth problem, in which a large number of small growth cycles are expected, it is essential that the near threshold

region of the fatigue crack growth curve is accurately represented by the fatigue crack growth model used in the analysis.

***Table 1:*** *Proposed fatigue crack growth models*

| Equation | Author |
|---|---|
| $\frac{da}{dN} = C\,(\Delta K)^n$ | Paris |
| $\frac{da}{dN} = C\,(\Delta K)^n\left(1-\frac{\Delta K_{th}}{\Delta K}\right)^p$ | Mod. Paris |
| $\frac{da}{dN} = C\left(\frac{\Delta K}{(1-R)^{1-p}}\right)^m$ | Walker |
| $\frac{da}{dN} = C\left(\frac{\Delta K^m}{(1-R)K_c - \Delta K}\right)$ | Forman |
| $\frac{da}{dN} = C\left(\left(\frac{1-f}{1-R}\right)\Delta K\right)^n\left[\left(1-\frac{\Delta K_{th}}{\Delta K}\right)^p / \left(1-\frac{K_{\max}}{K_c}\right)^q\right]$ | FNK/ NASGRO |
| $\frac{da}{dN} = \frac{C_1}{\Delta K^{n1}} + \frac{C_2}{\Delta K^{n2}} - \frac{C_2}{[K_c(1-R)]^{n2}}$ | Saxena |
| $\frac{da}{dN} = C\,(\Delta K - K_{th})^2\left(1+\frac{\Delta K}{K_c - K_{\max}}\right)$ | McEvily |
| $\frac{da}{dN} = C\left(\Delta K^p \Delta K_{\max}^q\right)$ | Roberts/Klesnil |
| $\frac{da}{dN} = C\left(K_{\max}^{\ 2} - K_{\min}^2\right)^m$ | Arad |
| $\frac{da}{dN} = C(\Delta G)^m$ | Mostovoy |

Since the early 1960's when Paris [5] initially proposed the relationship between the fatigue crack growth rate and the stress intensity factor range, many models have been developed to represent the fatigue crack growth rate curve for various materials. Several researchers have proposed different models of varying complexity including Forman [6], Walker [7], Erdogan and Ratwani [8], among others. A more comprehensive, but far from exhaustive, list of models is included in *Table 1*. As mentioned previously, for the high cycle fatigue crack growth problem, in which a large number of small growth cycles

are expected, it is essential that the near threshold region of the fatigue crack growth curve is accurately represented, and therefore future discussion will focus on those models that meet this minimum requirement.

Under constant amplitude loading conditions, the fatigue life of the structure can be found by simple integration of the fatigue crack growth rate model given in Eqn. (1). However, most finite-life structures are subjected to random variable amplitude loading while in service, which makes the fatigue life calculation significantly more difficult. The most common method for dealing with crack growth propagation under variable amplitude loading conditions is through the use of a cycle-by-cycle prediction method in which the crack growth increment ($da/dN$) is evaluated for a given $\Delta K$, and $R$ corresponding to each cycle within the variable amplitude history. However, relying on a cycle-by-cycle calculation can become computationally expensive, particularly within a probabilistic reliability analysis framework in which many life predictions must be evaluated. This computational burden is again increased when a multiaxial variable amplitude load is applied to a structure. Chapters 3 and 5 will further comment on the challenges inherent to fatigue crack growth modeling under multi-axial variable amplitude loading and will develop methods to address these issues for planar and non-planar fatigue crack growth modeling within a probabilistic framework.

Since the damage tolerance methodology assumes an initial flaw/defect in the material, and the key result of the analysis is focused on accurately predicting the number of cycles for this initial crack to grow to a critical crack length. Key questions that need to be addressed before crack analysis can be performed include:

1.) What initial crack shape should be used?

2.) What initial crack size should be used?

3.) How will crack propagation be modeled (single point, two-point, multiple points along crack front)?

4.) What direction is the crack allowed to propagate (planar, non-planar)?

Although seemingly simple questions, clear answers are not always obvious and can be problem dependent and subject to engineering judgment. Several different approaches have been developed and reported within the literature to address each of these issues, and the remaining portion of this section presents many of the methods that have been used within previous research. However, most of these questions currently remain open areas of research within the fatigue and fracture research community, where improved methods and techniques are currently under investigation.

Most cracks and planar flaws can be classified within one of five general categories: i.) surface-breaking flaws, ii.) through flaws, iii.) subsurface/embedded flaws, iv.) corner flaws, and v.) edge flaws [9]. Although actual flaws contained within structural components may have irregular shapes, these flaws are typically represented by simpler, idealized shapes within crack growth studies. Two main factors are responsible for the common practice of crack shape idealization; insufficient information of true crack shapes within components and limited theoretical and modeling capabilities of highly complex crack shapes. Most common nondestructive evaluation techniques are incapable of characterizing detailed crack front profile, providing only limited crack characterization information on crack size and location. Although advanced techniques such as the scanning electron microscope (SEM) can be used to see microstructure level defects, this technology is not widely available and can be expensive to operate.

Additionally, even if realistic crack front shapes were known, standard fracture mechanics solutions as well as reliable crack front modeling capabilities are generally only available for simple shapes. As a result, the shapes of surface, subsurface, embedded, and corner flaws are typically represented as semi-elliptical, elliptical, and quarter elliptical respectively, and through and edge cracks are generally assumed to have a rectangular shape [9].

For any fatigue critical structural component, the smaller the initial crack size, the higher the residual strength capacity, and the longer the overall fatigue life. Therefore, the estimation of the initial flaw size is of critical importance. Several different methods are available for determining initial crack sizes within as-manufactured components, and are briefly discussed below.

If the size and shape of the true flaws can be identified using SEM or by some other means, or if initial flaws are known to exist in the component (such as notches or surface scratches), idealized crack sizes should be defined as the maximum extent of the actual flaw [9]. That is to say, the idealized crack shape should fully inscribe the actual shape, thus making the area of the idealized crack greater than that of the true crack shape. In doing so, a larger crack size is assumed and a conservative fatigue life prediction can be expected.

Another typical method for quantifying initial crack sizes within as-manufactured material is by using nondestructive inspection techniques. Nondestructive inspection (NDI) can be defined as the use of nonintrusive methods to ascertain the integrity of a material or structure. Many different inspection methods have been developed to evaluate the existence of flaws including liquid penetrant, magnetic particle, eddy current,

ultrasonic, and radiographic, among others [10]. NDI techniques are typically used on fracture critical parts to detect flaws that are *equal to* or *larger than* a threshold crack size. The threshold crack size is defined as the minimum crack size that can be consistently detected using a given inspection method, and varies depending on the inspection method used. Using information obtained from NDI techniques, engineers are able to characterize initial flaw sizes based on the flaw sizes found within the inspected components. Since NDI techniques are not capable of reliably detecting crack sizes less than their threshold values, if no flaws are detected, engineers typically set the initial flaw size as the minimum detectable flaw size for the specific NDI technique used. The U.S. air force damage tolerant design handbook [11] reported ranges of approximate crack lengths that are reliably detected using different NDI techniques, the results are summarized in *Table 2*.

***Table 2:*** *Approximate limits of reliable crack size detectability limits*

| | | **Solid Cylinder** | | **Hollow Cylinder** | |
|---|---|---|---|---|---|
| | Specimen Type | Straight | Filleted | Straight | Filleted |
| Liquid Penetrant | Lab | 0.16 | 0.09 | x | 0.31 |
| | Production | x | x | x | x |
| Ultrasonic | Lab | 0.14 | 0.09 | 0.10 | 0.13 |
| | Production | 0.14 | 0.07 | x | 0.13 |
| Eddy Current | Lab | 0.20 | 0.23 | x | 0.14 |
| | Production | 0.16 | 0.30 | x | x |
| Magnetic Particle | Lab | 0.12 | 0.07 | 0.10 | 0.13 |
| | Production | 0.12 | 0.13 | x | x |

* x represents cases where data was not reported

When no additional information is available for the characterization of initial flaw sizes within a fatigue critical part, handbooks and standards can be used as references to

identify suitable values. Within the aerospace industry, the USAF damage tolerant design handbook [11] specifies conservative initial flaw size assumptions for intact structures. For edge cracks and corner cracks at holes the handbook suggests an initial flaw size of 0.05 inches, whereas for through and surface cracks at locations other than holes it suggests an initial half crack length ($c$) and depth of 0.125 inches (for surface crack configurations in slow growth components). These values can be used for subsequent fatigue life analyses.

The concept of equivalent initial flaw size (EIFS) has also been used for determining the size distribution of initial cracks. The equivalent initial flaw size approach has been used to derive initial flaw sizes from the distribution of fatigue cracks occurring later in the service life of a component, typically using back extrapolation techniques. Although mentioned here for completeness, the concept of EIFS will be discussed in more detail within Section 3.2.

Several approaches, of various levels of sophistication, have been used within the literature to extend the crack front of pre-existing flaws. Crack front extension at a single point (surface), two points (along the semi-major and semi-minor axis locations corresponding to surface and depth positions), or multiple points (all along the crack front) have been used for 2D and/or 3D crack propagation. In selecting one of these approaches for crack modeling, the engineer imposes one of three crack shape development schemes, namely; circular, elliptical, or a general case.

For illustration, suppose an initial semi-circular surface crack is under consideration. The usual method of dealing with propagating cracks is to assume that a particular crack shape is maintained during the fatigue process. This is equivalent to a

single point extension modeling approach where the stress intensity factor is determined at a single point (typically at the surface location where the highest stress intensity factor is commonly found), and the entire crack front is extended by a single value [12]. Implementing this approach will result in an initially circular crack remaining circular for the entire duration of the crack modeling process. The next level of sophistication considers crack growth at the semi-major and semi-minor axis locations [13] where the stress intensity factors and crack growth are performed at the semi-major and semi-minor axis locations only. Using this method an initial semi-circular crack may develop into an elliptical surface crack if the crack growth rate at one location (surface or depth) is calculated to be faster than the other point. In a general case, the crack front may be divided into *n* points. For each point along the crack front, a stress intensity factor is determined, crack growth rate is calculated and each point is extended accordingly [14]. This modeling approach allows an initially semi-circular crack to develop into a general crack shape that may not necessarily be easily captured by a simple geometric shape (e.g. semi-circular or semi-elliptical).

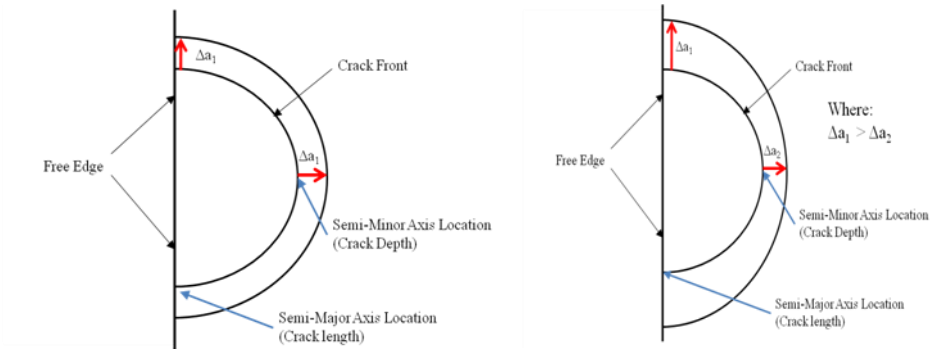


*(a.)* *(b.)*

***Figure 4:*** *Schematic of crack growth methods a.) semi-circular extension (constant along crack front) b.) semi-elliptical extension (different crack extension at semi-major and semi-minor locations)*

Obviously, there exists a tradeoff between accurate/meaningful crack shape evolution and crack modeling complexity. Although the multiple point advancement scheme may provide the most flexibility in terms of crack shape development, it also provides several additional modeling and computational complexities including multiple stress intensity factors and crack extension computations, as well as complicated remeshing requirements that simpler methods may avoid. It is mentioned here to make the reader aware not only of the necessary considerations for accurate crack shape representation, but also of the realistic computational limitations that exist for performing fatigue crack growth propagation analysis within a probabilistic framework. These issues will be discussed in later chapters as the crack modeling frameworks are developed for both planar and non-planar analyses.

Fracture mechanics concepts provide the tools to enable fatigue life assessment of structural components through crack growth analysis. In principle, the prediction of crack growth using fracture mechanics requires the following steps:

(1) Identify the relevant crack growth properties (crack growth rate as a function of the stress intensity factor, fatigue threshold, fracture toughness, etc) for the material used in design

(2) Determine the initial flaw size, shape, and location

(3) Establish the cyclic stress time history

(4) Determine the stress intensity factor solution as a function of crack size, shape, geometry, and loading

(5) Select a fatigue crack growth rate model and damage accumulation rule

(6) Propagate fatigue crack from initial flaw size to final (critical) flaw size

Each of these steps must be performed in order to obtain a prediction for the fatigue life of a component, and several different methods and techniques which are available to engineers, have been presented within this section. Inherent to each available method are certain benefits, drawbacks, and limitations that must be considered when performing this type of analysis. This research will focus on investigating various tools and techniques, which are based on fundamental fracture mechanic principles, for fatigue crack growth analysis under uncertainty.

The previous discussion within this section has focused on traditional, deterministic fracture mechanics (DFM) principles and procedures. The DFM approach assumes single, well defined, deterministic values for all model inputs. The result of the deterministic approach is a single model prediction value. Traditional methods employing deterministic approaches lack the ability to consider model predictions under uncertain conditions and cannot answer "what-if" questions under operating or environmental conditions which differ slightly from the values under which they were evaluated. In fact, all the necessary inputs to a fracture mechanics analysis are rarely accurate to a high degree of certainty, leaving the deterministic approach less than desirable [15]. To overcome this limitation, engineers have used a worst-case scenario approach, in which conservative values for all model inputs were assumed and used within a deterministic analysis. If a system could perform safely under the worst-case conditions, then it also would be functional under less severe load conditions. However, tradeoffs usually exist between those factors that increase safety and those which increase performance or economic considerations, and an optimal design for system safety under worst case

considerations may lead to an overdesigned structure with poor performance capabilities (e.g. larger and thicker components have more strength, but result in increased vehicle weight leading to decreased speed or maneuverability).

Probabilistic fracture mechanics (PFM) can be used to remove the unrealistic conservatism that is inherent to the worst-case approach (i.e. simultaneous occurrence of several improbable events), by combining known, assumed, or proposed statistical variations of the controlling parameters within traditional engineering models [15]. Fracture mechanics and probability theory are implemented within the PFM framework to account for both mechanistic and stochastic aspects of the fracture problem and PFM is gaining popularity as a method for realistic evaluation of fracture response and reliability of cracked structures [16]. PFM is based on the fundamental principles of deterministic fracture mechanics but considers one or more of the input variables to be random rather than having deterministic values. Therefore, rather than calculating a single fatigue life prediction and using a safety factor based on engineering judgment, a range of fatigue life predictions are calculated and appropriate values are selected to maintain a sufficiently low, but cost effective, failure probability [17].

Early work using PFM in aircraft applications mainly focused on capturing the inherent random nature in the applied loads or stresses in structural components. Much of this work addressed crack initiation, rather than crack growth [18,19]. More recent work has proposed additional methods in the area of PFM by treating various fracture mechanics inputs as random variables (initial crack size, crack detection probability, material properties, and service conditions [15]) with increased emphasis on crack propagation methods. Examples of PFM analysis where certain input variables, such as

stresses, yield strength, and fracture strength, have been treated as random variables can be seen in ref [15].

The failure probability at any given time may be determined by combining conventional fracture mechanics calculations with an appropriate statistical approach. Generally, the component failure is defined through some limit state function, *g(…)*, which defines the boundary between the region of safe operating conditions and that of failure. Typically, the limit state function is expressed in terms of structural capacity and structural demand. Failure is expected when the demand exceeds the capacity of the system and is typically expressed as the limit state being < 0. The probability of failure is the multiple integral of the joint probability density function in the region of failure ($g(x_i) < 0$) given by

$$P_f = P\left(g(x_i) < 0\right) = \int_D \ldots \int f\left(x_1 \ldots\ldots x_n\right) dx_1 dx_n \qquad (5)$$

where $D=\{(x_1 \ldots x_n): g(x_1 \ldots x_n) < 0\}$ is the region of failure, $P_f$ is the probability of failure, $f(x_1 \ldots x_n)$ is the joint probability density function of the parameters $x_1 \ldots x_n$, and the function *g()* is the limit state function defined above. The driving parameters, $x_1 \ldots x_n$, for fatigue failure may be the component strength and the applied load, flaw size and critical size, or stress intensity factor and fracture toughness [20]. Numerical based techniques are then used to evaluate the failure probabilities of complex problems. Monte Carlo simulation is broadly applicable to the generation of numerical results from PFM models [21] and will be used within this work due to its scope, depth, and relative ease of implementation for evaluating probabilistic component life predictions considering multiple sources of uncertainty.

The probabilistic approach is capable of identifying the sources of variables affecting the fatigue life and fatigue strength of the structure in terms of risk, while eliminating the over-conservatism that maintains safety. It has been proven that the probabilistic method can be extended to provide useful information to help managers in making decisions regarding the operation and inspection time of the fleet in order to maintain airworthiness [3]. The probabilistic method for damage tolerance analysis presents the foundation on which this work is built and enables a systematic framework for uncertainty quantification considering physical variability, data uncertainty, and modeling uncertainty to be included within an overall component life prediction.

## 1.3 Problem Statement and Research Objectives

As the overall population of our aviation fleet (both fixed wing and rotary) ages and existing aircraft are required to function long beyond their initial design life, increasing emphasis has been placed on improving the understanding and modeling of the fatigue crack growth problem. Amid ever shrinking budgets and resources, engineers are tasked with the enormous responsibility of developing lower weight structures with increased design lives, which still meet the high reliability requirements that have become expected within the aviation industry. However, uncertainties exist at all levels of the fatigue damage tolerance modeling process, resulting in unknown confidence bounds on component life predictions made by engineers. In order to overcome this limitation, a systematic framework for stochastic fatigue crack growth modeling must be developed which accounts for uncertainty at all levels of the damage tolerance analysis. It is the goal

of this dissertation to provide a methodical and practical framework for quantifying various sources of uncertainty and analyzing their effects on component reliability predictions over time. The objectives of this dissertation are:

1.) Develop statistics based uncertainty quantification techniques for fatigue crack model inputs and model parameters. Fatigue crack growth modeling involves numerous input quantities such as initial flaw size, loading, and material properties as well as various model parameters which should be treated in a probabilistic manner. Each input may have a different form or use within the fatigue modeling procedure and quantification must be performed in such a way that additional new information can be easily incorporated into the overall framework.

2.) Develop a methodology to perform fatigue crack growth analysis for components subjected to multi-axial variable amplitude loading within a probabilistic framework. The methodology must incorporate the random input and parameter values which are quantified in the previous objective and provide an accurate component reliability prediction over time. Uncertainty quantification requires multiple analyses, therefore, the overall methodology must also be computationally efficient to implement.

3.) Develop and implement necessary methods for quantification of error and uncertainty in model predictions considering numerical solution error and model form error. Each model within the crack growth process introduces additional error, and this error must be accounted for and included within the overall component reliability prediction.

4.) Implement methods developed in objectives 1, 2, and 3 for planar and non-planar crack growth analysis. Three dimensional crack growth modeling introduces additional uncertainties arising from model form (extension and direction criteria) and numerical modeling approximations. These uncertainties need to be evaluated from a statistical viewpoint and included within the probabilistic fatigue life prediction.

Relatively little work has been completed on the application of the damage tolerance method to rotorcraft structures due to their complex geometries, high frequency dynamic loading, and mixed mode loading conditions. This research will help address some of the limitations posed by the traditional damage tolerance modeling approach for rotorcraft structures by further investigating the near threshold crack growth behavior and material properties, overcoming small crack growth modeling restrictions, and developing efficient computational methods which are suitable for mixed mode loading conditions. These improvements to the current analysis methodology are developed to be compatible with a probabilistic treatment of the fatigue crack growth process.

The overall goal of this research is to develop and implement an overarching framework for fatigue crack growth under multi-axial, variable amplitude loading which includes systematic uncertainty quantification at all levels of the fatigue crack growth modeling process. Key contributions have been made to both planar and non-planar crack growth analysis. A significant contribution contained within this work for planar crack growth analysis is the development of a new framework for probabilistic fracture mechanics which enables fatigue crack growth modeling under multi-axial, variable

amplitude loading conditions incorporating finite element analysis, surrogate modeling, and cyclic crack growth modeling methods. Included in this area are novel approaches to fatigue crack growth rate representation, surrogate model development, and model error assessment. Contributions to the area of non-planar crack growth analysis include uncertainty assessment in fatigue crack growth models resulting from the use of different crack extension and direction criterion as well as an 'equivalent planar' fatigue crack growth modeling approach which reduces the computational expense of numerical simulations while retaining valuable features of a full scale non-planar crack growth analysis.

*Demonstration Problem Description*

The methods developed throughout this research will be applied to a demonstration problem which is of general interest to the rotorcraft community. In evaluating potential candidate problems several key characteristics were desired including:

1. Metallic component
2. Principal structural element
3. Non-redundant part
4. Complex structural geometry
5. Subject to multiaxial, variable amplitude fatigue loading
6. Fatigue failure observed in the field

The rotorcraft mast structural component meets the above criteria and was identified as a suitable demonstration problem that will be used throughout this research for application

of developed techniques to a practical problem. In order to allow practical considerations to be presented directly alongside the methodology development, the application of techniques developed within each section of this dissertation will be evaluated on the rotorcraft mast problem. Relevant numerical results will be presented in each section following the technical considerations and methodology development.

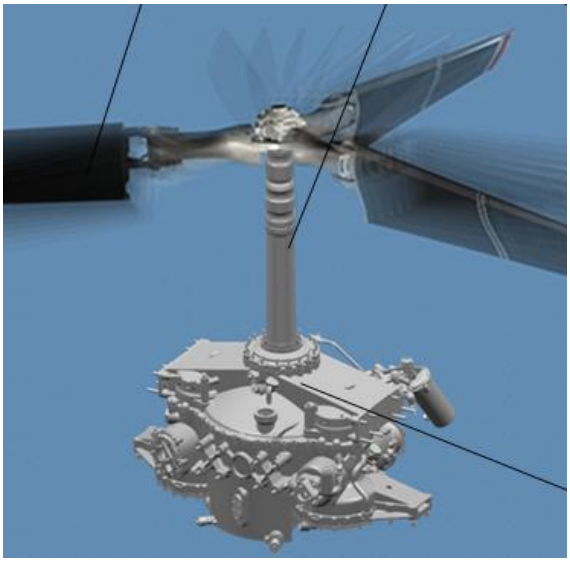

***Figure 5:*** *Schematic showing typical rotorcraft mast component, rotorcraft blades, and gearbox assembly*

Materials that are used in aerospace structural components are generally restricted to steels (4340, 9310, D6AC), and aluminums (7000 and 2000 series) as a result of their high strength and high fracture toughness [22, 23]. Special focus will be placed on analysis of the 4340 steel alloy and Aluminum 7075 within this work, as they are most commonly used materials for rotorcraft masts and other critical structural components.

Analysis results using data from other common aerospace grade materials will also be shown on occasion.

Mixed mode loading conditions are known to exist within the mast structure. Typically, tension, torsion, and bending forces are present during regular in-service conditions. As the rotor system operates, upward thrust is generated by the blades and is transferred to the rotorcraft body through the mast system. This causes tension loading to exist within the mast system, and is the primary force that keeps the system air-born. Torsion exists due to the twisting of the rotor system and the torque that is applied at the top of the mast system from the rotating rotor blades. Finally, bending forces are introduced as a result of the centrifugal force, resulting from the rotor system rotation, which causes forces to act outward and perpendicular to the rotorcraft mast system. Although all three loading conditions exist within the main rotor mast during in-service conditions, tension typically only accounts for less than 5% of the overall applied loading within the structure and can be deemed relatively insignificant for this problem. For this reason, only bending and torsion are considered within this research, however, their application does induce all three modes of loading (I, II, and III) within the cracked structural component.

The rotorcraft mast component (and associated materials) will be referred to throughout this work and will be used to demonstrate the applicability of methods for probabilistic damage tolerance analysis presented in this research to a realistic structural component.

## 1.4 Organization of the Dissertation

The content of this dissertation can be considered to address three major topics with respect to the overall stochastic fatigue crack growth analysis process, namely; quantification of the inherent uncertainty in model inputs, development of a flexible and efficient fatigue crack growth propagation method, and quantification of the resulting uncertainty in model outputs including modeling errors. A schematic showing the various components of this work as related to the overall component fatigue life prediction modeling approach is included in *Figure 6*.

The first topic is concerned with statistically quantifying model inputs and model parameters. When individual variables are under consideration, statistical methods can be used to fit probability density functions to experimental data sets. Chapter 2 addresses uncertainty quantification techniques for parameters/processes that are common to both the planar and non-planar crack growth methods. Additional sources of uncertainty that are unique to the planar and non-planar crack growth analysis are addressed within Chapter 3 and Chapter 5, respectively.

The second major topic covered within this dissertation focuses on developing a framework to accurately model the fatigue crack growth process while including those uncertainties which were previously identified and quantified. This task is addressed within Chapter 3 for the planar fatigue crack growth modeling scenario and again in Chapter 5 for non-planar crack growth analysis.

The last major topic analyzes the uncertainty of model outputs. Again, this topic is addressed in two different chapters, corresponding to model output resulting from the planar and non-planar fatigue crack modeling frameworks. Uncertainties in model

outputs are addressed in Chapter 4 and Chapter 6 for planar and non-planar crack growth, respectively. Included in this topic is the quantification of modeling errors for each of the models included in the overall crack modeling methodology. Discretization errors, surrogate modeling errors, and various crack growth model form errors are identified and statistically evaluated. Additionally, Chapter 6 analyzes the uncertainties in fatigue crack shape and model prediction resulting from the use of different crack growth extension and direction modeling criteria within the non-planar fatigue crack growth analysis framework.

The final chapter summarizes the overall work contained within the dissertation and provides recommendations for areas of future research.

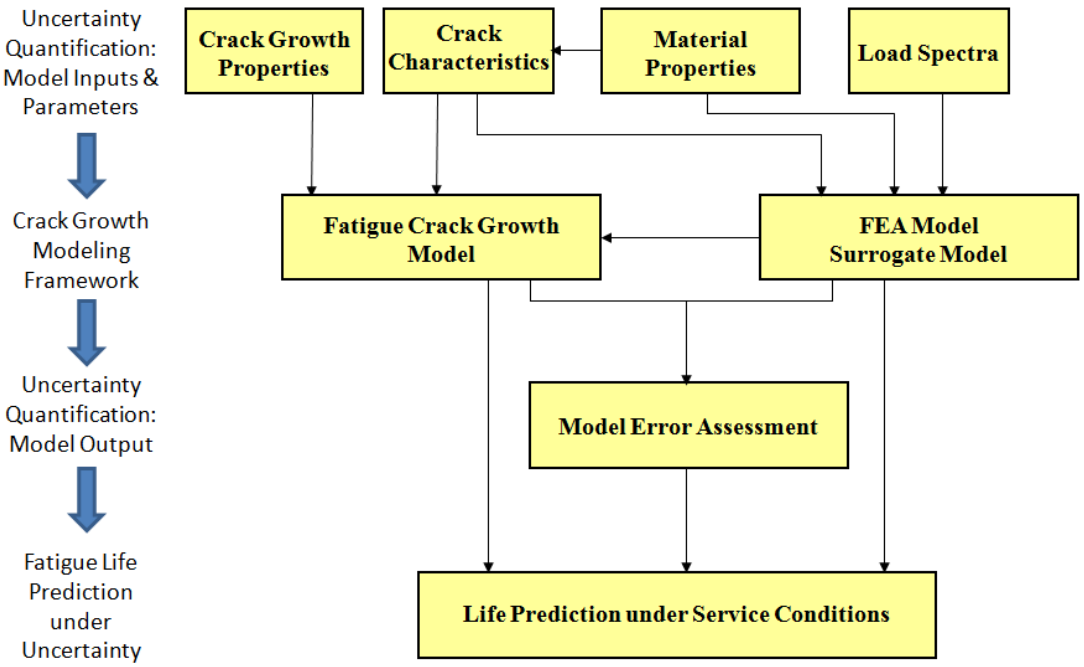


***Figure 6:*** *Flow chart depicting dissertation outline and of methodology development for stochastic fatigue crack growth evaluation*

# CHAPTER II

# UNCERTAINTY QUANTIFICATION OF MODEL INPUTS AND PARAMETERS

## 2.1 Introduction

The reliability of an engineering system can be defined as the ability to fulfill its design purpose for some time period [24]. For structural systems, reliability can be most simply viewed as the capacity of the structure exceeding some demand. Typically capacity is expressed in terms of structural strength, and demand is given by loads or stress. Engineers are expected to design these systems so that the capacity of the structure is maintained despite uncertainties in system performance over time (typically due to degradation) and/or uncertain use and environmental conditions. Traditional engineering approaches simplify the analysis by considering uncertain variables to be deterministic, and then apply empirical safety factors on top of deterministic solutions. However, empirical safety factors are typically based on past experience and/or engineering judgment, and statistical justification for the choice of their values is not always available. As a result, structural systems designed using empirical safety factors can be either significantly overdesigned or operating at unacceptably low reliability levels.

The probabilistic approach to engineering design provides a method for incorporating uncertainty within the structural analysis in a logical and meaningful way. Uncertainty exists in the architecture, parameters, abstraction, and unknown aspects of an engineering system. Additional uncertainty is introduced as a result of the predictive models, simplifying assumptions, and analysis methods used [24]. Quantification of the

uncertainty inherent in each of these sources needs to be implemented within a structural analysis to better understand the overall uncertainty within the analysis and how each affects the overall variability in system performance.

Generally, uncertainties can be identified to be of two types; aleatory or epistemic. Aleatory uncertainty can be defined as uncertainty arising from or associated with the inherent, irreducible, natural randomness of a system or process. Additional knowledge about this type of uncertainty is aimed not at reducing the uncertainty, but in better quantifying the actual physical state of the system or process. Examples of aleatory uncertainty are seen in material properties data and loading. Typically, a probabilistic interpretation can be developed to capture this type of uncertainty assuming enough statistically relevant data is available. Epistemic uncertainty is also known as reducible uncertainty, or subjective uncertainty, and is associated with a general lack of knowledge of the system or process under consideration. The epistemic uncertainty can, in principle, be eliminated with sufficient study. However, for complex systems or processes, this may not always be possible in practice. Typically, epistemic uncertainty exists when there is non-existent, sparse, or incomplete experimental data, when multiple plausible models are available or model approximations are made, when subjective expert opinions/observations are used, and in any other cases where there exists a general lack of information or knowledge about the behavior of the physical process or system.

Much of the traditional damage tolerance (DT) research has used deterministic modeling approaches under well defined, simple loading conditions. Deterministic fatigue failure analysis has been described as non-representative of the conditions during flight, too conservative due to the application of generic safety factors, or inaccurate due

to the limited information and uncertain knowledge [25]. Melis and Zaretsky [26] state that deterministic methods assume full and certain knowledge exist for service conditions and material properties, which is hardly practical. For actual structural systems, elements of uncertainty are inherent to the system and operating conditions themselves and result in unpredictable behavior to some extent. As explained in Lust [27] and Xiaoming [28], the non-deterministic nature of fatigue failure is the result of material and geometric tolerance uncertainties, environmental conditions, uncertainty in service loading, as well as variations in manufacturing and assembly processes. Additionally, the physical modeling process itself introduces many additional sources of uncertainty that need to be accounted for in addition to the natural variability previously discussed. These sources of uncertainty should be included in the component analysis, and their influence on the overall life prediction should be evaluated.

Svensson [29] identified five categories that contribute to the uncertainty in life prediction namely; material properties, structural properties, load variation, parameter estimation, and model error. The first three categories represent inherent variability through random variables, whereas the last two categories focus on the uncertainty associated with model and parameter selection. Much research and experimental testing has been performed for better estimation of the mechanical properties of materials which has reduced some of the uncertainty resulting from material and structural property estimation.

Several researchers have worked on uncertainty quantification of some aspects of the damage tolerance problem, however a systematic analysis which incorporates multiple sources and multiple types of uncertainty that are inherent in the fatigue crack

growth modeling procedure has not been completed. In this chapter, focus will be placed on statistically quantifying the model inputs and parameters that are particularly relevant to the high cycle fatigue crack growth problem. Additionally, stochastic variable amplitude loading conditions will be considered and addressed in an effort to more realistically represent in-service loading conditions.

The remaining sections within this chapter focus on the uncertainty within model inputs for fatigue crack growth analysis. Topics which are covered include uncertainty in material properties, uncertainty in fatigue crack growth rate parameters, and uncertainty in variable amplitude, multi-axial loading. Each source of uncertainty will be detailed and suitable methods for quantification will be implemented and demonstrated for rotorcraft damage tolerance analysis.

## 2.2 Uncertainty in Material Properties

Several researchers have attempted to address uncertainties in material properties through statistical distribution functions. Among the material properties that have been considered relevant to the fatigue damage tolerance analysis are the threshold stress intensity factor, fracture toughness, ultimate tensile strength, and yield strength [30, 31, 32, 33, 34].

*Threshold Stress Intensity Factor Range*

Experimental data shows that the fatigue crack propagation rate tends to zero at some critical value of the stress intensity factor, $\Delta K$. The threshold exists because fatigue

crack growth rates of less than about one lattice spacing per cycle are not possible on physical grounds [35]. The threshold stress intensity factor range, $\Delta K_{th}$, is the parameter which defines separation between no crack growth and slow crack growth in the near threshold region of the fatigue crack growth rate curve and is critical for accurately assessing the fatigue lifetimes for components subjected to high cycle fatigue.

However, the threshold is not sharply defined [36], and has been shown to be sensitive to loading factors, such as stress ratio, which is important when performing analysis under variable amplitude loading conditions. The threshold stress intensity factor tends to decrease with increasing R ratio and has been expressed by Backlund [37] to be related to the stress ratio, $R$, and the threshold stress intensity factor at $R$=0, $\Delta K_o$, through the relationship

$$\left(\Delta K_{th}\right)_R = \left(1 - C_o R\right)^d \Delta K_o \qquad (6)$$

where $C_o$ and $d$ are fitting constants. For this relationship to be determined, it is essential that the quantity $\Delta K_o$ is available through experimental testing. Klesil and Lukas [38] proposed a simpler version of Eqn. (6) by setting the constant $C_o$=1. Barsom [39] further simplified the expression by enforcing the fitting constant $d$ to be set equal to 1. In cases where the two fitting constants are not available, the value of $C_o = d = 1$ will give conservative results for the threshold stress intensity factor, $\Delta K_{th}$ for $R \geq 0$ [40], and will result in the relationship:

$$\left(\Delta K_{th}\right)_R = \left(1 - R\right)\Delta K_o \qquad (7)$$

Under variable amplitude load conditions, it is necessary to properly account for load ratio effects (min load/max load) that exist in experimental data prior to any

uncertainty quantification method. Rather than constructing distribution functions for each of the threshold stress intensity factors obtained under different loading conditions, it is preferable to first remove the underlying loading effects and quantify a baseline material property that can be used for a variety of loading conditions. As a result, the Backlund equation given in Eqn. (6) will be used within this work prior to distribution fitting.

Fatigue crack growth rate data collected under different load ratios for Steel 4340, representative of the material typically used in rotorcraft mast components, has been used within this section for numerical investigation. A parametric study is first performed to identify fitting parameter $C$ and $d$ for the Steel 4340 experimental data set with threshold data collected at multiple R ratios. It was determined that $C$=0.4 and $d$=1 provided the best results and effectively reduced data to single curve that could be used for baseline analysis. Statistical distribution fitting techniques were performed to identify the most appropriate distribution function for accurately representing the scatter found in the threshold stress intensity factor experimental data.

The lognormal distribution was compared to the experimental data through the chi-squared test, the Kolmogorov-Smirnov (K-S) statistical test at a 5% significance level, as well as through traditional probability plot techniques as shown in *Figure 8* [41]. The lognormal distribution function was found to accurately represent the data using all three techniques. The histogram of the threshold stress intensity factor along with the probability density function (PDF) of the fitted lognormal distribution are shown in *Figure 9*, and the corresponding cumulative distribution function (CDF) is shown in *Figure 10*. By quantifying the baseline condition without the effect of load ratio, the

fitted distribution function can be used, along with the Backlund equation (Eqn. (6)) to sample statistical-based realizations of the baseline threshold stress intensity factor which can be adjusted for particular load cases.

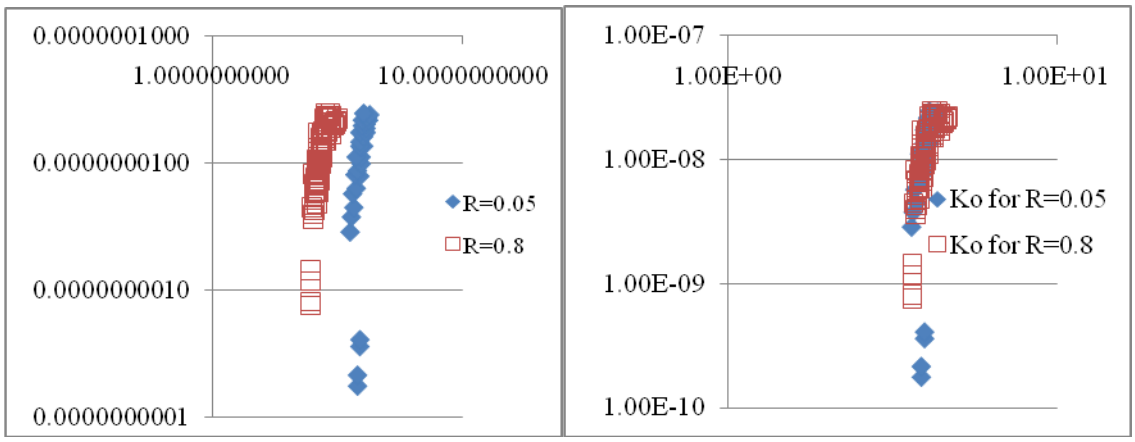


***Figure 7:*** *Fatigue crack growth rate threshold data for 4340 steel a.) raw data b.) adjusted $K_o$ data using Backlund equation [37]*

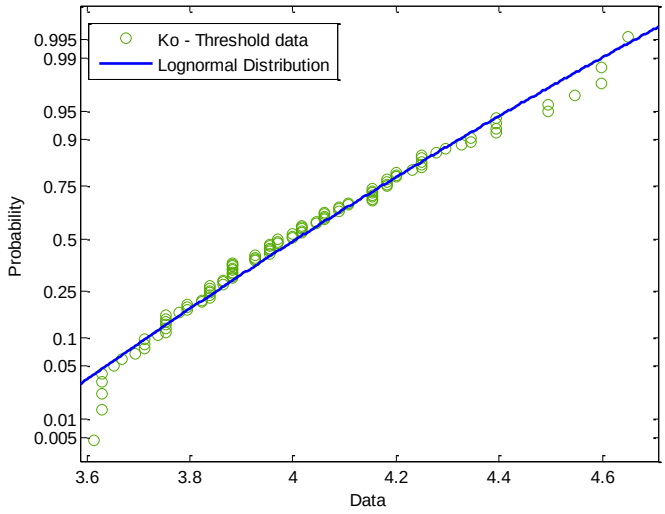


***Figure 8:*** *Probability plot showing Adjusted $K_o$ data to lognormal distribution function*

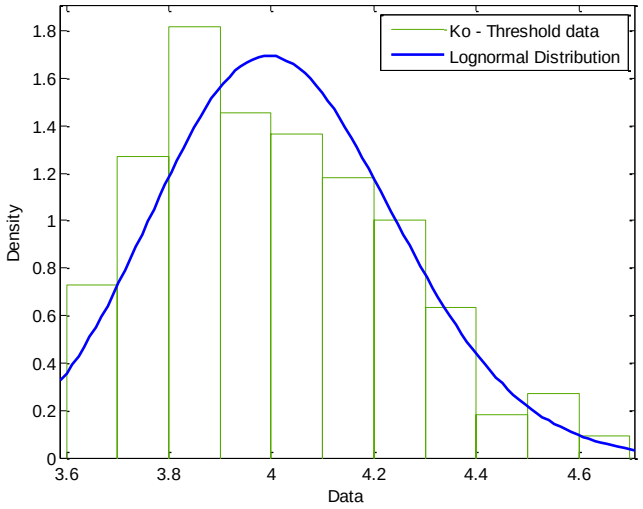


***Figure 9:*** *Histogram of Adjusted $K_o$ data from experiment data and PDF of fitted lognormal distribution function*

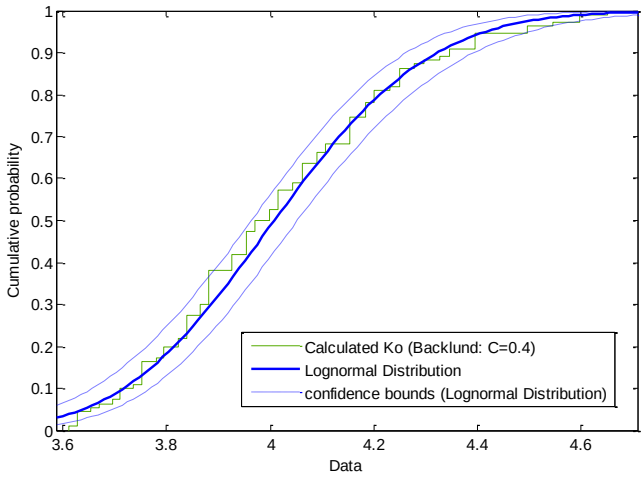


***Figure 10:*** *Adjusted $K_o$ data from experiment data and CDF of fitted lognormal distribution function*

*Fatigue Limit*

The fatigue limit has been traditionally used within the safe-life design methodology as a means of matching the infinite fatigue life of specimen subjected to

low magnitude cyclic loading. The fatigue limit is the amplitude (or range) of cyclic stress that can be applied to the material without causing fatigue failure [42]. The fatigue limit has generally been determined through traditional S-N experiments, in which a known stress is repeatedly applied to the specimen, and the number of cycles to failure is recorded. Ferrous and titanium alloys tend to have a distinct fatigue limit, whereas other materials, such as aluminum, tend to not have as well defined thresholds. Typically, for these materials, the stress which corresponds to a value of $10^7$ cycles is taken as a good approximation for the fatigue limit of the material. The metallic materials properties development and standardization (MMPDS) handbook [43] is recognized as a reliable source of aircraft materials data from which accurate materials strength data and material properties can be obtained.

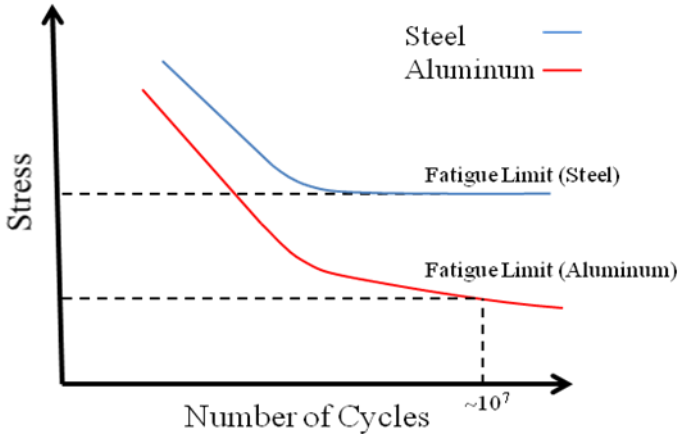


***Figure 11:*** *Typical S-N Curves for Steel and Aluminum materials*

However, performing material tests to define the fatigue limit of the material can be time consuming and costly, because of the large number of cycles that must be applied

before structural failure is observed and the numerous test that are required to fully capture the S-N curve. For this reason, sparse data may again exist for the statistical quantification of the fatigue limit of the material of interest.

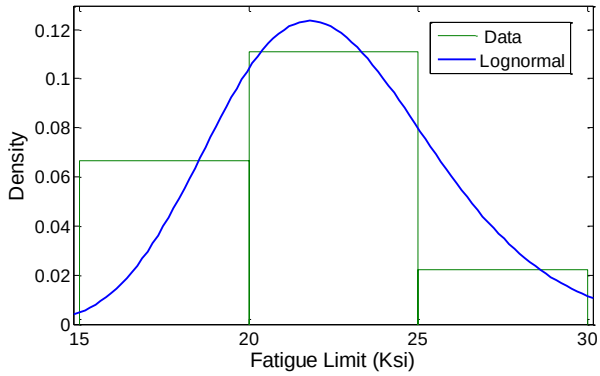


***Figure 12:*** *Fatigue Limit data for aluminum alloy 7075-T6 and fitted lognormal distribution function*

When only sparse experimental data sets are available for distribution fitting purposes, confidence in statistical quantities, such as mean and variance, may be somewhat limited. That is to say, uncertainties may exist in the statistical fitting parameters themselves. To overcome the limitations that sparse data pose to statistically meaningful parameter estimation, resampling methods can be used. McDonald et al.[44] proposed a method to account for data uncertainty, in which in the quantity of interest can be represented using a probability distribution, whose parameters are in turn represented by probability distributions. The accurate distribution representations of the fatigue limit and the threshold stress intensity factor are important within this work as they are later used for the numerical evaluation of the equivalent initial flaw size (EIFS) which describes the statistical characteristics of the initial flaws sizes to be considered in the material. Sparse experimental data is common for both of these material properties as a

result of the expensive and time consuming experimental tests which are necessary for their determination. As a result, uncertainty may exist in the probability density functions which are used to represent the statistical characteristics, which will directly affect the statistical representation of other parameters which are derived from this quantity, such as the equivalent initial flaw size (EIFS). The uncertainty resulting from sparse data is addressed below and can easily be included within the overall uncertainty quantification approach. Additional information on the specific EIFS formulation used within this research is presented within Section 3.2.

A variety of resampling methods exist within the field of statistics, including both bootstrapping and jackknifing. The bootstrap technique is a statistical method for estimating the sampling distribution of an estimator by sampling with replacement from the original sample set [45]. The jackknife technique is similar to bootstrapping, and can be used to estimate the bias and standard error in a statistic, when a random sample of observations is used to calculate it. The jackknife estimator technique systematically recomputes the statistic estimate leaving out one observation at a time from the sample set [46].

Consider a random variable $X$ whose statistics are to be determined from experimental data, given by $\boldsymbol{x} = \{x_1, x_2 .. x_n\}$. For the sake of illustration, suppose that the random variable $X$ follows a normal distribution, then the parameters ($\boldsymbol{P}$) of this distribution, i.e. mean and variance, of $X$ can be estimated from the entire data set $\boldsymbol{x}$. However, due to sparseness of data, these estimates of mean and variance are not accurate. Using resampling techniques such as bootstrapping method, jackknifing etc. the probability distributions ($f_{\boldsymbol{P}}(\boldsymbol{P})$) of the parameters ($\boldsymbol{P}$) can be calculated. Hence for each

instance of a set of parameters (***P***), $X$ is defined by a particular normal distribution. However, because the parameters (***P***) themselves are stochastic, $X$ is defined by a family of normal distributions. For a detailed implementation of this methodology, refer to McDonald [44].

The current research uses similar resampling techniques to calculate the distribution of the parameters (***P***), however does not define a family of distributions. Instead, it recalculates the unconditional distribution of the random variable $X$ [41]. The probability density of $X$ conditioned on the set of parameters (***P***) is denoted by $f_{X|\boldsymbol{P}}(x)$. The parameters are represented by the joint probability density $f_{\boldsymbol{P}}(\boldsymbol{P})$. Hence, the unconditional probability distribution of $X$ ($f_X(x)$) can be calculated as shown in Eqn.(8).

$$f_X(x) = \int f_{X|P}(x) f_{\mathbf{P}}(\mathbf{P}) \mathrm{d}\mathbf{P} \qquad (8)$$

The integral in Eqn. (8) can be evaluated through quadrature techniques or advanced sampling methods such as Monte Carlo integration or Markov chain Monte Carlo Integration. Hence, the unconditional distribution of $X$ which accounts for uncertainty in input data can be calculated. This method can be used to be able to better characterize the distribution of threshold stress intensity factor ($\Delta K_{th}$) and fatigue limit ($\Delta\sigma_f$) when only limited experimental data is available.

*Yield Strength and Ultimate Tensile Strength*

The probability distributions used to represent fracture toughness are also often used to characterize the yield strength and ultimate tensile strength and include normal, lognormal, and Weibull [47, 30]. In reality, these parameters may be variable and might

require probabilistic treatment. However, these properties are regularly monitored, have tight manufacturing tolerances, and are easily tested by standard techniques. Therefore, within this work it is assumed that these properties have limited uncertainties and will be treated as deterministic values.

## 2.3 Uncertainty in Fatigue Crack Growth Rate Parameters

As mentioned previously, numerous crack growth rate empirical models have been proposed within the literature. For the high cycle fatigue crack growth problem, only those models which are capable of capturing the non-linear behavior within the near-threshold region are relevant, since strictly linear models will drastically overestimate crack growth rates within this region leading to unnecessarily short fatigue life predictions. For the purpose of demonstration and general application of the methods developed in the research, the modified Paris model [85] will be used as a result of the multiple fitting parameters included in the model, the near threshold and linear region modeling capabilities, and the familiarity of fatigue community with its functional form. The modified Paris model is given by the relation:

$$\frac{da}{dN} = C(\Delta K)^n \left(1 - \frac{\Delta K_{th}}{\Delta K}\right)^p \qquad (9)$$

By fitting crack growth rate models to available experimental data, it is observed that natural scatter is seen in the data resulting in some fitting parameters remaining relatively constant, while others tend to vary significantly. Stochastic parameters have been introduced into various empirical crack growth models by Yang [48], Provan [49],

Moore [50], Cruse [51], and others to try to capture this phenomenon. By using experimental data to fit model parameters to distribution functions, the uncertainties in model parameters can be quantified. Various forms of probabilistic fatigue crack growth models have been proposed, and can generally be divided into two distinct categories.

The first type of method accounts for the stochastic behavior in fatigue crack growth data by treating the crack growth rates at specific stress intensity factors as random variables that are completely uncorrelated to each other. This assumption is equivalent to treating the crack growth process as a white noise process. This approach will be referred to as the statistical FCG approach and results in the smallest statistical variability (underestimates the variance) [52]. Yang's [48, 53] method using a hyperbolic sine (SINH) fatigue crack growth model with an additional term representing a homogeneous Gaussian random process fits into this category. By defining the correlation function of the Gaussian random process equal to zero, the Gaussian term represents a random white noise process. Although computationally feasible, this approach artificially introduces randomness in the model prediction through a noise term, and ignores the intuitive physical relationship that exists between stress intensity factor and crack growth rate data. It has been inferred within the literature that the white noise process is not valid for fatigue crack propagation, and therefore will not be included within this research.

The second type of method treats coefficients of the deterministic crack growth models as random variables. The statistics of the parameters are described using common distribution functions, such as lognormal or Weibull distributions, and are determined by fitting the model to available fatigue crack growth rate data. In numerous

reliability studies, the fatigue crack growth model coefficients, such as the Paris *C* and *n* parameters, have been assumed to follow the lognormal distribution [54,55,56, 57, 58]].

By treating these parameters as random variables, the fatigue crack growth model is randomized and probabilistic analysis is possible. This approach is equivalent to assuming the random variables are fully correlated and is commonly referred to as a percentile crack growth curve approach. Due to its broad applicability and understanding, as well as its straightforward implementation, this method will be further evaluated within this work for the high cycle fatigue crack growth problem and numerical parameter distribution fitting to relevant experimental data will be presented following this initial discussion.

A more realistic approach to this problem is to model the correlation of the random variables somewhere between the two extremes mentioned above, that is, $0 < \rho < 1$. This approach will be referred to as the partial correlation based approach. Yang and Manning [59] considered the correlation effect and proposed a second-order approximate method to calculate the failure probability. The underlying assumption is that a lognormal random process could be added to deterministic fatigue crack growth models as

$$\frac{da(t)}{dt} = X(t)\, f(\Delta K, .....) \qquad (10)$$

where *a(t)* is the crack size at time *t*, $\Delta K$ is the stress intensity factor, and *X(t)* is a stationary lognormal random process with median value of 1 and a standard deviation of $\sigma_x$.

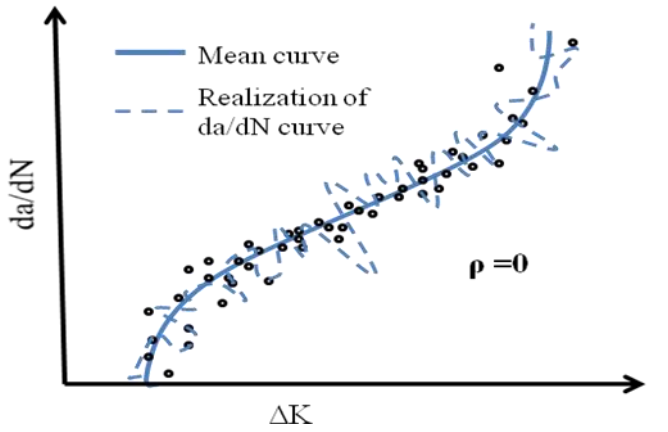


*(a.)*

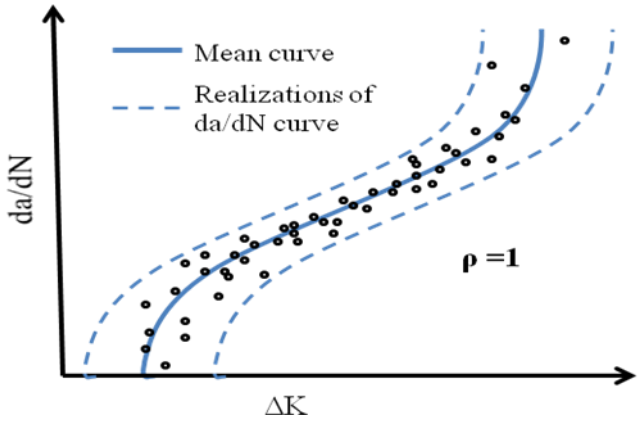


*(b.)*

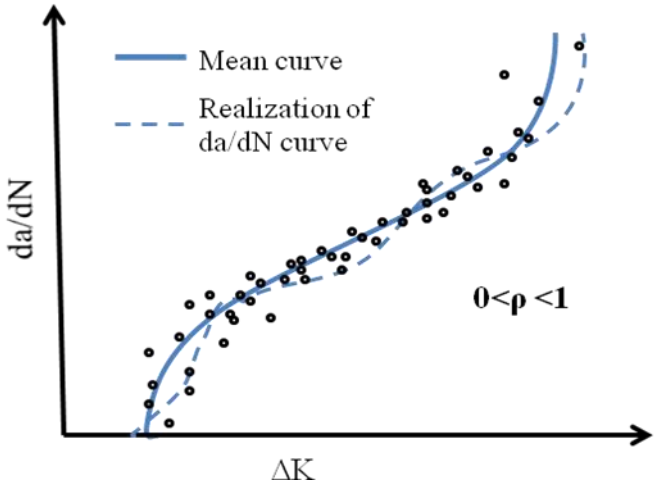


*(c.)*

***Figure 13:*** *Stochastic fatigue crack growth curves using; a.) no correlation; b.) full correlation; c.) partial correlation*

Liu and Mahadevan [52] have proposed a Karhunen-Loeve random process expansion technique for stochastic SN analysis that accounts for realistic correlation effects in fatigue damage accumulation simulation. The KL expansion technique is not dependent on the Gaussian assumption and non-Gaussian methods for random field representation are easily adopted. The KL expansion technique has been shown to agree well with experimental data collected from various types of steel [52]. Some of the benefits of approaching stochastic modeling by this approach are that the Gaussian assumption is not necessary, the correlation is accurately represented to be $0 < \rho < 1$, and the variance is not restricted to a constant value.

Two distinct methods for probabilistic fatigue crack growth rate modeling are the percentile and partial correlation based crack growth models. The percentile approach offers a simple, straightforward method for representing the randomness seen in experimental data, but may not realistically represent the correlation structure between the stress intensity factor and the crack growth rate due to the method's implicit assumption of a perfect correlation structure. The partial correlation based approach overcomes this deficiency by providing the flexibility to represent any correlation value between 0 and 1, however, in doing so, adds model complexity in the form of representation and implementation. Each of the methods provides a benefit to the analyst, and, therefore, both are implemented within this work and are presented below. First, the percentile crack growth method is detailed and statistical distributions are fit to common fatigue crack growth model parameters using experimental data. Following the discussion of the percentile based approach, a partial correlation based method is presented and implemented for the same experimental data set. The methodology

developed by Liu and Mahadevan [52] for stochastic fatigue damage modeling using the stochastic SN approach is extended for fatigue crack growth rate modeling using fracture mechanics principles. The mathematical construct of the method is provided in detail for the new application. By extending this methodology to fatigue crack growth modeling, it is possible to not only use state of the art fatigue crack growth modeling techniques, but also maintain all of the above benefits from stochastic representation. Details of the numerical implementation of each method are included below.

It should be noted that initial implementation of both the percentile crack growth approach and the partial correlation based crack growth approach will be presented assuming adequate data is available. It is clear that material crack growth data has to be available to justify the choice of the type and value of the distribution function used for the stochastic parameter estimation.

*Percentile crack growth approach*

In order to quantify the uncertainties from experimental data using this approach, *Eqn.* (9) was randomized. This process is performed by using a multi step approach in which the data in each region is used to fit the corresponding parameters. The parameters are first estimated by solving a non-linear curve fitting problem in the least squares sense. This is accomplished by finding the coefficients that best fit the equation

$$Min(x) \quad \frac{1}{2}\sum_{i=1}^{m}\left(F\left(x, xdata_i\right) - ydata_i\right)^2 \qquad (11)$$

given input data *xdata*, and the observed output *ydata*, where *xdata* and *ydata* are vectors of length *m,* and *F(x,data)* is a vector-valued function. After the parameters have been estimated, some are held as constants while others are assumed to be random variables.

For each data point within a given data set, a realization of the random variable is obtained, and, after all the realizations are collected, the parameter can be fitted to a probability distribution. In order to choose the best fit for a given distribution, the Anderson-Darling (A-D) statistic is used. The main fitting parameters corresponding to the linear region of the Modified Paris fatigue crack growth model are *C* and *n* shown in Eqn. (9). Using the non-linear curve fitting procedure outlined above, data within the linear region could be used to evaluate Eqn. (11) to determine the best values for the parameters *C* and *n*. After estimates for both parameters where obtained, *n* was held at its mean value, and realizations of *C* were obtained for each data point within the data set. The experimental data fitting results could then be fit to a well defined distribution function.

Experimental fatigue crack growth rate data collected for Steel 4340 is included for demonstration purposes. The analysis is limited to only the fatigue crack growth rate data that corresponds to the linear region of the crack growth rate curve (see *Figure 3*). The experimental data is analyzed to determine the statistical distributions of fatigue crack growth rate model parameters corresponding to the linear region of the curve. The results from this numerical study are presented here to demonstrate uncertainty quantification of fatigue crack growth model parameters, and the uncertainty quantification results obtained here are applied to the overall probabilistic fatigue crack growth modeling analysis presented in Chapter 3.

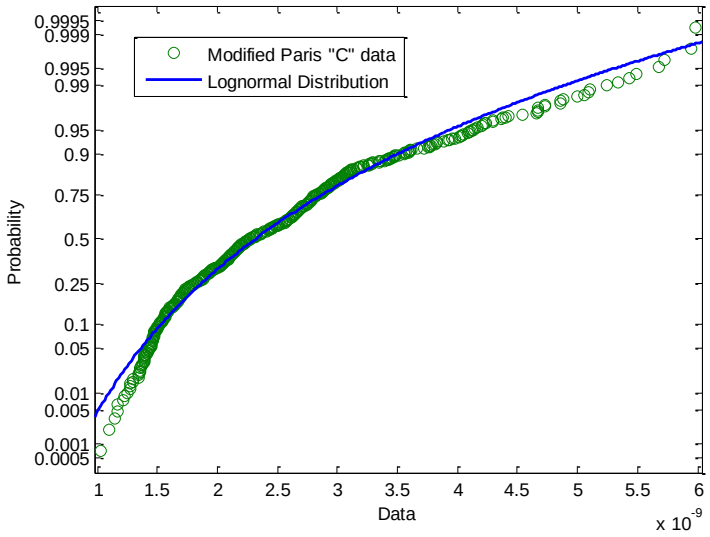


***Figure 14:*** *Probability plot showing Modified Paris parameter C data and lognormal distribution function*

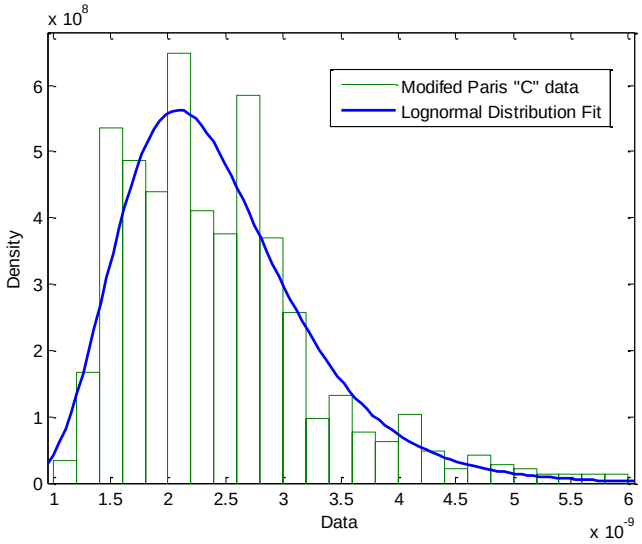


***Figure 15:*** *Histogram of Modified Paris parameter C calculated from experiment data and PDF of fitted lognormal distribution function*

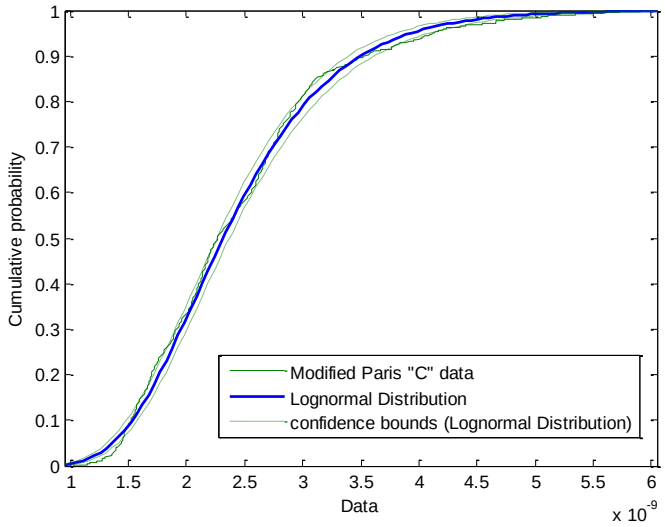


***Figure 16:*** *Modified Paris parameter C calculated from experimental data and CDF of fitted lognormal distribution function*

Statistical goodness of fit tests are used to analyze the experimental results with theoretical distribution functions. Several common distribution functions were compared to the experimental data set and it was determined that the lognormal distribution well characterized the data. The lognormal distribution was compared to the experimental data through the chi-squared test, the Kolmogorov-Smirnov (K-S) statistical test at a 5% significance level, as well as through traditional probability plot techniques, and was found to pass all of the statistical tests considered. The numerical analysis revealed that the fatigue crack growth parameter *C* could be well characterized by the lognormal distribution function with a mean value of $2.4378*10^{-9}$ and a standard deviation of $8.074*10^{-10}$, corresponding to a coefficient of variation (COV) of approximately 0.33.

For the high cycle fatigue crack problem, it is not only necessary to capture the uncertainty in the linear region of the fatigue crack growth rate curve, but also critical to incorporate the uncertainty in the near threshold region. Similar to the statistical method

outlined above for the linear region parameters $C$ and $n$, so too can the statistics of the model parameters in the near threshold region be treated as random variables. The main parameters corresponding to the near threshold region of the Modified Paris fatigue crack growth model are $\Delta K_{th}$ and $p$ shown in Eqn. (9).

The parameter $p$ in Eqn. (9) is used to help capture the transition from the near threshold to the linear region of the fatigue crack growth rate curve. The transition from the near vertical threshold region to the sloped linear region appears smoother and more gradual when $p$ increases, and becomes increasingly sharp as $p$ decreases. Values of $p$ found for aerospace grade aluminum and steel materials are generally $\leq 1$. When compared to experimental data, it is seen that the gradient of the fatigue crack growth rate in the transition zone from the near threshold to linear region appears consistent, indicating that $p$ can be treated as a deterministic value. As a result, $p$ is treated as an empirically fitted deterministic constant within this dissertation and can be best fit using the least squares method outlined above.

The other primary parameter within the near threshold region is the threshold stress intensity factor, $\Delta K_{th}$. The threshold stress intensity factor range, $\Delta K_{th}$, is the parameter which defines separation between no crack growth and slow crack growth in the near threshold region of the fatigue crack growth rate curve. $\Delta K_{th}$ should be treated as a random variable and a detailed discussion of its significance as related to the high cycle fatigue problem as well as appropriate techniques for statistical characterization has been previously included in Section 2.2. It was found that the baseline near-threshold stress intensity factor (lacking load ratio effects) for steel 4340 could be well represented by the lognormal distribution function as shown in *Figure 8*, *Figure 9*, and *Figure 10* in Section

2.2. The reader is encouraged to refer to the previous section for additional details and discussion on this topic.

Methods to fit model parameters from fatigue crack growth rate models to statistical distribution functions using experimental data sets has been presented. Crack growth rate models within the near-threshold and linear regions should be analyzed separately using only experimental data contained in the region which is relevant to the model parameters. It was found that for the 4340 steel data set which was considered, the lognormal distribution function provided the best fit for both the $C$ and $K_{th}$ parameters contained in Eqn. (9). However, it should be noted that different distribution functions such as Normal, or Weibull distributions may provide a better fit when considering different datasets or different materials, and the most accurate distribution function should be used within subsequent analysis. The framework proposed within the following chapter is flexible and allows for the use of any distribution function for the representation of fatigue crack growth rate model parameters.

Once the crack growth rate parameters are fit to distribution functions, the percentile approach offers a simple, straightforward method for representing the randomness seen in experimental data by treating the stress intensity factor and fatigue crack growth rate as perfectly correlated random variables. The result of this assumption is shown schematically in *Figure 13 b.* Uncertainty in fatigue crack growth rate data can be captured using this technique by randomly sampling the statistical distributions of each random parameter for each fatigue crack growth analysis performed.

*Partial Correlation based crack growth approach*

The partial correlation based crack growth approach treats the crack growth rate at any specific stress intensity factor as a random variable and a stochastic process modeling method is used to avoid the assumption that crack growth rates at different stress intensity factors are either completely correlated or completely uncorrelated as previously developed methods assume [52]. The method detailed below is an extension of a stress life (SN) based approach developed by Liu and Mahadevan [52] and details of the methodology as they relate to crack growth modeling using fracture mechanics principles is included below.

Within this section, for the sake of illustration, the fatigue crack growth rates at given stress intensity factors are assumed to follow the lognormal distribution. The lognormal assumption makes $log(da/dN(\Delta K))$ a Gaussian process with a mean value process of $E[log(da/dN(\Delta K))]$ and a standard deviation of $\sigma_{log(da/dN(\Delta K))}$. It should be noted that non-Gaussian methods for random field representation are available, and that the Gaussian assumption is not a requirement, but has been made to simplify the discussion [52]. The mean value, $E[log(da/dN(\Delta K))]$, is representative of the mean $da/dN$ vs. $\Delta K$ curve found through deterministic analysis. The mean curve can be found using any available general crack growth model.

It can be seen within experimental data that the variance of $da/dN$ is not constant, but rather is a function of stress intensity factor range, $\Delta K$. Significant scatter may exist in both the near threshold and linear crack growth regions. If $\sigma_{log(da/dN(\Delta K))}$ represents the

scatter in the data, then the process given by Eqn. (12) is a normal Gaussian process with zero mean and unit variance.

$$Z(\Delta K) = \frac{(\log(da/dN(\Delta K)) - E[\log(da/dN(\Delta K))])}{\sigma_{\log(da/dN(\Delta K))}} \qquad (12)$$

The random process, *Z(ΔK)*, can be expressed using the Karhuenen-Loeve expansion technique [60, 61] as a sequence of statistically independent random variables. Generally, the expansion is expressed as

$$Z(\Delta K) = \sum_{i=1}^{\infty} \sqrt{\lambda_i}\, \varepsilon_i(\theta)\, f_i(\Delta K) \qquad (13)$$

where $\varepsilon_i(\theta)$ is a set of independent random variables, and $\sqrt{\lambda_i}$ and $f_i(\Delta K)$ are the $i^{\text{th}}$ eigenvalues and eigenfunctions of the covariance function $C(\Delta K_1, \Delta K_2)$, evaluated by solving the homogenous Fredholm integral equation analytically or numerically. The homogenous Fredholm integral equation is given by

$$\int_D C(\Delta K_1, \Delta K_2)\, f_i(\Delta K_2) = \lambda_i\, f_i(\Delta K_1) \qquad (14)$$

The autocovariance function, $C(\Delta K_1, \Delta K_2)$, can be expressed through the exponential decay function of *Z(s)* as:

$$C(\Delta K_1, \Delta K_2) = e^{-\mu|\Delta K_1 - \Delta K_2|} \qquad (15)$$

where $\mu$ is a measure of the correlation distance of *Z(ΔK)* and depends on the material. Through the control of the parameter $\mu$, the exponential decay function can model covariance structures ranging from fully correlated ($\mu \rightarrow 0$) to fully uncorrelated ($\mu \rightarrow +\infty$). These two extreme cases correspond to the percentile and statistical stochastic models respectively.

Based on Eqns. (13) through (15), the fatigue crack growth rate can be modeled as:

$$(\log(da/dN(\Delta K)) = \sum_{i=1}^{\infty} \sqrt{\lambda_i}\,\varepsilon_i(\theta)\, f_i(\Delta K) * \sigma_{\log(da/dN(\Delta K))} + E[\log(da/dN(\Delta K))]) \quad (16)$$

This equation not only expresses the fatigue crack growth rate as a function of *ΔK* through the deterministic mean term, but also includes terms from the KL expansion which introduces stochastic behavior in the crack growth prediction and captures the correlation structure. A typical fatigue crack growth curve representation which is obtained after applying this method can be seen in *Figure 13 (c)*. Only a finite number of terms within the KL expansion are necessary to effectively model the stochastic behavior seen in most practical applications. Usually, 10-20 terms suffice for providing sufficiently precise results under the standard Gaussian assumption [52].

Since *da/dN* increases with increasing stress intensity factor range, *ΔK*, it is a non-stationary random process. In order to accurately model the variance of *da/dN* over the entire range of *ΔK* values, the crack growth rate curve can be subdivided into *n* sections (or regions), with the variance determined within each section from experimental data. As the number of sections, *n*, increases, the general trend of variance of *da/dN* over the range of *ΔK* values can be determined and can be closely approximated by a common functional form (linear, power, etc). Once the variance is determined, the standard deviation ($\sigma$) can easily be found and used within Eqn. (16). *Figure 17* shows the standard deviation determined over the each interval of *da/dN* (standard deviation evaluated from data within each order of magnitude) for data collected under several

different R-ratios for 2024-T3 Aluminum alloy. As can be seen in the figure, the standard deviation appears to be independent of R ratio, thus allowing it to be modeled by a single function for all R ratios.

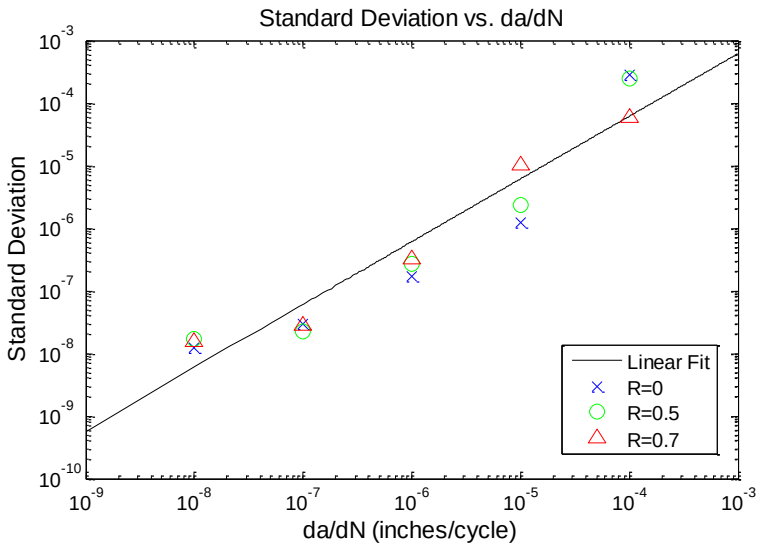


***Figure 17:*** *Standard deviation of fatigue crack growth rate data*

*Figure 18* shows 5 realizations of the fatigue crack growth rate curve obtained by using the partial correlation method along with experimental crack growth rate data. A random realization of the fatigue crack growth curve can be generated for each simulation within the overall stochastic fatigue crack growth modeling framework.

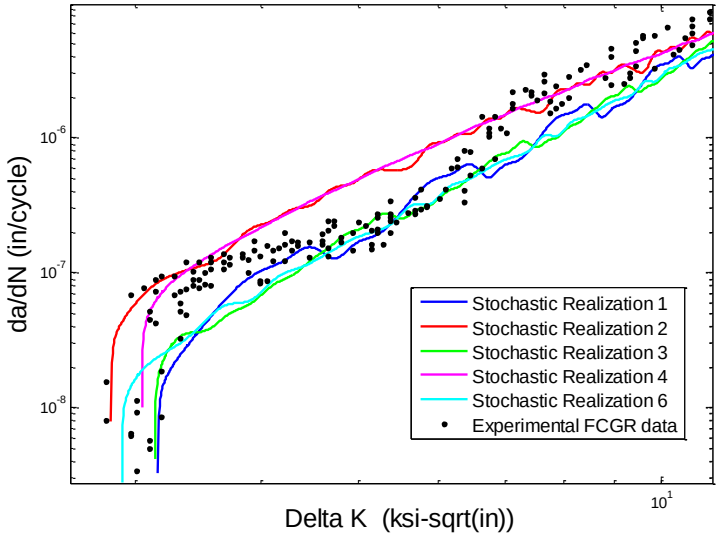


***Figure 18:*** *Ensemble of 5 stochastic fatigue crack growth curves generated using partial correlation technique*

Either the partial correlation method or the percentile fatigue crack growth rate modeling approach can be used to represent the variability that exists in experimental fatigue crack growth rate data. Additionally, each can be easily incorporated within an overall crack growth probabilistic analysis. However, the partial correlation based fatigue crack growth rate modeling approach using a K-L expansion technique offers several advantages over previous methods, including:

1.) More realistic correlation structure representation of the crack growth rate at different stress intensity factor ranges

2.) Can be used to exactly model statistical and percentile crack growth representations

3.) Capability of modeling Gaussian and non Gaussian stochastic behavior

4.) Flexibility to include changes in variance within specific regions of the crack growth rate curve as dictated by the data set under consideration

The partial correlation method for representation of fatigue crack growth rate data can be used within a Monte Carlo simulation method for stochastic fatigue crack growth prediction in order to account for the natural scatter observed in experimental fatigue crack growth rate data.

## 2.4 Uncertainty in Variable Amplitude, Multi-axial Loading

As part of the certification process for rotorcraft and fixed wing aircraft, assumed design load spectra must be verified on the basis of actual flight load measurement. These lengthy, irregular time histories contain the fatigue relevant load information that is necessary for life prediction. Measured time histories contain all of the information about the loading history including all phasing, frequency, sequence, magnitude, and mean effects [62], however they contain so much data that they are difficult to decipher and compare. In order to accurately characterize load histories in a meaningful way, the content of a measured signal must be able to be summarized and quantified in an efficient and concise way [63]. Various methods exist to quantitatively assess recorded time histories, and are generally grouped into two distinct categories; frequency domain methods and time domain methods [35].

Different harmonic analysis methods can be used to determine the "frequency content" of the signal by characterizing the frequencies or wavelengths of the built up

signal. Although some research has been published that uses traditional frequency domain based methods for fatigue evaluation [64,65], such analysis is generally relevant only to determine the vibration characteristics of the structure, and is not very descriptive of the fatigue damage of the loading [63].

It is generally agreed that the structural load variations used in metal fatigue analysis should be characterized in the time domain since it is the maxima and minima, and the number of cycles (rather than time) which are the main controlling parameters [35, 66], and the shape of the intervening curve between a maximum and a minimum is of little importance [67]. Time domain methods typically work by identifying occurrences of specific "events" in a load-time sequence. Typical events of interest include the occurrence of load peaks/maximums at specific levels, the exceedance or crossings of specific levels, and the occurrence of load changes or ranges of a specific size [63]. Methods which help identify fatigue relevant "events" within a complex load history are generally referred to as simply *counting methods*. Many counting techniques are available including: level crossing, peak count, mean crossing peak count, range count, and range-pair counting techniques [68,69], however, the rain-flow counting method (range pair-range) is widely recognized as the most accurate and meaningful way of representing variable amplitude loading [66].

It is obvious that in-service operational loading on many structures is a stochastic process and typically cannot be adequately characterized by a single constant or variable amplitude load history. Statistical investigation of the variable amplitude load cycle distribution is often a critical task, as the structural reliability under service loading has strong dependence on the accurate quantification and representation of such loads. The

majority of research has been performed under constant amplitude conditions, and only limited effort has been put into developing statistical tools for fatigue load characterization when the loads are both variable amplitude and stochastic [70]. An efficient and accurate method is needed for quantification and characterization of the fatigue content (load reversals) contained within a variable amplitude load spectrum. Additionally, methods are needed to capture and represent the inherent uncertainty that exists within the environmental loading condition.

Several counting techniques are discussed in detail below and implemented in this research for initial load quantification purposes. Load characterization using the rainflow counting method is presented first, followed by methods using the Markov method. The results obtained from each of these methods are later used within Chapter 4 to generate stochastic load simulations with similar loading characteristics as the original measured history within a probabilistic crack growth framework.

*Load Quantification using Rainflow Counting Method*

The majority of the previous research that includes rainflow counting methods has been used in combination with the stress-life (S-N) or strain-life ($\varepsilon$-N) methods [69] in which the damage in each cycle is computed based on data gathered from constant amplitude tests using a damage accumulation rule such as Miner's Rule. This research uses the rainflow counting method as an initial fatigue loading quantification method and then implements a stochastic regeneration technique for variable amplitude load spectrum simulation which can be used within a fracture mechanics based crack growth analysis procedure. The load quantification method using the rainflow cycle counting procedure

will be presented within this section, whereas the stochastic generation of additional load histories will be presented later in Chapter 3.

The rainflow method was originally proposed by Matsuiski and Endo [71], and is viewed by many to be the most popular and best method of cycle counting. The method separates high and low amplitude load cycles and records them in a physically meaningful way. To briefly summarize the method, for each local peak ($s_{max}$) within the time history, the rainflow algorithm finds the corresponding local trough ($s_{min}$) to form a hysteresis loop. The stress range as well as the mean stress for each cycle is determined, and the results are stored in matrix form. In this way, the complex load history is reduced to a simple rainflow matrix which contains information about the stress amplitudes, mean values, and number of occurrences of each loading cycle. Additional details of the rainflow counting method are available in various literature sources [68, 69].

The objective of the *rain-flow method* or the *range pair-range method* is to extract and count cycles of various sizes. These load cycles are considered to be the basic elements of a load sequence. The final counting result is contained in a matrix A of size ($k+1$) x ($k+1$), in which the element $a_{ij}$ gives the number of counted cycles from load level $i$ to load level $j$, and $k$ is a user defined number of discretization levels, usually set to 32, 64, or 128 depending on accuracy and computational efficiency desired [72,73]. Plots of a generated load history signal and its corresponding rainflow matrix are shown within *Figure 19.*

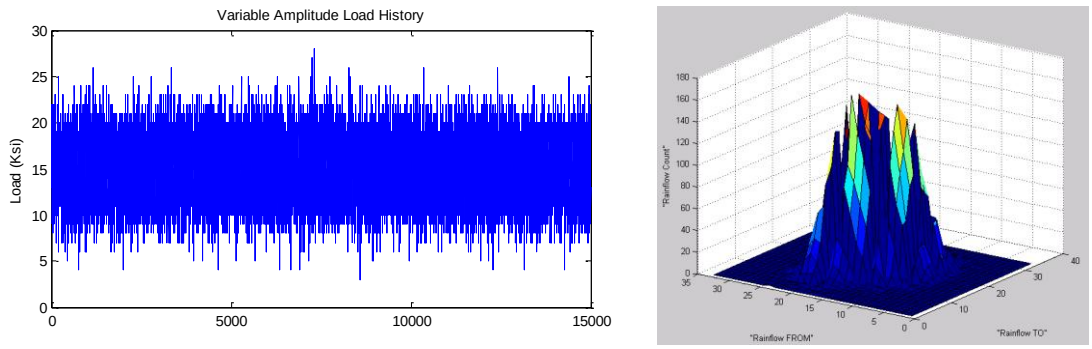


(a.) (b.)

***Figure 19:*** *(a.) Generated variable amplitude load history (b.) Graphical representation of rainflow matrix showing cycle counts for discrete load levels as calculated from (a)*

Although cycle counting methods have typically been viewed as deterministic methods for characterizing load histories, the obtained results from such methods can be easily transformed for use within a statistical framework in one of two ways. The first method simply uses the counted load cycles within the rainflow matrix within a stochastic regeneration technique to produce random fatigue load history simulations. The second method fits the elements in the rainflow matrix to a joint distribution, for full statistical representation of the loading characteristics. In order to accomplish this, both the "from" load level and "to" load level within the rainflow matrix are considered as random variables, say *x* and *y*, respectively. Assuming that the rainflow counting results are discrete values, the joint probability mass function (PMF) of *x* and *y* is denoted as $p_{X,Y}(x,y)$ and the joint cumulative distribution function (CDF) given by [74]:

$$F_{X,Y}(x,y) = \sum_{x_i<x} \sum_{y_j<y} p_{X,Y}(x_i, y_j) \qquad (17)$$

The variables *x* and *y* can also be approximated as continuous variables with their joint PDF denoted by $f_{X,Y}(x,y)$ and the joint CDF given by:

$$F_{X,Y}(x,y) = P(X \le x, Y \le y) = \int_{-\infty}^{x}\int_{-\infty}^{y} f_{X,Y}(u,v)dvdu \qquad (18)$$

The histogram of extracted values as well as the marginal PDF (obtained from the rainflow matrix shown in *Figure 19* is shown in *Figure 20.*

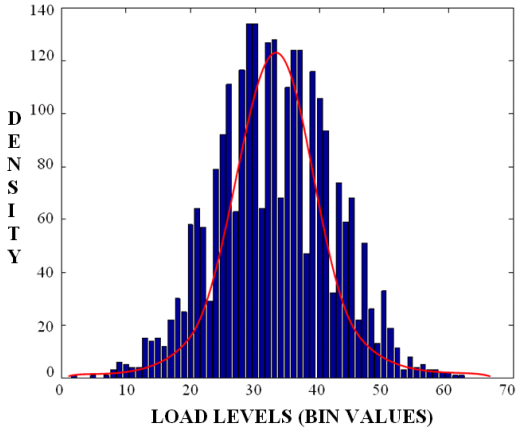


***Figure 20:*** *Plot of histogram and fitted marginal PDF of load cycles from rainflow matrix*

A schematic of the procedure for the uncertainty quantification of the variable amplitude load spectrum is shown in *Figure 21*. By using the rainflow counting procedure in combination with statistical distribution fitting techniques, a complex load history can be easily broken down into its elementary cycles and efficiently represented by a joint probability density function.

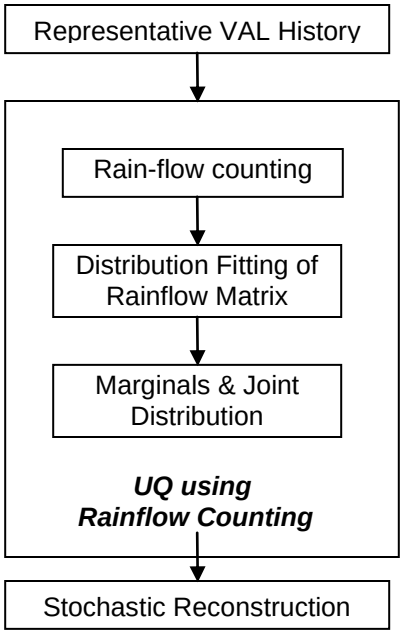


***Figure 21:*** *Elements of the uncertainty quantification (UQ) procedure using rainflow representation*

*Load Quantification using Markov Chain Method*

The Markov method uses the loading information contained within a representative fatigue cycle history to construct a probability based transition matrix. The transition matrix contains discretized load levels with the "from" load level and "to" load level composing the axes, and is populated by placing all level transitions contained within the stress history in the discrete *(i,j)* position according to the nominal stress values ($\sigma_i$, $\sigma_j$) that they represent.

For a realistic loading history, not only the load amplitude at a certain time instance is random, but also the load amplitudes at adjacent time instances may be correlated, i.e., the amplitude at time instance $T_k$ can affect the amplitude at time instance $T_{k+1}$. Given this assumption, the fatigue loading history with $m$ discrete load levels are

modeled as a discrete time Markov chain $\{X_n\}$, which is a Markov stochastic process whose state space (the set of discretized load levels) is a finite set, and for which $n$ is a discrete time instance ( $n = T_0, T_1, T_2, \ldots,$ ) [75]. Let event $E_{k,i}$ denote that the loading amplitude at time instance $T_k$ equals to load level $i$, and let event $E_{k+1,j}$ denotes that the loading amplitude at $T_{k+1}$ equals load level j. With a further assumption that the one-step transition is independent of time instances, i.e., the transition between $E_{k,i}$ and $E_{k+1,i}$ depends on $i$ and $j$ only, and not on previous values, a stationary Markov chain transition matrix is constructed as:

$$I = \begin{bmatrix} 0 & I_{1,2} & \cdots & I_{1,n} \\ I_{2,1} & 0 & & \vdots \\ \vdots & & 0 & I_{n-1,n} \\ I_{n,1} & \cdots & I_{n,n-1} & 0 \end{bmatrix} \qquad (19)$$

where $I_{i,j}$ is the one-step stationary transition count between $E_{k,i}$ and $E_{k+1,i}$, which can be obtained directly from the original load spectrum. The elements above the main diagonal in $I$ represent the transitions from minima to maxima, whereas the elements below the main diagonal represent the transition from maxima to minima.

Given a load spectrum with discrete load levels from time $T_0$ to $T_e$, the element of the stationary Markov chain transition probability matrix $P_{i,j}$ can be estimated using the number of occurrences of that the event $E_{k,i}$ is followed by the event $E_{k+1,i}$, i.e.,

$$C_{i,j} = \sum_{k=0}^{e-1} I_{i,j}(k) \qquad (20)$$

$$P_{i,j} = \begin{cases} C_{i,j} / \sum_{j=i+1}^{m} C_{i,j} & i < j \\ C_{i,j} / \sum_{j=1}^{i-1} C_{i,j} & i > j \end{cases} \qquad (21)$$

where $I_{i,j}(k)$ is a indicator function,

$$I_{i,j}(k) = \begin{cases} 0 & \text{if } E_{k,i} \text{ is followed by } E_{k+1,j} \\ 1 & \text{if } E_{k,i} \text{ is not followed by } E_{k+1,j} \end{cases}$$

*Figure 23* shows the conversion of a Markov transition matrix given by Eqn. (19) to a transition probability matrix as determined from Eqn. (21) for the simple turning point load history shown in *Figure 22*. A proper transition matrix satisfies the property that the sum of cycle counts in each cell of a row above the diagonal must equal the sum of cycle counts in each cell of the column opposite and below the diagonal. Once the transition probability matrix is constructed, random samples of loading history can be easily generated using random number generators.

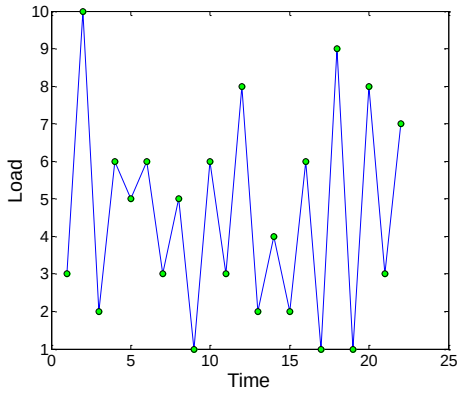


***Figure 22:*** *Simple turning point load history*

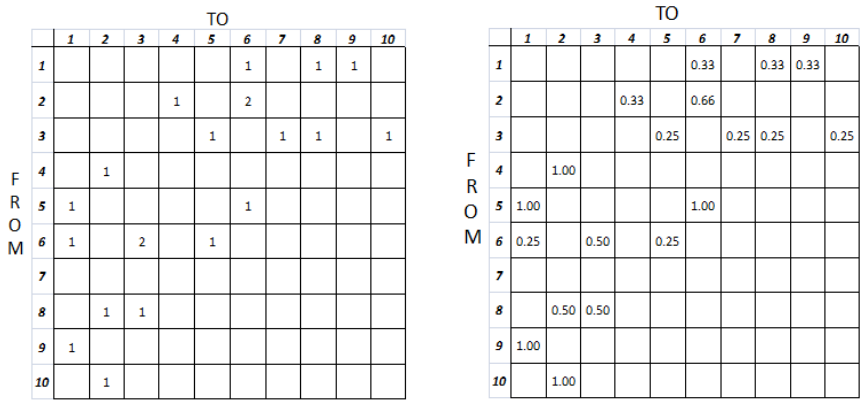


*a.)* *b.)*

***Figure 23:*** *a.) Transition matrix b.) Transition probability matrix*

Although measured time histories contain all of the information about the loading history, it is difficult to obtain a clear understanding of the key characteristics of the data when it is in this format, and makes load comparison between different histories virtually impossible. To accurately characterize load values in a meaningful way, the content of a measured signal must be summarized and quantified in an efficient and concise way. Within this section, rainflow and Markov-based methods are presented as tools which simplify the representation of fatigue loading within a complex, variable amplitude load history. Additionally, methods are presented to more generally express the fatigue loading content contained within a history by joint distribution functions and transition probability matrices. Each of the load quantification methods contained within this section is further developed within Chapter 3 to enable stochastic load simulation within a probabilistic crack growth framework.

## 2.5 Summary

Much of the traditional damage tolerance (DT) research has used deterministic modeling approaches under well defined, simple loading conditions. However, several sources of uncertainty exist and each needs to be statistically quantified and included within subsequent analyses for meaningful component life prediction results. The probabilistic approach to engineering design is offered as a method for incorporating uncertainty within the structural analysis in a logical and meaningful way.

A general overview of uncertainty with respect to the fatigue life prediction method is presented within Section 2.1. The different sources of uncertainty in model inputs identified for this class of problem include material properties, model parameters, and applied loading. Section 2.2 applies statistical techniques for uncertainty quantification to material properties, such as the threshold stress intensity factor and the fatigue limit. Each of these material properties is treated as a random variable, whose statistics are determined and compared to common distribution functions. Two different methods for characterizing the randomness in fatigue crack growth rate model parameters are given in Section 2.3. The first method assumes a perfect correlation structure exists between the crack growth rate per cycle, $da/dN$, and the stress intensity factor, $\Delta K$, and is referred to as the percentile approach. Different fatigue crack growth rate model parameters may be treated as random variables using this approach, and each can be fit to standard distribution functions using experimental crack growth rate data. A new approach to fatigue crack growth rate modeling is developed which includes a more realistic representation of the correlation that exists between crack growth rate and stress intensity factor data. This approach is called the partial correlation based method. Section

2.4 investigates two different methods for quantification and representation of variable amplitude fatigue loading data. The rainflow cycle counting method can be used for this purpose, and detailed methods of further fatigue relevant fatigue representation is provided. The Markov based method is also presented within this section as an alternative method for load characterization and quantification.

The different statistical methods presented within this chapter are given as useful tools which can be used to characterize the randomness that exists in several of the model inputs and/or model parameter values that are typically used within a damage tolerance based fatigue life prediction analysis. Each method can be used individually to represent a single random input, or collectively to more fully represent the overall stochastic nature of inputs to the fatigue crack growth analysis. Chapter 3 develops a fatigue crack growth modeling framework which enables systematic and efficient probabilistic fatigue life prediction considering the uncertainty in model inputs identified and quantified within this chapter.

# CHAPTER III

# PLANAR FATIGUE CRACK GROWTH MODELING

## 3.1 Introduction

This chapter explains the overall methodology that has been developed to model fatigue crack propagation under multiaxial loading conditions using a planar fatigue crack growth approach. The methodology has been developed with probabilistic analysis in mind, where uncertainties at various levels of modeling can easily be included within the overall framework.

For each deterministic analysis within the Monte Carlo scheme, input variables such as initial crack size, crack shape, and crack growth model parameter values are sampled from their given distributions. A stochastic load history is simulated based on fatigue relevant statistics determined from a representative load history. A cycle by cycle approach is adopted where a stress intensity factor is evaluated for the current loading cycle and crack configuration using a trained surrogate model. Crack growth rate calculations can be performed along the crack front using a stochastic fatigue crack growth rate model and the crack front can be appropriately extended. Cyclic crack growth analysis is repeated using the same load history from the initial crack size until a user defined critical crack size is reached, at which time the results are stored and the procedure is repeated for the next realization of input variables. After many simulations are completed, it is possible to extract probabilistic information such as the probability distribution of the crack size at any given time, *t*, or, conversely the probability

distribution of the time necessary for a crack to reach a critical size, as shown in *Figure 24*. This information can ultimately allow for prognosis, risk assessment and inspection scheduling. A flowchart of the overall approach is presented in *Figure 25*. Details of the methodology can be found in the following sections.

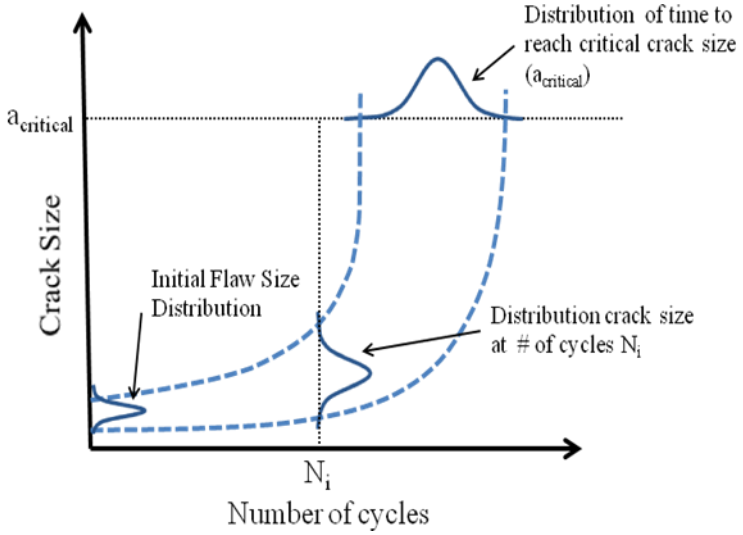


***Figure 24:*** *Summary of typical results using proposed methodology*

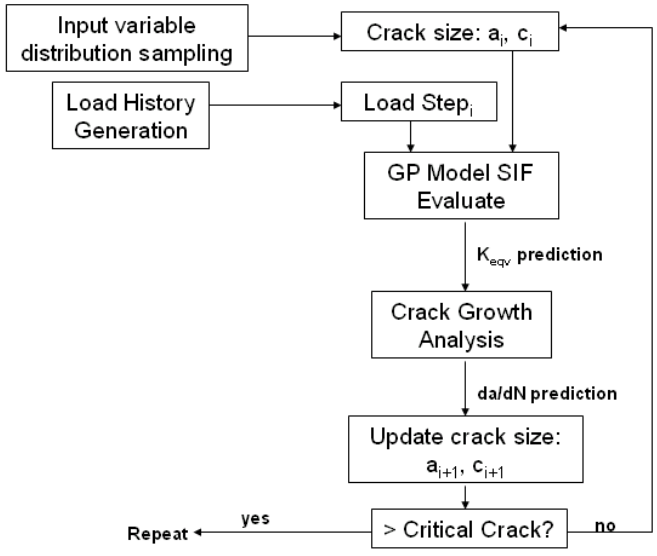


***Figure 25:*** *Monte Carlo simulation scheme for fatigue crack growth using proposed methodology.*

## 3.2 Initial Flaw Size & Location

The first step in performing a damage tolerance analysis, in which an initial flaw is assumed to be contained within the component of interest, is to fully characterize the flaw which is to be modeled. For this research, only surface crack configurations will be considered. The surface crack configuration is controlled by two parameters, namely; crack length (*2c*) and aspect ratio. Here, aspect ratio is defined as the ratio of half the crack length over the crack depth (*c/a*) as shown in *Figure 26*.

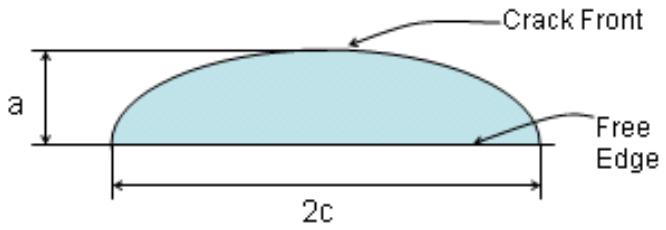


***Figure 26:*** *Semi-Elliptical Crack showing crack length (2c) and depth (a) definitions*

It is clear that different locations within the component will be subjected to different stresses based on the type of applied loading and the geometry of the component of interest. Since fatigue crack propagation depends not only on the crack size and shape, but also on the stress concentration at the crack front, cracks with the same initial configuration but at different locations within the component will have different propagation rates, and thus, will cause different component life predictions. Based on this information, the most critical location is that which will cause the crack to grow the fastest, causing the component to break in the least amount of time. MIL-A-83444 handbook [76] states that "the analyses shall assume the presence of flaws placed in the

most unfavorable location and orientation with respect to the applied stresses and material properties."

In order to identify this critical location, a preliminary stress analysis of the uncracked component can be completed. Loading conditions similar to those expected in-service are applied to the component and the stress field can then be analyzed to identify the region with the highest stress concentration. By performing this analysis on an uncracked component, the critical location can be identified and a crack can be inserted in the structural model such that it is perpendicular to the maximum principal stress direction at that location.

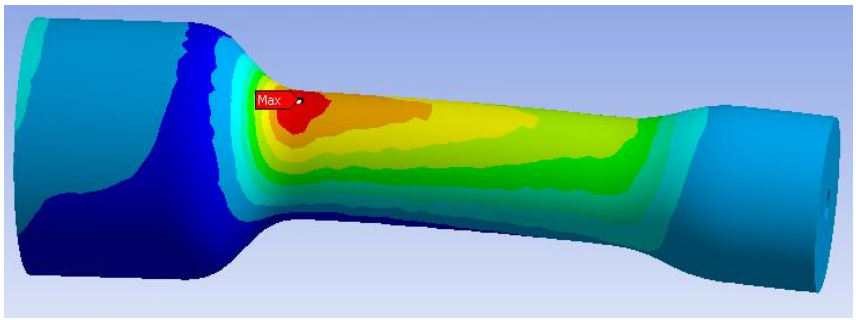


***Figure 27:*** *Plot of typical stress profile within rotorcraft mast component under applied mixed mode loading*

Ideally, fatigue life prediction could be performed starting from an actual, as-manufactured initial flaw size, accounting for actual voids, non-metallic inclusions, or surface scratches contained within the material. However, determining the true distribution of initial flaw sizes within an as-manufactured part is, often times, difficult to accomplish due to inadequate resources and/or the limited capability of non-destructive evaluation (NDE) techniques for reliably detecting small crack sizes. If the actual initial

crack size can be accurately determined and is found to be large (> 0.02 inches), then long crack growth models such as the Paris, Walker or Forman models can be used directly. However, this is not the case in many applications, and initial flaws contained within the material might be on the order of the grain size of the material. When cracks of this type are present, their growth is controlled by grain boundaries and cannot be described by linear elastic fracture mechanics [40]. Additionally, the crack growth rate behavior of small cracks (on the order of grain size) is not easily characterized and cannot be represented by traditional crack growth rate laws. The concept of an equivalent initial flaw size (EIFS) was proposed to bypass the poorly understood small crack growth analysis and make direct use of a long crack growth law for fatigue life prediction.

However, EIFS does not represent any physical quantity and cannot be directly measured using experiments. Initially, certain researchers used empirical crack lengths between 0.25 mm and 1 mm for metals (JSSG [77]; Gallagher [78]; Merati [79]). Later, several researchers (Yang [80]; Moreira [81]; Fawaz [82]; White [83]; Molent [84]) used back-extrapolation techniques to estimate the value for equivalent initial flaw size. Recently, Liu and Mahadevan [85] proposed a methodology based on the Kitagawa-Takahashi diagram [86] and the El-Haddad Model [87] to derive an analytical expression for the equivalent initial flaw size. The value of EIFS is calculated from material properties and is given by the expression

$$a_o = \frac{1}{\pi}\left(\frac{\Delta K_{th}}{\Delta \sigma_f Y}\right)^2 \qquad (22)$$

where $a_o$ is the EIFS, $\Delta K_{th}$ is the threshold stress intensity factor range, $\Delta\sigma_f$ is the fatigue limit, and $Y$ is the geometry correction factor.

The current research work uses Eqn. (22) to calculate the statistics of EIFS by using the probability distribution functions of the threshold stress intensity factor and fatigue limit. The distribution functions of these material properties were determined within Chapter III of this work, considering both natural variability in experimental data and data uncertainty due to sparse data. By using this physics based approach, the analytical expression in Eqn. (22) can be used to determine a distribution of the EIFS. The distribution of EIFS for 7075-T6 Aluminum alloy is included within *Figure 28* and can be sampled within the subsequent probabilistic crack growth analysis. Since both the threshold stress intensity factor and the fatigue limit have been determined to fit the lognormal distribution function for this material, the EIFS will also be a lognormal variable. However, this is not a necessary condition, and the distribution of EIFS can be easily determined (despite the distribution functions of $\Delta K_{th}$ and $\sigma_f$, through simple sampling techniques.

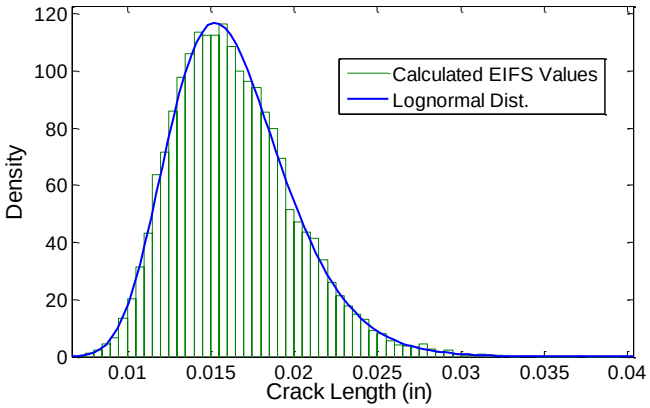


***Figure 28:*** *10,000 calculated EIFS value and best fit lognormal distribution function for Aluminum Alloy 7075-T6*

## 3.3 Component Stress Analysis

For standard fatigue specimen subjected to uniaxial loading conditions, handbook solutions for stress intensity factors are available [88]. For structures having complicated geometry or complex multi-axial loading conditions, a handbook solution for the stress intensity factor, $\Delta K$, may not be available and finite element analysis (FEA) may be required. Although the computational expense can be significant for high fidelity models, FEA analysis is still necessary in some capacity to determine the stress state at the crack tip, and must be performed for complex geometry and loading conditions.

A two level approach is adopted for finite element analysis within this work, using a global model and a submodel. The crack region represents a relatively small volume of material that lies within the larger volume of the overall component and is constructed within a submodel for better computational efficiency and accuracy. The submodel method is a technique to obtain a more accurate numerical value for the specific region in the analyzed model with high efficiency, and is sometimes referred to as the cut-boundary displacement method or the specified boundary displacement method. The boundary of the sub model represents a cut through the coarse model, where displacement boundary conditions are enforced.

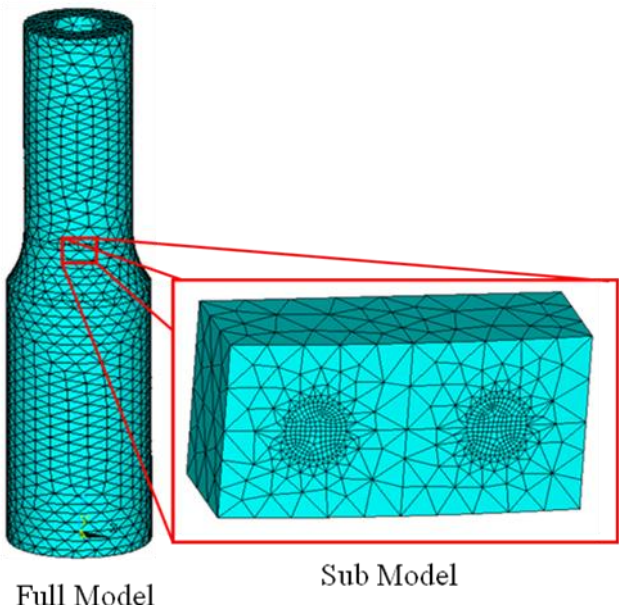


***Figure 29:*** *Depiction of full model and sub model used in FEA for planar crack analysis*

The submodel is composed of a crack 'block' and a crack 'tunnel' in the vicinity of the surface crack location and has a much more refined mesh than does the full model. In order to create the cracked configuration within the submodel, an auxiliary area is first swept through the semi-elliptical arc defining the crack front shape (as defined by crack length and aspect ratio) and is then reflected about the crack plane. This volume is generally referred to as the crack 'tunnel'. The crack tunnel volume is meshed using a very fine mesh with singular elements around the crack front and non-singular elements elsewhere in order to have accurate representation of the stress field around the crack tip. By merging all coincident nodes and keypoints within the crack block, except for those along the crack faces, connectivity is ensured between the crack tunnel mesh and the slightly coarser mesh created in the remainder of the crack block. The submodel technique is based on the St. Venant's principle, which states that if an actual distribution

of forces is replaced by a statically equivalent system, the distribution of stress and strain is altered only near the regions of load application. That is to say, if the boundaries of the sub model are far enough away from the stress concentration along the crack front, accurate results can be expected. *Figure 30* shows a stepwise schematic of the FEA submodel creation process.

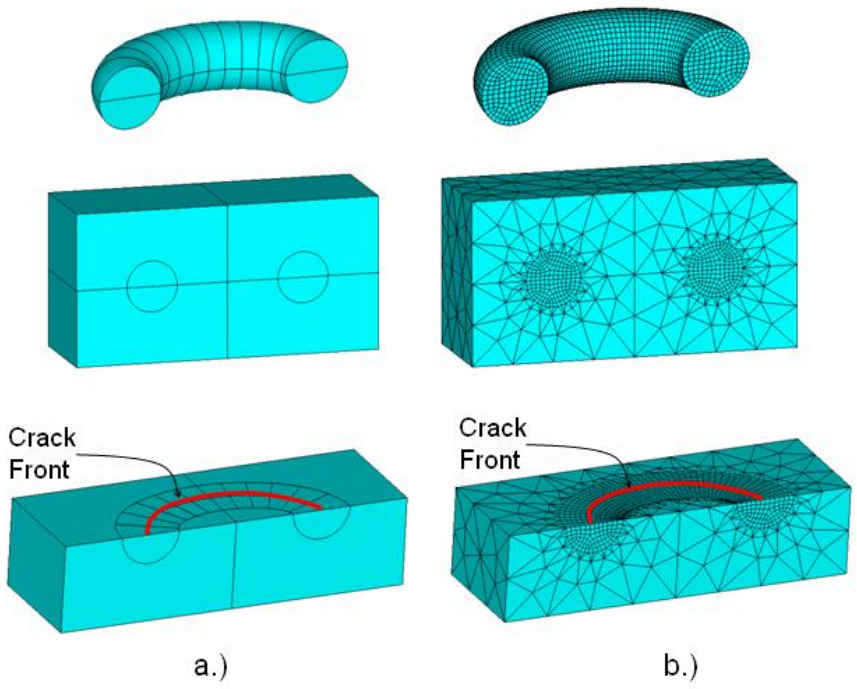


***Figure 30:*** *Detailed view of finite element crack submodel volume a.) unmeshed and b.) meshed configurations*

The finite element software package ANSYS [89] version 11.0 is used to build and analyze the finite element model. The crack configuration is built by extruding a projection of the semi-circular crack through the mast body at the crack location. The immediate volumes on either side of the crack face are identified and subdivided in order to allow for SIF evaluation at various locations along the crack front. The crack faces (coinciding upper and lower surfaces of the previously mentioned volumes) are then

modeled as surface to surface contact elements (CONTACT174 and TARGET170 elements) in order to prevent the surface penetration of the crack's upper and lower surfaces. The augmented Lagrangian method is the algorithm used for contact simulation. Additionally, friction effect is included in the material properties of the contact element, in which a Coulomb friction model is used. This model defines an equivalent shear stress which is proportional to the contact pressure and the friction coefficient. Friction coefficients between two crack faces are difficult to measure and are generally assumed to vary between 0 and 0.5 [90]. The friction coefficient, $\mu$, used within this study is assumed to be a deterministic quantity and taken to be equal to 0.1.

Since the primary quantity of interest is the stress intensity factor at the crack tip, the volume along the crack front is subdivided into many smaller blocks, which allows for better mesh control and enables SIF evaluation at various locations along the crack front. The ¼ node displacement method proposed by Henshell and Shaw [91] and Barsoum [92] has been commonly used to enable the square root singularity of stresses and strains at the crack tip to be modeled accurately by shifting the mid-point nodes to the quarter-point locations in the region around the crack front. Stress intensity factors at the surface and depth locations are calculated and are used within fatigue crack growth models for crack extension calculations, allowing for initial semi-circular surface cracks to develop into semi-elliptical cracks over time.

## 3.4 Equivalent Mixed-Mode Stress Intensity Factor

Many mechanical and structural components are subjected to some combination of tension, bending, bearing, and torsion, in which some combination of mode I, mode II, and mode III loading conditions exist (e.g. mast in rotorcraft, railroad wheels, turbine blades, shafts of automobiles [93,94,95]), however only limited research has been reported in the literature. Carpinteri [96,97] analyzed hollow pipes with elliptical surface cracks under bending moment and axial loading separately. Fonte [98] applied bending moment to a round bar with a circumferential elliptical crack and validated his results with previously published results in the literature, followed by an analysis of torsion loading only. He then applied both bending moment and torsion loading, and checked the superposition principle. Results showed that the application of bending moment induced only Mode I at the crack front, whereas the application of torsion induced all three modes of loading at the crack front.

The stress intensity factor is the primary parameter used for fatigue crack growth rate prediction and is typically used with many commonly used fatigue crack growth rate models including the Walker [7], Forman [6], and Forman-Newman-de Koning [99] models.

Several parameters have been used to correlate fatigue crack growth rates under mixed mode conditions. These include equivalent stress intensity factors, equivalent strain intensity factors, strain energy density, and the J-integral [69]. These methods develop different expressions for an equivalent stress intensity factor range, $\Delta K_{eqv}$, which has been used to obtain the crack growth rate for mixed-mode loading condition in a Paris-type equation [69].

This research uses a characteristic plane-based model for multi-axial fatigue damage modeling proposed by Liu and Mahadevan [100,101], which is applicable to a wide range of metallic materials and has been validated using multiaxial fatigue experimental data. The characteristic plane-based model enables the calculation of an equivalent mixed mode stress intensity factor which can be used for mixed mode fatigue crack propagation and life prediction calculations. A detailed derivation and explanation of the model can be found in Liu and Mahadevan [101] and the concepts will only be briefly summarized within this section as necessary for basic understanding of the methodology.

The characteristic plane-based approach seeks to reduce the dimension of the multiaxial fatigue problem by considering the stress components on a given plane, the characteristic plane, so that traditional crack growth models can be implemented, and in doing so, also reduces the necessary computational effort [101]. The formula under general mixed mode I+II+III loading is derived as

$$\sqrt{\left(\frac{k_I}{K_{I,th}}\right)^2+\left(\frac{k_{II}}{K_{II,th}}\right)^2+\left(\frac{k_{III}}{K_{III,th}}\right)^2+A\left(\frac{k^H}{K_{I,th}}\right)^2}=B \qquad (23)$$

where $k_I$, $k_{II}$, and $k_{III}$ are the mode I, II and III loading factors with the same unit of stress intensity factors, and $K_{I,th}$, $K_{II,th}$, and $K_{III,thI}$ are the fatigue crack threshold values, respectively. $k^H$ is the hydrostatic stress related term, and $A$ and $B$ are material parameters which can be determined by tension and shear fatigue limits. The characteristic plane for a given material is determined through minimizing the contribution of the hydrostatic stress amplitude to zero.

***Table 3:*** *Material Properties for fatigue damage accumulation using characteristic plane approach*

| **Material Property** | $s = \frac{t_{-1}}{f_{-1}} \le 1$ | $s = \frac{t_{-1}}{f_{-1}} > 1$ |
|---|---|---|
| $\gamma$ | $\cos(2\gamma) = \frac{-2 + \sqrt{4 - 4\left(1/s^2 - 3\right)\left(5 - 1/s^2 - 4s^2\right)}}{2\left(5 - 1/s^2 - 4s^2\right)}$ | $\gamma = 0$ |
| **A** | A=0 | $A = 9\left(s^2 - 1\right)$ |
| **B** | $B = \left[\cos^2(2\gamma)s^2 + \sin^2(2\gamma)\right]^{\frac{1}{2}}$ | $A = s$ |

Following the derivation outlined by Liu [101], the equivalent mixed mode stress intensity factor using the characteristic plane approach can be expressed as

$$\Delta K_{mixed,eqv} = \frac{1}{B}\sqrt{(\Delta k_I)^2 + \left(\frac{\Delta k_{II}}{s}\right)^2 + \left(\frac{\Delta k_{III}}{s}\right)^2 + A\left(\frac{\Delta k^H}{s}\right)^2} = f\left(\frac{da}{dN}\right) \qquad (24)$$

The equivalent uniaxial stress intensity factor, $\Delta K_{mixed,eqv}$, could be used within any available fatigue crack growth model by a simple substitution of the mode I stress intensity factor, $\Delta K_I$, used in the original formulation with the newly defined parameter $\Delta K_{mixed,\,eqv}$.

## 3.5 Surrogate Model Development

The previous two sections within this chapter presented methods for the multiaxial stress analysis of a fatigue critical component using FEA, and a stress intensity factor dimension reduction technique for calculation of equivalent, uniaxial stress intensity factor. Within a damage tolerance analysis, where initial cracks are grown incrementally until they reach a critical crack size, each of these steps is necessary for each crack growth increment within the analysis, requiring substantial computational effort. The computational expense associated with the stress intensity factor calculation typically results from the need to implement an expensive finite element code for the current crack size and loading conditions. In order to implement this type of analysis within a probabilistic framework, where many full simulations are necessary, a more efficient method for determining the stress intensity factor at the ever evolving crack front must be developed.

Response surface methodology can be used in place of expensive finite element models for iterative fatigue analysis to reduce the computational effort needed to calculate the stress intensity factor at the crack tip. A response surface approximation is constructed to approximately capture the relationship between the input variables (crack length, location, and load values) and the output variables (stress intensity factors), using only a few sample points within the design space. Instead of using a finite element model to determine the stress intensity factors at *every* load step within every simulation, the model is analyzed for a small number of crack configurations and loading conditions to "train" a surrogate model to an acceptable degree of accuracy. Once trained, the surrogate model is used in place of the full finite element model. By developing an accurate

surrogate model and drastically reducing the computational effort needed at load cycle within the analysis, it is possible to use a Monte Carlo simulation technique for component reliability assessment.

Many different types of surrogate models have been developed and reported within the literature including: locally weighted polynomial regression, quadratic response surface regression (QREG), random forest regression (RF), gradient boosting machine (GBM), multivariate adaptive regression splines (MARS), support vector and relevance vector regression, neural networks and Gaussian process models [102,103]. An initial study of several methods was performed to evaluate the relative performance of each as applied to the FEA/stress analysis problem. Results from the study are included in *Table 4*, and revealed the Gaussian process model to have an overall better performance when compared to the other methods with the same level of training. The Gaussian process model will be implemented within this research due to its flexibility and relative performance when compared with other available methods.

***Table 4:*** *Comparison of surrogate model performance for stress analysis application*

| Surrogate Model | Sum of Squares of Errors |
|---|---|
| Polynomial Chaos Expansion | 57.7 units |
| Support Vector Regression | 55.1 units |
| Relevance Vector Regression | 54.9 units |
| Gaussian Process Interpolation | 50.3 units |

Gaussian process (GP) modeling (which is in most cases equivalent to the family of methods which go by the name of "Kriging" predictors) is a powerful technique based on spatial statistics for interpolating data. Gaussian process models are increasingly being

used as surrogates to expensive computer simulations for the purposes of optimization and uncertainty propagation [104,105], and will be investigated within this paper as method to improve computational efficiency by replacing the expensive stress intensity factor calculation.

The basic idea of the GP model is that the response values, *Y*, are modeled as a group of multivariate normal random variables, with a defined mean and covariance function. A recently developed greedy point selection technique can be used to select training points for the GP model to build up the response surface to a desired level of accuracy [106]. The benefits of GP modeling is that the method requires only a small number of sample points (usually 30 or less), and is capable of capturing highly nonlinear relationships that exist between input and output variables without the need for an explicit functional form. Additionally, Gaussian process models can be used to fit virtually any functional form and provide a direct estimate of the uncertainty associated with all predictions in terms of model variance.

In order to accurately capture the functional relationship between input and output quantities, the Gaussian Process model must be "trained" using a set of observed inputs and outputs. The Greedy Point algorithm [106] can be used to identify which points within the design space would be the most advantageous to use as training points. As mentioned previously, the variance associated with model predictions is available as a result of the Gaussian Process formulation. The Greedy Point algorithm uses this information to identify the set of input variable values (design space location) which correspond to the largest variance in the design space, and selects the next training point to be at that location, thus improving the model by minimizing the model prediction

error. By repeating the Greedy Point algorithm iteratively, training points can be identified that minimize the variance of the surrogate model until a sufficiently accurate model is generated, say within 1% or 5% of FEA. This training point selection method eliminates the subjectivity associated with typical design of experiments methods which use a pre-determined fixed set of training points, and ensures that the identified training points are adding the most value (accuracy) to the surrogate model per additional full simulation run.

Suppose that there are $n$ training points, $x_1$, $x_2$, $x_3$ … $x_n$ of a $d$-dimensional input variable (the input variables being the crack size and loading conditions here), yielding the resultant observed random vector $Y(x_1)$, $Y(x_2)$, $Y(x_3)$ … $Y(x_n)$. R is the $n$ x $n$ matrix of correlations among the training points. Under the assumption that the parameters governing both the trend function ($f^T(x_i)$ at each training point) and the covariance ($\lambda$) are known, the conditional expected value of the process at an untested location $x^*$ is calculated as in Eqn. (25) and Eqn. (26) respectively.

$$Y^* = E\left(Y \mid x^*\right) = f^T\left(x^*\right)\beta + r^T\left(x^*\right)R^{-1}(Y - F\beta) \qquad (25)$$

$$\sigma_{Y^*} = Var\left(Y \mid x^*\right) = \lambda\left(1 - r^T R^{-1} r\right) \qquad (26)$$

In Eqn. (25) and Eqn. (26), $F$ is a matrix with rows $f^T\left(x_i\right)$, $r$ is the vector of correlations between $x^*$ and each of the training points, $\beta$ represents the coefficients of the regression trend. McFarland [106] discusses the implementation of this method in detail.

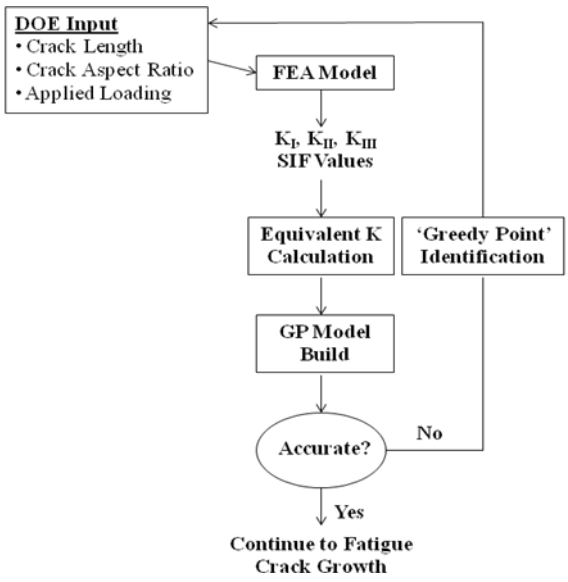


***Figure 31:*** *Schematic of GP training process using iterative greedy point algorithm*

The GP surrogate modeling technique offers several advantages which prove useful. The first is that the GP modeling approach is a non-parametric technique, meaning that assumptions about the functional form (linear, quadratic, power, etc.) are not necessary. The framework is flexible and can capture linear and non-linear relationships that exist within the design space. A second significant attribute of the GP modeling approach is that the method has the ability to provide a direct representation of the uncertainty associated with its interpolative approximation [106]. This uncertainty representation has been shown to provide usefulness in improving both the efficiency of optimization [107] and reliability estimation [108].

## 3.6 Variable Amplitude Load Generation

By reducing the complex load history into its elementary load cycles and storing the information in a rainflow or Markov transition matrix representation, significant advantages are gained in terms of ease of quantification of the measured load spectrum. However, the sequence of the loading is lost. Loading sequence is of importance since it is well known that amplitude changes in fatigue loading conditions can result in significant retardation or acceleration of fatigue crack growth rates [109]. This section address this issue and presents stochastic regeneration techniques that can be used to produce multiple realizations of load histories that contain the same fatigue loading characteristics as the original representative load history

It is well known that crack growth can be significantly affected by prior events in the load history [69]. There is vast literature showing that tensile overloads can cause retardation or arrest in fatigue crack growth and compressive overloads can also have significant effects on the rate of subsequent crack propagation [110]. Ignoring such effects can lead to significant error in fatigue life estimation. Therefore, it is necessary to incorporate a methodology that uses the sequence of loadings in the life prediction. Several different reconstruction techniques have been reported within the literature including traditional power spectral density techniques [111], Markov simulations [72], rainflow [112], among others. It is proposed that by utilizing stochastic reconstruction methods in combination with the load quantification results developed in Chapter 2, it is possible to generate multiple realizations of the fatigue content to represent several different load sequences.

*Rainflow Stochastic Load Reconstruction*

The basic objective of the stochastic rainflow reconstruction algorithm is to create a systematic method to reconstruct a load history given a rainflow matrix and its residual. Dreβler [113] presents an algorithm for reconstruction and approaches the problem so that an optimal randomization of the reconstructed series is attained. Rainflow reconstructions are based on the idea of extracting cycles from the rainflow matrix and placing them in valid locations in the history under construction. Several rules exist to ensure that cycles are inserted within the residual in such a way as to yield a similar rainflow matrix as the original signal.

Reconstruction is performed in such a way that fatigue cycles are reinserted into the residual in order of their respective amplitudes, with largest amplitudes inserted first. Randomness is introduced into the load reconstruction process by first identifying all of the 'allowable' locations for reinsertion of the current load cycle under consideration, and then sampling from a distribution function to randomly select the insertion location. After insertion, the cycle is deleted from the rainflow matrix, and the cycle with the next largest amplitude is considered. This process is repeated until the rainflow matrix is empty and all cycles have been reinserted into the residual. Numerous random sequences can be generated in this manner, and used to quantify the effect of load sequence on fatigue life prediction.

Assuming a fully populated rainflow matrix is available, an algorithm can be implemented to reproduce a new turning point sequence, whose rainflow counting result is identical to that obtained from the original spectrum. Due to the fact that inserting a turning point pair (max-min or min-max pair) does not affect the possibility of inserting

any pair of equal or smaller amplitude, the reconstruction algorithm starts by selecting the largest cycle first. The size of any cycle pair is indicated within the rainflow matrix construction by its relative distance from the central diagonal, hence, small cycles are found near the main diagonal while larger ones are farther away. Cycle counts along the same sub-diagonal indicate the same amplitude. Once the largest cycle is inserted, the next largest amplitude cycle is identified and inserted. For illustration purposes, *Figure 32* shows a simple 5x5 rainflow matrix configuration with the relative order of cycle insertion indicated within each cell.

| FROM \ TO | | | | | |
|---|---|---|---|---|---|
| | | (17) | (10) | (5) | (2) |
| | (13) | | (18) | (11) | (6) |
| | (7) | (14) | | (19) | (12) |
| | (3) | (8) | (15) | | (20) |
| | (1) | (4) | (9) | (16) | |

***Figure 32:*** *Relative order for cycles contained in 5x5 rainflow matrix*

For each load cycle to be inserted, allowable locations for reinsertion are identified using the inverse rules for cycle extraction under the rainflow counting algorithm [112]. The reinsertion rules are as follows:

If the cycle that is to be inserted is ordered max-min (i.e. in the lower triangle of the rainflow matrix), then it can be placed anywhere within the turning point sequence provided:

1. If the receiving cycle is ordered min-max (row # < column #), then receiving row must be less than or equal to the inserting column, and the receiving column must be greater than or equal to the inserting row
2. If the receiving cycle is ordered max-min (row # > column #), then the receiving row must be greater than or equal to the inserting row, and the receiving column must be less than or equal to the inserting column

Similarly, if the cycle that is to be inserted is ordered min-max (i.e. in the upper triangle of the rainflow matrix), then it can be placed anywhere within the turning point sequence provided:

3. If the receiving cycle is ordered max-min (row # > column #), then receiving row must be greater than or equal to the inserting column, and the receiving column must be less than or equal to the inserting row
4. If the receiving cycle is ordered min-max (row # < column #), then the receiving row must be less than or equal to the inserting row, and the receiving column must be greater than or equal to the inserting column

Additionally, the reconstruction must alternate between local minimum and maximum values, i.e. maintain a turning point sequence. These rules ensure that the inserting cycle is smaller in amplitude than the receiving cycle and that all cycles within the rainflow matrix are guaranteed to have at least one feasible insertion location. As a result, the newly constructed load history is guaranteed to have the identical rainflow count as that obtained from the original history.

*Markov Chain Stochastic Load Reconstruction*

Stochastic load reconstruction using the Markov chain method is simple and straightforward. The reconstruction technique utilizes both the transition probabilities contained within the Markov transition probability matrix as well as random number generators. First, the transition probabilities contained within each row within the upper diagonal of the transition probability matrix given in Eqn. (21) are converted to cumulative density functions. Since the Markov transition matrix is composed of $n$ discrete load levels (as detailed in Section 2.4 and shown in Eqn. (19)), the cumulative distribution function for any load transition from level $i$ can be calculated by the summation of the individual transition probabilities. To maintain the turning point sequence, i.e. maintain minimum→maximum→minimum order, the cumulative discrete distribution function can be calculated as:

$$F(x) = P(X \le x) = \begin{cases} \sum_{j=i+1}^{n} p_{i,j} & i < j \\ \sum_{j=1}^{i-1} p_{i,j} & i > j \end{cases} \qquad (27)$$

Assume an initial load minimum at state $i$ is known. Stochastic simulation of the subsequent load state $j$ can be performed through the following steps

1. Calculate the CMF along row $i$ using the transition probability information above the main diagonal
2. Generate a uniform random number, $x$, within the bounds [0,1]
3. Compare the random number, $x$, to the CMF contained within each level $j$
4. Select the new load level $j$ for which $x$ is $\geq CMF_{j-1}$ and $\leq CMF_j$ and add to turning point history

5. Set $i = j$ and repeat steps 1→4

For the purpose of illustrating the applicability of the reconstruction methods outlined within this section, the scaled helicopter combat maneuver loading history as presented in Khosrovaneh [114] and shown in *Figure 33*, is presented with numerical reconstruction using both the rainflow and Markov chain stochastic methods. The reconstructed load histories using the rainflow technique are seen in *Figure 34* and closely resemble the original load sequence by retaining major sequence trends and load magnitudes.

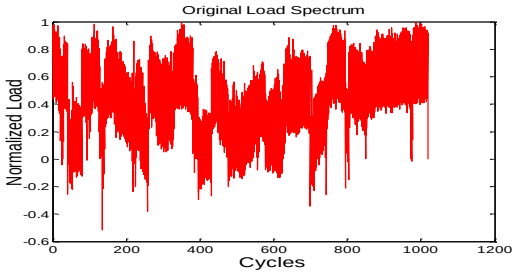


***Figure 33:*** *Original helicopter load spectrum*

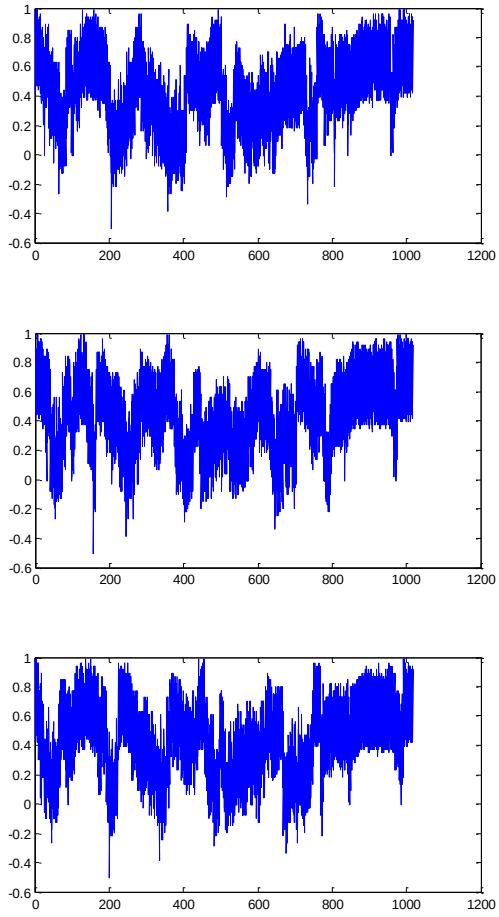


***Figure 34:*** *Three reconstructed helicopter load spectra using the rainflow method*

Similarly, load reconstruction can be performed for the same helicopter spectrum using the Markov method. Two simulated load histories obtained using this method can be seen in *Figure 35*.

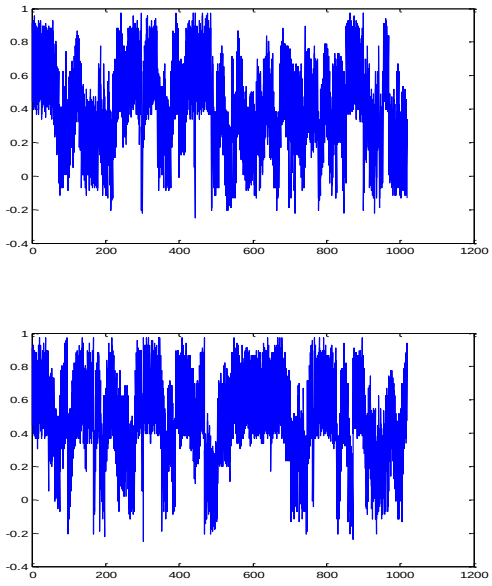


***Figure 35:*** *Reconstructed helicopter load spectra using the Markov transition method*

As can be seen within *Figure 35*, the Markov method appears to be capable of stochastic reconstruction of variable amplitude load histories, however, the newly constructed loads appear to be slightly more randomly structured than those histories constructed using the rainflow methods. This is evident by looking at the major trend contained within the original load history (*Figure 33*) between approximately the 400 and 1000 cycle. An overall positive trend is observed in both the original spectrum as well as the reconstructed rainflow spectra. Both of the reconstructions using the Markov method failure to capture this major trend, and appear to have a more stationary random behavior than the original data set. However, the simulated load history using the Markov method

still retains the same loading transition probability structure as that of the original history, and therefore remains a viable option for meaningful stochastic simulation of variable amplitude load histories.

It should be noted that both of these reconstruction methods assume that the original spectrum contains all relevant loading information and is representative of a typical load spectrum experienced by the component. This is an important distinction to make since all reconstructions are based on the original signal, and do not currently include extreme usage or load extrapolation methods. If desired, these extreme loading conditions can be adapted from regular use spectrum data using available methods, but should be performed prior to load quantification techniques such that the quantified history is representative of the use condition under consideration.

## 3.7 Fatigue Crack Growth Modeling

As discussed previously in Chapter 2, crack growth analysis can be performed using any number of published crack growth laws or crack growth rate representations, in which the crack extension, $da/dN$, for the current load step is calculated as some function of stress intensity factor range, $\Delta K$. For variable amplitude loading, load sequence effects can be significant, in which the order of the applied loading affects crack growth rate and component life prediction. Theses load sequence effects can be addressed through the use of crack growth retardation models such as those proposed by Wheeler [115], and Willenborg [116] which are available in the literature.

Within this research, the fatigue crack growth rate is modeled using the modified Paris fatigue crack growth law, as initially presented in Eqn. (9), along with Wheeler's crack retardation model to include load sequence effects given by Eqn. (28).

$$\frac{da}{dN} = \phi^r C(\Delta K)^m \left(1 - \frac{\Delta K_{th}}{\Delta K}\right)^p \qquad (28)$$

In Eqn. (28), $\varphi^r$ refers to the retardation parameter, and is equal to unity if $a_i + r_{p,i} > a_{OL} + r_{p,OL}$ where $a_{OL}$ is the crack length at which the overload is applied, $a_i$ is the current crack length, $r_{p,OL}$ is the size of the plastic zone produced by the overload at $a_{OL}$, and $r_{p,i}$ is the size of the plastic zone produced at the current crack length $a_i$. Else, $\varphi^r$ is calculated as shown in Eqn. (29)

$$\phi^r = \left(\frac{r_{pi}}{\left(a_{OL} + r_{p,OL} - a_i\right)}\right)^{\lambda} \qquad (29)$$

where $\lambda$ is the curve fitting parameter for the original Wheeler model termed the shaping exponent. Sheu et al. [117] and Song et al. [118] observed that crack growth retardation actually takes place within an effective plastic zone. Hence the size of the plastic zone can be calculated in terms of the applied stress intensity factor ($K$) and yield strength ($\sigma$) as:

$$r_p = \alpha\left(\frac{K}{\sigma}\right)^2 \qquad (30)$$

In Eqn. (30), $\alpha$ is referred to as the effective plastic zone size constant which is calculated experimentally [119]. Immediately following the overload, the retardation parameter $\varphi^r < 1$. As the crack growths through the overload plastic zone, $\varphi^r$ increases

monotonically to a value of 1, at which point the crack is assumed to have grown out of the influence of the overload, or until another overload is applied. The retardation parameter, $\varphi^r$, is required to be less than or equal to 1.

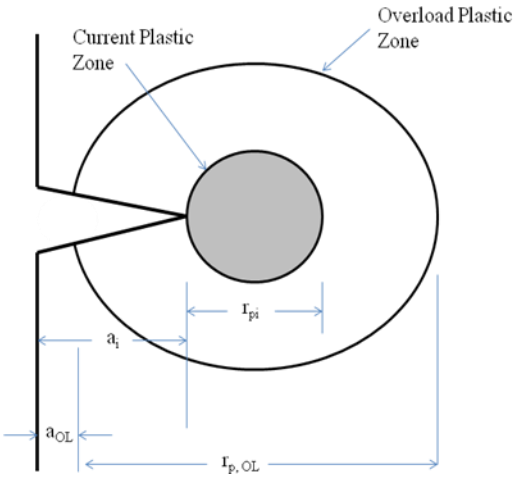


***Figure 36:*** *Schematic of crack front showing Wheeler model parameters for plastic zone based retardation correction*

The expressions in Eqn. (29) and Eqn. (30) can be combined with Eqn. (28) and used to calculate the crack growth as a function of number of cycles. By integrating the expression in Eqn. (28), the number of cycles ($N$) to reach a particular crack size $a_N$ can be calculated as shown in Eqn. (31).

$$N = \int dN = \int \frac{1}{\left( \phi^r C(\Delta K)^n \left( \frac{1 - \Delta K_{th}}{\Delta K} \right)^m \right)} da \qquad (31)$$

For structures with complicated geometry and loading conditions, the integral in *Eqn. (31)* is to be evaluated cycle by cycle, calculating the stress intensity factor in each

cycle of the crack growth analysis. Since the stress intensity factor varies along the periphery of the crack front, so too will the predicted crack growth rate.

Within this study, the stress intensity factor for a planar crack will be calculated at two points along the crack front; at the crack tip at the surface and at the crack tip at the depth (semi-major and semi-minor axis locations). This modeling approach allows for initially semi-circular cracks to develop into semi-elliptical cracks. For the planar crack growth analysis procedure, the crack growth direction remains in-plane with the initial crack orientation.

## 3.8 Summary

This chapter presented various methods which, when used in combination, enable efficient probabilistic fatigue crack growth analysis of planar, semi-elliptical surface cracks under multiaxial, variable amplitude loading conditions. Several different topics were covered including the statistical representation of the initial flaw size using EIFS concepts, efficient stress intensity factor determination using FEA and surrogate modeling techniques, stochastic load representation, and crack growth modeling.

The methodology incorporates some key features which enable efficient probabilistic fatigue crack growth analysis considering multiple sources of uncertainty. One key improvement over previous research includes the statistical representation of the initial crack size by sampling the statistical distributions of material properties (threshold stress intensity factor and fatigue limit). The EIFS concept enables the use of well defined, long crack growth modeling which overcomes the limitations associated with

small crack growth modeling and provides a physics-based approach for EIFS formulation. Another key contribution is the development of a new modeling construct for fatigue crack growth analysis which allows for accurate and efficient component stress analysis and stress intensity factor determination using finite element models and surrogate modeling techniques. The Gaussian process interpolation response surface is used to replace the computationally expensive hierarchical finite element analysis and provides quick and accurate stress intensity factor solutions for any combination of crack sizes, shapes, and loading parameters that are within the design space, without the need for constant remeshing at the crack front. A new method is implemented to determine which input variable combinations should be evaluated within the FEA by identifying regions within the design space which are not well characterized by the current model. Two methods for variable amplitude stochastic load reconstruction are also developed for use within the cyclic fatigue crack growth analysis in order to consider the uncertainty in load sequence which may result from different use conditions. Both methods appear to be capable of regenerating stochastic load realizations based on the statistical characterization of the original load sequence.

The uncertainty quantification techniques presented in Chapter 2 can be used with the proposed framework developed in this chapter by implementing a sampling based strategy within a Monte Carlo framework. Chapter 4 will investigate the additional uncertainties introduced by the numerical methods introduced in this chapter and will develop suitable methods for quantifying and incorporating these additional uncertainties within the overall component fatigue life prediction.

# CHAPTER IV

# UNCERTAINTY QUANTIFICATION IN PLANAR CRACK GROWTH ANALYSIS

## 4.1 Introduction

As our dependence upon both numerical and finite element models increases for stress intensity factor calculation and fatigue life estimation, it is important that we acknowledge that modeling error exists in each model used. Contained within each model, be it numerical or some other form, simplifications and assumptions are made in order to enable analysis of a real system by means of the model. Therefore, some errors will exist in the model predictions when compared with reality. By improving the resolution or complexity of the models and limiting the number of simplifications and assumptions contained within them, it is possible to reduce model error, but at the expense of computational efficiency.

The use of various numerical simulation models for the analysis of complex system performance incorporates many approximations and assumptions which result in errors in model predictions. Before higher system level analysis can be performed, it is first necessary to evaluate the accuracy of the simulation model itself in order to accurately assess and quantify model errors. Model errors can generally be categorized into numerical solution errors and model form errors [120] and each type may be significant.

Model uncertainty typically begins at the conceptual modeling stage, due to inadequate understanding, information, or assumptions made about the actual physical phenomenon [121]. These errors become quantifiable at the mathematical modeling stage, when a mathematical model is chosen to represent the physical process of interest. At this stage, model form error exists (discrepancy between the mathematical model and the physical reality) as a result of the incorrect or inexact mathematical representation of the true process, improper selection of input parameters and values, and other assumptions.

Additional errors can occur in the form of numerical solution errors that can occur as a result of data error, discretization error, and measurement error. Numerical error can result from finite element discretization (finite mesh size), convergence tolerances, and truncation (from response surface methods) [121]. A general schematic of sources of errors that occur during modeling can be seen in *Figure 37*.

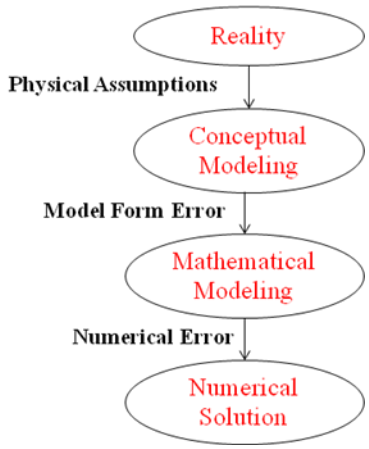


**Figure 37:** *Schematic showing sources of error during various stages of modeling and simulation*

All of these different sources of error contribute to the overall model error. Typically these errors combine in a nonlinear form that is impossible to derive explicitly. However, several methods exist to try to estimate the different types of errors that may exist within the model prediction. The true value can be assumed to be equal to the observed test result plus the experimental error as given by the expression

$$y_{true} = y_{obs} + \varepsilon_{\exp} \tag{32}$$

where $y_{true}$ is the true value, $y_{obs}$ is the experimental observation, and $\varepsilon_{exp}$ is the error in the experimental observation and generally consists of both systematic and random error [122]. It can then be stated that the following relation exists

$$y_{obs} + \varepsilon_{\exp} = y_{pred} + \varepsilon_{mf} + \varepsilon_{num} \tag{33}$$

where $y_{pred}$ is the model prediction, $\varepsilon_{mf}$ is model form error, and $\varepsilon_{num}$ is numerical errors. Several methods will be examined and investigated to determine the best way to estimate the various sources of model error. The error in experimental error, $\varepsilon_{exp}$, may be estimated from repeated observations and experimental measurements, if available, or may need to be estimated based on expert opinion and data availability.

If multiple models exist, as is the case when deciding between which crack growth model to use (i.e. Walker vs. Forman vs. Forman-Newman-de Koning models), Bayesian model averaging (BMA) can be implemented to reduce the model form uncertainty and help with selection of the most relevant model [123] and model form errors, $\varepsilon_{mf}$, can be evaluated using sensitivity analysis. Additionally, the statistics of numerical errors, $\varepsilon_{num}$, within the finite element model may be estimated by using the distribution of model outputs at both course and fine element meshes [121].

Although there may be different types of errors existing throughout the modeling process, some may be more relevant and significant than others. This chapter will present methods for uncertainty quantification of model outputs from the primary models used in fatigue crack propagation analysis. Model errors will be evaluated and the results of these assessments will be systematically included within the overall component reliability framework.

## 4.2 Finite Element Discretization Error

Theoretically, an infinitesimally small mesh size will lead to the exact solutions but this is difficult to implement in practice. Hence, finite element analyses are carried at a particular mesh size and the error in the solution, caused due to discretization needs to be quantified. To reduce the finite element modeling error and due to the stress singularity near the crack front, a very high-resolution model (i.e., very fine mesh) is desired. However, the fatigue crack propagation problem usually spans different length scales from micro-level to macro-level, and the requirement for a high resolution model at all levels makes the analysis extremely time consuming and computationally demanding.

Several methodologies have been proposed to calculate the stress (or stress intensity factor) efficiently and accurately, such as Automated, Global, Intermediate, Local Evaluation (AGILE) method by Chen and Le [124]. The key idea is to break down the problem into several smaller scale analyses. In each stage (global, intermediate, local), a different resolution can be used to reduce the overall computational cost. This

type of approach is proven to provide efficient and effective solutions for relatively small cracks in highly complex structures as compared with other available methods. This hierarchical method has been demonstrated to offer substantial improvement in computational efficiency for RCDT analysis [125]. Liu and Mahadevan [126] proposed a similar computational methodology for fatigue crack propagation analysis and applied the methodology to fatigue cracking in railroad wheels. Similar to AGILE, the problem is broken down to hierarchical stages: Full-model, Sub-model and Local crack model (FSL).

The results obtained from any finite element analysis are dependent on the mesh density used with finer density models producing the most accurate results. If a coarse meshed model is used in place of highly refined meshed model, in order to improve computational efficiency, what errors are introduced into the solution? Since a two level model is used within this research, discretization is performed at two distinct length scales; the full component model and the cracked sub model. Therefore, it is possible that the level of discretization used at both the full model level and the sub model level will introduce some level of modeling error in the solution. First, in order to determine the effect the full model discretization had on the overall solution, the sub model mesh density was held constant while the full model mesh density was refined. Results could then be analyzed using the Richardson extrapolation technique as described within the next section. After this analysis was performed, the full model mesh density was held constant while the sub model mesh was refined. The analysis was again performed to determine the errors introduced by the sub model discretization. By using this approach, it is possible to identify and quantify the magnitude of the modeling errors introduced at

each level of the modeling process and include these errors within future fatigue crack growth analysis.

Several methods are available in literature for discretization error assessment but many of them quantify some surrogate measure of error to facilitate adaptive mesh refinement. The Richardson extrapolation (RE) method has been found to come closest to quantifying the actual discretization error and this method has been extended from Richards original formulation [127] to stochastic finite element analysis by Rebba [120]. It should be noted that the use of Richardson extrapolation to calculate discretization error requires the model solution to be convergent and the domain to be discretized uniformly [120]. Sometimes, in the case of coarse models, the assumption of monotone truncation error convergence is not valid.

In the Richardson extrapolation method, the discretization error due to grid size, for a coarse mesh is given by Eqn.(34)

$$\varepsilon_h = \left( \frac{f_1 - f_2}{r^P - 1} \right) \qquad (34)$$

In Eqn. (34) $f_1$ and $f_2$ are solutions for a coarse mesh and a fine mesh respectively. If the corresponding mesh sizes were denoted by $h_1$ and $h_2$, then the grid refinement ratio, denoted by $r$ is calculated as $h_2/h_1$. The order of convergence of $p$ is calculated as:

$$p = \frac{\log\left( \frac{f_3 - f_2}{f_2 - f_1} \right)}{\log(r)} \qquad (35)$$

Where $f_3$ represents the solution for a coarse mesh of size $h_3$, with the same grid refinement ratio, i.e. $r = h_3/h_2$.

The estimated discretization error will not be accurate if even the finest mesh used in an analysis is not fine enough [121]. For this reason, initial convergence studies should be performed to ensure that solution convergence is obtained from the model. The Richardson extrapolation technique also requires that asymptotic convergence of the finite element solution is observed when the mesh size is reduced, i.e. y1,y2,y3 in Eqn. (35) should either progressively decrease or increase [128].

When using a global-local hierarchical finite element approach, it is necessary to perform the Richardson Extrapolation technique on both the full model and sub model in order to accurately represent the overall discretization error introduced within the modeling process. As a result, finite element solutions were needed for 3 different mesh densities within the full model while the sub model refinement was held constant, and then solutions were needed for 3 different mesh densities within the sub model while the full model refinement was held constant. By analyzing the solutions obtained from the different mesh densities, modeling error could be estimated for each crack configuration and loading condition.

The solutions $f_1$, $f_2$, $f_3$ are dependent on the inputs (loading, current crack size, aspect ratio and angle of orientation) to the finite element analysis and hence the error estimates are also functions of these input variables. For each set of inputs, a corresponding error is calculated and this error is added to the (coarse mesh) solution from finite element analysis to calculate the true solution.

A series of finite element analyses were performed for various model input combinations. For each model input combination, the model error resulting from the meshing of the finite element model was evaluated using the Richardson extrapolation

technique. This analysis required three levels of discretization within the full model in order to determine the rate of convergence and ultimately quantify the discretization error associated with the coarsest mesh density. After performing the error analysis, it was found that absolute value of error caused by the coarse mesh in the full model ranged from 0.58% up to 3.53% depending on the crack configuration (length and aspect ratio) and loading condition considered. A histogram of the model error is shown in *Figure 38*. As indicated within the figure, it was determined that the distribution of the model error fit the lognormal distribution function well, with a mean value of 2.144 and a variance of 0.154.

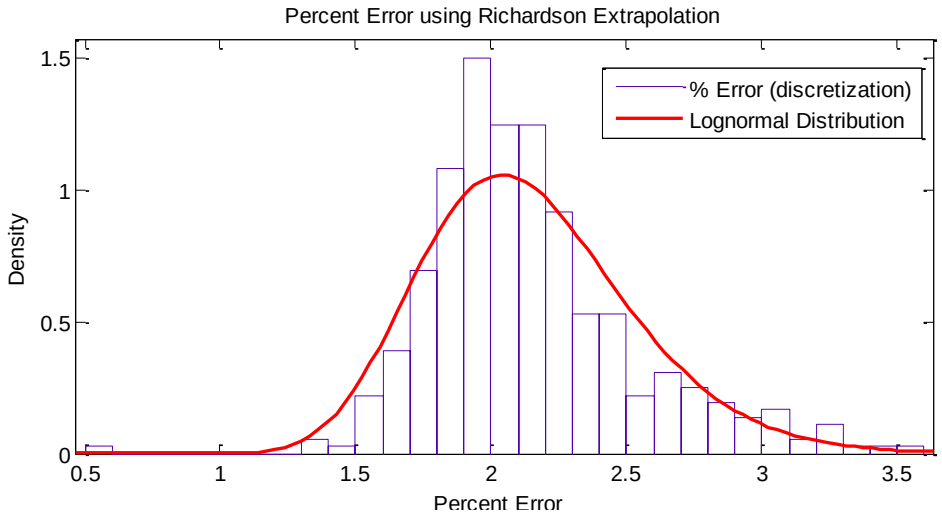


***Figure 38:*** *Histogram of Percent Errors found during full-model refinement analysis with results compared to lognormal distribution*

Similar analysis can be performed to evaluate the discretization error caused by the mesh choice within the sub model. In order to determine its effect on the overall stress intensity factor solution, the full model mesh size is held constant while the mesh density within the sub model is varied. For the sub model analysis, it is important to

accurately model the crack front with singular elements of adequate shape and size in order to capture the stress state within the region, as more fully discussed in Section 3.3. As a result, some limitations on the mesh density are necessary to ensure basic solution convergence and non-irregular element shapes. After performing the Richardson extrapolation analysis on the results obtained from the sub model refinement analysis, it is found that the error caused by using even the coarsest mesh is relatively insignificant, less than 1% for all cases. This is not a significant source of error for the purposes of component life prediction and the discretization errors within the submodel are not included in the overall probabilistic crack growth analysis.

It is not surprising that the discretization error evaluated for the submodel is determined to be insignificant. This result can be explained by comparing the relative size and mesh densities of the sub model when compared to the full model. The overall size of the sub model is very small compared to that of the full model. As a result, the relatively large elements in the full model are replaced by thousands of smaller elements within the sub model. In order to maintain minimum element shape tolerances and provide suitable mesh configurations for stress intensity factor calculations, even the coarsest mesh density in the sub model analysis maintained a relative high mesh density and provided accurate solutions.

The Richardson extrapolation technique has been shown to be a suitable way to evaluate the inherent modeling errors that result from using a coarse mesh within a finite element model, and has been applied to a hierarchical rotorcraft mast demonstration problem. The method requires evaluating the model for three distinct mesh densities to determine solution convergence rates. It should be noted that the discretization error

obtained using this method is a discrete error (as opposed to random error) that arises due to the specific geometric configuration of the problem under consideration. As a result, the modeling errors determined through this analysis should be directly added to the corresponding stress intensity factors to provide adjusted solutions that more closely match the true solution (void of any discretization errors). These "adjusted" model solutions can be used to train the surrogate model as initially described in Section 4.5 and analyzed within the next section. The histogram and distribution functions shown in *Figure 38* are included only to provide an overall summary of the individual results obtained in this study and are not meant to (nor should they be) used for sampling purposes in subsequent model evaluations.

## 4.3 Surrogate Model Error

The use of an efficient surrogate model allows for efficient cycle by cycle fatigue crack growth evaluation for components subjected to variable amplitude multiaxial loading by eliminating the computational burden that otherwise exists for calculation of the stress intensity factor at the crack front. However, the surrogate model is itself an approximation method to an already uncertain model, thus its use introduces another uncertainty within the modeling framework that needs to be addressed.

The successful use of any surrogate modeling technique depends on the ability of the surrogate to accurately match the underlying function shape, and a successful method for identifying suitable data to most effectively train the surrogate. As discussed in Section 3.5, the Gaussian process model is capable of accurately modeling the non-linear

relationship that exists between the input variables and output variables within the fatigue crack growth modeling application. Therefore, the primary question is, if only limited training points can be generated, which set of training points should be used to most effectively train the surrogate model? The answer to the question depends on what criteria (maximum error, average error, maximum variance, etc) is used to evaluate the effectiveness of training, and several methods have been developed which approach this problem from different perspectives. Three main methods offered within the literature for training point selection are the traditional design of experiments [129], model error minimization [130], and model variance minimization [106]. Within this research, traditional DOE methods are first used to select a small set of initial training points, followed by an iterative model variance minimization method using the Greedy point algorithm. Details of the model error assessment resulting from the Gaussian Process surrogate model is discussed below.

As detailed in Section 3.5, one of the advantages of using the Gaussian Process surrogate modeling technique is that the method has the ability to provide a direct representation of the uncertainty associated with its interpolative approximation. The uncertainty in the model prediction is given by the model variance. The Greedy Point algorithm can utilize the model variances across the entire design space to determine the precise location which proves to have the largest model uncertainty (variance). The next training point is set to be the combination of input variable values corresponding to that particular location within the design space, the full FEA is evaluated to provide the "correct" solution and is used to update the surrogate model. By repeating the Greedy Point algorithm iteratively, training points can be identified that minimize the variance of

the surrogate model. This training point selection method eliminates the subjectivity associated with typical design of experiments methods which use a pre-determined fixed set of training points, and ensures that the surrogate model is iteratively improved by adding new information that most efficiently reduces the maximum uncertainty in model predictions.

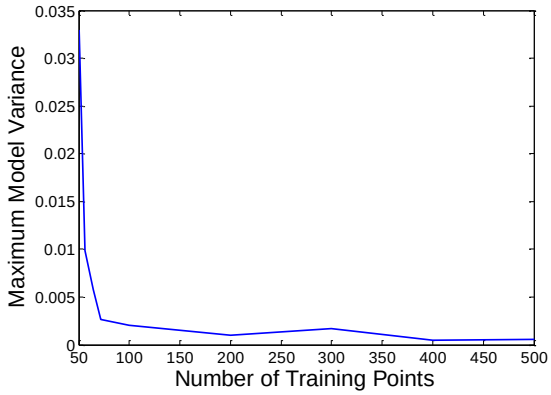


***Figure 39:*** *Maximum GP model variance vs. # of Training points used*

***Table 5:*** *Number of Training Points used in surrogate vs. Maximum Model Variance*

| # of Training Points | Max. Model Variance |
|---|---|
| 16 | 54.787240 |
| 24 | 1.145149 |
| 32 | 0.065271 |
| 40 | 0.040791 |
| 48 | 0.040660 |
| 56 | 0.009858 |
| 64 | 0.005758 |
| 72 | 0.002637 |
| 100 | 0.002064 |
| 200 | 0.000975 |
| 300 | 0.001683 |
| 400 | 0.000511 |
| 500 | 0.000542 |

Since the surrogate model is built using an iterative process, it is easy to track the maximum model variance for different numbers of training points used. The maximum model variance (model prediction uncertainty) is observed to decrease as additional training points are used to train the surrogate. This trend can be clearly seen within *Figure 39* and *Table 5* as the maximum model variance within the surrogate is shown as a function of number of training points used. Since the model variance at any untested location $x^*$ is based on its relative proximity to available training points as well as the correlation structure between them, the overall variance is expected to decrease with increasing training points within the design space.

The Greedy Point method which uses a model variance minimization technique for training point selection has been compared to a recently proposed method which uses a hierarchical decomposition of the approximation error for training point selection method [130]. Comparisons of model predictions at different levels of training for the fatigue analysis application described herein show the model variance and model error minimization techniques to have very similar performance in terms of overall solution accuracy.

For demonstration purposes, the Gaussian process model shown in *Figure 39* was trained for an overly large number of training points, as reflected by the small values of model variance near the bottom of *Table 5*, resulting in a very small value of surrogate model uncertainty. However, in practical applications where only limited finite element runs may be possible, the associated surrogate model prediction uncertainty at different locations within the design space may be more significant. The Gaussian process model provides an easy and convenient method for quantifying the uncertainty in model

predictions when limited training points are available. Under these circumstances, model predictions made using the surrogate model can be treated as Gaussian random variables with closed form solutions for their mean values given by Eqn. (25) and variances given by Eqn. (26). In doing so, the associated model uncertainty can be easily included within the fatigue crack growth modeling framework.

## 4.4 Methodology to Incorporate Uncertainty in Final Prediction

The physical modeling process itself introduces many additional sources of uncertainty that need to be accounted for in addition to the natural variability that is inherent in physical processes. This chapter identified several uncertainties associated with different types of numerical models that are typically used in fatigue crack growth analysis. It is important that each of these uncertainties is quantified and included within the stochastic fatigue crack growth modeling framework for component life prediction. A systematic and rigorous probabilistic component life assessment can be performed by combining the various sources of uncertainty detailed in Chapter 2, the modeling errors discussed within this chapter, and the overall fatigue crack growth framework developed in Chapter 3. Each input variable and modeling technique introduces additional uncertainty that must be carefully combined within the analysis to provide a meaningful and useful component life prediction under uncertainty.

The overall objective of a probabilistic damage tolerance analysis is to determine the probability of component failure over the lifetime of the component. A sampling methodology is used within this research to include many different sources of uncertainty

including physical variability, data uncertainty, and modeling errors. The approach enables the evaluation of the distribution of the amount of time, $t$, for an initial flaw to grow to a critical size, or conversely, the distribution of crack sizes at any time $t$ . This type of information can be used by fleet managers and maintenance personnel for inspection planning and decision making. The various steps in this procedure are outlined here.

I. Initial uncertainty quantification is performed to determine statistical distributions of model parameters and input values including: material properties, crack growth rate model parameters, and loading.

II. Component stress analysis is completed to identify critical crack location and orientation

III. EIFS distribution is constructed from distributions of material properties (obtained in step I) to statistically characterize the initial flaw size

IV. Finite element analysis is performed to provide necessary training points for the Gaussian process surrogate model. Discretization error is evaluated and FEA results using the coarse model are adjusted accordingly.

V. Updated FEA results are used for construction of initial GP model, and the Greedy point algorithm is implemented to identify additional training points until a satisfactory level of performance is reached

VI. The fully trained GP model is used exclusively for calculating the stress intensity factor as a function of crack size, loading, aspect ratio and angle of orientation.

VII. A realization of a variable amplitude loading history is reconstructed using either the rainflow or Markov reconstruction techniques.

VIII. A single realization of EIFS is sampled from its statistical distribution as calculated based on material properties.

IX. For the current load cycle (obtained from history generated in Step VII), the stress intensity factor is sampled from the GP model (where the mean and variance are accounted for in model prediction) and the corresponding stress intensity factor is used within a crack growth rate model to determine crack extension magnitude.

X. Cycle-by-cycle crack growth is evaluated at both the semi-major and semi-minor locations along the crack front, thus allowing for semi-elliptical to semi-elliptical crack shape development. Crack growth rate modeling is randomized by using either the percentile or partial correlation approach detailed in Section 2.3. The crack front is grown in plane and Steps IX and X are repeated until a critical crack length is obtained.

XI. Steps VII → X are repeated within a Monte Carlo scheme

The straightforward sampling procedure in combination with an efficient cycle-by-cycle fatigue crack growth evaluation enables a multiple realization of fatigue crack growth analyses to be performed quickly and without the need for much user intervention. The analysis method enables the determination of statistical characterization of fatigue crack sizes over time. Despite the addition of probabilistic representation of model inputs, the computational efficiency afforded by the modeling framework enables many simulations within the Monte Carlo framework to be performed without significant computational expense.

A numerical example is included to show typical results that are obtained through the use of this method. For this example, the material considered is aluminum alloy 7075-T6. The material properties of the aluminum alloy are included within *Table 6*.

***Table 6:*** *Material Properties of 7075-T6 Aluminum alloy*

| 7075-T6 Aluminum Alloy | | |
|---|---|---|
| | SI Units | US Units |
| Modulus of Elasticity | 71.7 GPa | 10400 Ksi |
| Poisson Ratio | 0.33 | 0.33 |
| Yield Stress | 503 MPa | 73 Ksi |
| Ultimate Stress | 572 MPa | 83 Ksi |

A Monte Carlo based method is used to perform the analysis method outlined above. Typical results obtained within each step have been previously presented within the original sections in which they were presented, and therefore, will not be repeated here. As mentioned previously, the Monte Carlo implementation generates a random realization of each stochastic variable and performs a cyclic fatigue crack growth analysis from an initial size to a final size using either the percentile or partial correlation fatigue crack growth rate representation. The crack growth results obtained from all realizations can then be used to determine the statistics of the fatigue life predictions under uncertainty.

*Figure 40* and *Figure 41* show numerical crack growth modeling results obtained from the stochastic fatigue crack growth analysis procedure using both the percentile and partial correlation crack growth rate modeling approaches. Similar simulation results are obtained using either stochastic crack growth rate representations indicating that the choice in stochastic crack growth rate representation (percentile and partial correlation)

does not have a significant effect on the overall fatigue life prediction. Each method appears to equally represent the scatter in the fatigue crack growth rate data and results in the same overall model prediction when all the other sources of uncertainty are considered. A typical crack profile which results from the planar crack growth analysis is shown in *Figure 42* after many crack growth increments are completed.

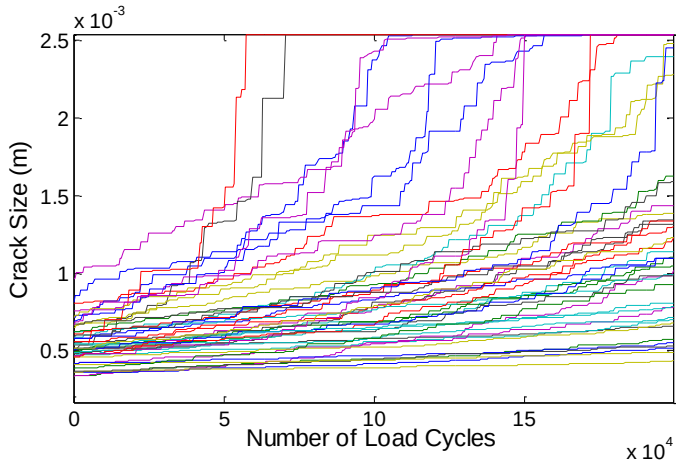


***Figure 40:*** *Plot showing simulated fatigue crack growth curves considering natural variability, information uncertainty, and modeling error*

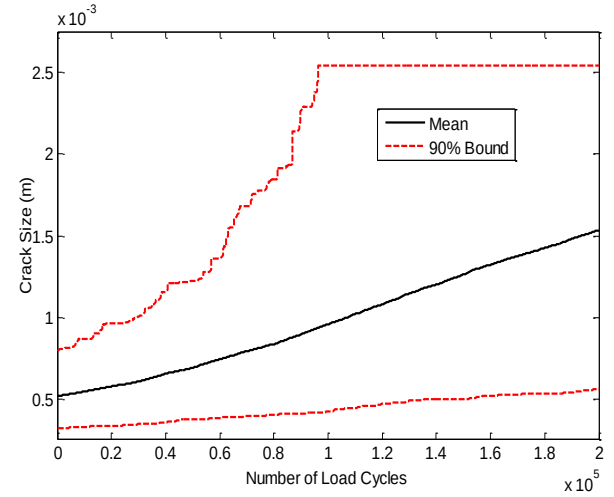


*(a.)*

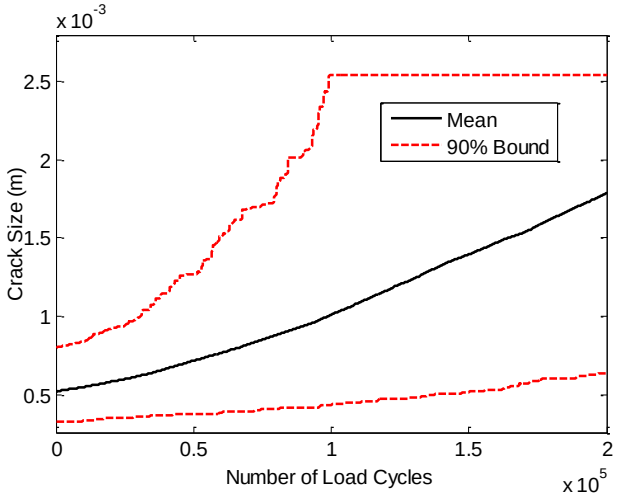


*(b.)*

***Figure 41:*** *Plot showing mean and 90% confidence bounds on component life prediction obtained using the a.) percentile b.) partial correlation crack growth rate representations*

The probabilistic crack growth method not only can provide a mean prediction for component fatigue life, but can also estimate the variance to be expected in life prediction considering uncertainty, as seen in *Figure 41 a)* and *b.)*. One of the key benefits of using the probabilistic based modeling approach is the ability to extract from the simulation results a crack size probability distribution at any given time, *t*, or, conversely the probability distribution of the time necessary for a crack to reach a critical size. These

results can be easily expressed through statistical distributions functions. *Figure 43 a.)* and *b.)* show simulation results with the lognormal probability density function and cumulative density function, respectively, for the number of load cycles necessary for an initial crack to grow to a critical size extracted from the results obtained using the percentile crack growth rate representation. Similar statistical distributions can be evaluated to represent the crack size population after any given number of load cycles.

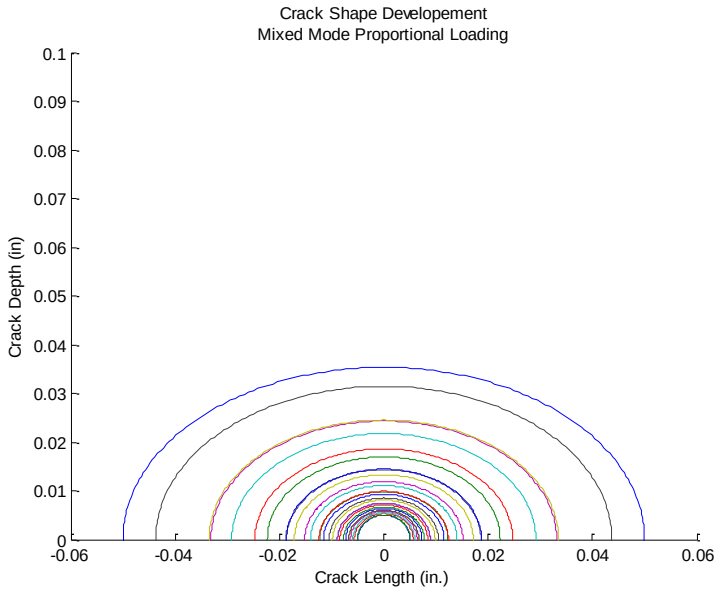


***Figure 42:*** *Typical fatigue crack profile showing crack growth due to fatigue loading*

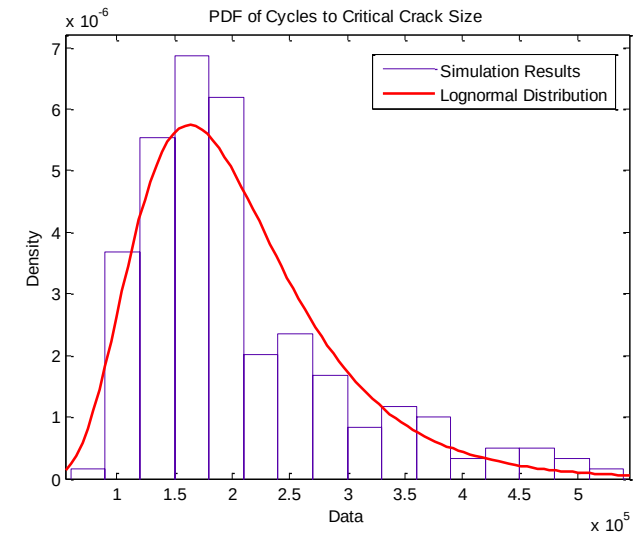


*(a.)*

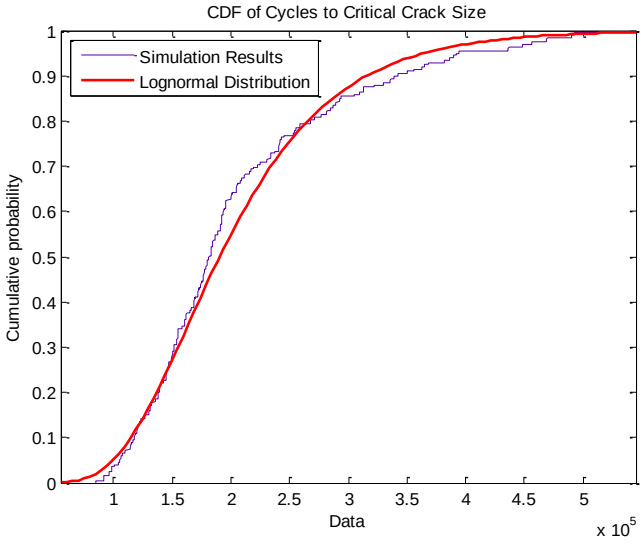


*(b.)*

***Figure 43:*** *a.) PDF and b.) CDF of Lognormal distribution function of number of cycles to reach a critical crack size shown with simulation results*

The use of various models for the analysis of complex system performance incorporates many approximations and assumptions which result in errors in model predictions. This chapter has presented methods to evaluate different types of modeling errors including finite element discretization error and surrogate modeling error and has

demonstrated how uncertainties at all levels of the crack growth modeling approach can be incorporated within an overall probabilistic fatigue life assessment.

Both deterministic and random errors have been addressed within this work and can easily be included within the overall probabilistic crack growth modeling framework. Finite element discretization errors represent deterministic errors that result from the specific mesh densities used within finite element models. Error resulting from using a coarse mesh density is determined using a Richardson extrapolation technique and is a deterministic error should be evaluated and directly applied to the model prediction. Deterministic errors should not be treated using sampling techniques as their effects are directly related to specific configurations. The stress intensity factors evaluated using the Gaussian Process (GP) surrogate model represent uncertain model predictions, which produce random model errors. These types of errors can be included by sampling techniques.

Multiple sources of uncertainty including natural variability, data uncertainty, and modeling errors can be incorporated into the methods developed in previous chapters. The methods for implementation of the developed methodology to a realistic rotorcraft component have been provided within this chapter and executed on the rotorcraft mast demonstration problem. Overall, the fatigue crack growth framework developed in Chapter 3 is capable of performing cycle-by-cycle fatigue crack growth analysis while considering several different sources of uncertainty in model input values and parameters described in Chapter 2 as well as model errors which have been classified in this chapter.

# CHAPTER V

# NON-PLANAR FATIGUE CRACK GROWTH MODELING

## 5.1 Introduction

Damage tolerance based design has increased the necessity for better understanding of fatigue crack growth mechanisms in mechanical components. Traditional applications of fracture mechanics, as well as most experimental testing, have focused on cracks growing under pure mode I conditions. Characterization of fatigue crack growth under Mode I loading conditions using the stress intensity factor range is based on the assumption that the path of the crack is linear and that its plane of growth is normal to the loading axis [131]. Therefore, the crack growth direction remained in plane with the original crack orientation, resulting in planar (non-kinked) cracks even after the occurrence of several crack growth increments. The fatigue crack growth modeling framework developed in Chapter 3 adopted this approach for probabilistic fatigue life prediction under uncertainty.

It is, however, well known that on a microscopic level, cracks seldom propagate in a linear fashion (even under Mode I loading), and on a macroscopic level, cracks in structures are often subjected to mixed-mode conditions, resulting in crack kinking and other non-planar propagation paths. As a result, there is a growing interest in investigating the mechanics and crack growth modeling capabilities associated with the nonlinearities in the crack path. When considering non planar crack growth modeling, it is important to be able to predict and model both the crack extension magnitude and the

crack path direction. Nonlinearities in the crack path have been generally ignored in fatigue life prediction because of the difficulties in incorporating crack meandering effects in estimates of the stress intensity factor range [131], crack extension criteria, and crack model meshing capabilities. In order to try to capture the nonlinear crack extension behavior that has been seen in both experimental results and realistic applications, numerous crack growth direction and extension criteria have been proposed within the literature by different authors over the past few decades. This chapter will investigate the fatigue crack growth modeling capabilities for non-planar fatigue cracks. Additionally, it will provide a suitable method for fatigue crack growth simulation with the goal of investigating the uncertainty in crack path and component life predictions resulting from different criteria for crack extension magnitude and direction.

There are two dominant modes of fatigue crack propagation: tensile and shear dominated crack growth [132]. Tensile dominated crack growth is also sometimes referred to as maximum principal stress dominated, and is the class most often observed in metal fatigue. Under the tensile dominated case, a Mode I crack usually (but not always) tends to propagate in a direction that is perpendicular to the maximum principal tensile stress within the uncracked specimen [133]. The second dominant mode is shear dominated crack propagation (Mode II type), which usually takes place on planes of maximum shear stress and is an important exception to the tendency to Mode I fatigue crack propagation [134]. In metal fatigue, the shear dominated mode of crack propagation is often observed when the crack tip plastic zone becomes large, and is generally applicable to micro cracks that are characterized as stage I cracks in Forsyth's notation [143] (as shown in *Figure 45*). Additionally, a third mode of fatigue crack propagation is

sometimes observed and is called slant crack propagation. This type is another exception to Mode I, and is often observed in thin sheets and is characterized by a transition zone between Mode I and Mode III fatigue growth. A schematic of generalized crack growth under mixed mode loading is shown in *Figure 44*.

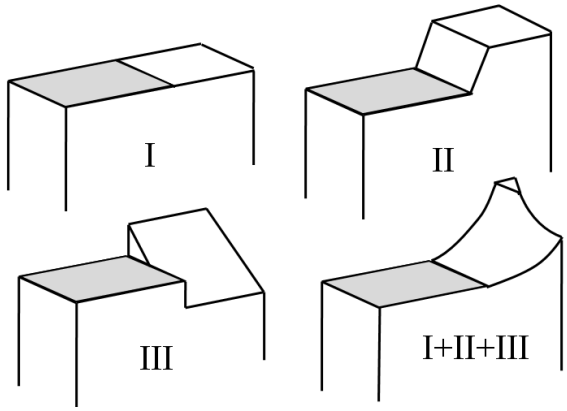


***Figure 44:*** *Schematic showing development of fracture surface for a.) in plane crack opening subjected to mode I; b.) crack kinking under mode II; c.) crack front twisting under mode III; d.) deflected crack for superimposed modes I, II, and III*

In the last four decades there have been substantial advances in the understanding of macroscopic aspects of fatigue crack paths and their prediction [134]. However, at the present state of the art, the factors controlling the path taken by a propagating fatigue crack are not completely understood, and, in general, crack paths are difficult to predict [134]. Under mixed mode loading, the fatigue crack growth rate is typically expressed [134,163] with the same functional relation as that of the uniaxial case where the stress intensity factors in multiple modes are replaced by a single equivalent stress intensity factor range, $\Delta K_{eqv}$.

$$\frac{da}{dN} = f\left(\Delta K_{eqv}\right) \qquad (36)$$

One approach that is commonly seen within the literature is to ignore any nonlinearity in the crack path direction due to the difficulties in incorporating crack meandering effects in estimates of the stress intensity factor range. Fatigue crack path prediction for a planar crack is essentially two dimensional, regardless of whether a single point, two point, or multiple point extension criterion is used. Ultimately, it reduces to making the assumption that crack propagation direction is perpendicular to the current crack front, and calculating crack growth increment (s) using a standard crack growth law, such as one listed in *Table 1*. Many of the existing three-dimensional fracture simulation codes actually fall under this category since only planar crack extension is considered.

Theoretical justifications for a planar crack growth assumption are that local variations in the path of a long fatigue crack are normally overcome during subsequent propagation over a short distance under certain loading conditions [131], and that projection of the initial mixed mode crack onto an appropriate plane can provide an accurate method for estimating SIFs for a kinked crack [135]. Additionally, it has been pointed out by numerous authors that on a macroscopic scale, and under essentially elastic conditions, most fatigue cracks in isotropic metallic materials tend to propagate in Mode I [134], that is, approximately perpendicular to the maximum principal tensile stress. These authors include Borberg [136], Cotterell [137], Knauss [138], Minoshima [139], Parton[140], Pook [133,141], and Vinas-Pich [142]. Under this observation, cracks that are classified to stage II in Forsyth's notation [143] often show crack growth behavior that is confined to a particular plane [143].

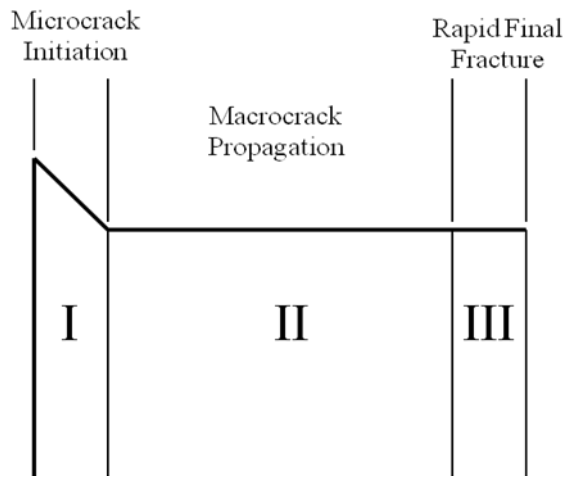


***Figure 45:*** *Forsyth's notation of fatigue crack growth evolution [143]*

Although many commercial software codes can perform accurate stress analysis of cracked structures, most have difficulty in implementing a suitable propagation scheme for non-planar, three-dimensional crack growth. Various three-dimensional fracture simulations have been reported within the literature with emphasis on numerical analysis development [144, 145, 146, 147]. However, most programs do not acknowledge the critical issues of crack representation and automated propagation, which are necessary for efficient implementation on realistic structures [148]. To model an evolving crack efficiently and automatically in a complex three-dimensional structure, one requires two integral components in a simulator: crack representation and crack growth mechanics. Here, crack representation includes the geometry of the cracked body and updating the description to reflect crack growth; which includes both the real geometry and the mathematical representation (i.e. the mesh), and crack growth mechanics refers to stress analysis, extraction of relevant crack growth parameters, and determination of shape, extension, and direction of crack growth [148].

For the case in which the initial fatigue crack is allowed to grow in a non-planar fashion, both crack extension and crack direction model predictions are necessary and lead to an increase in the complexity of the crack shape development and computational modeling considerations. The following section discusses many of the existing non-planar crack growth criteria which have been reported within the literature with particular emphasis on the various theoretical and empirical forms available for the crack kink angle and equivalent stress intensity factor under mixed mode I, II, and III conditions. Section 5.3 provides details of the specific methods which are used for component stress analysis and non-planar crack modeling within this research. The remaining sections of this chapter focus on the challenges associated with surrogate modeling development for non-planar crack growth analysis and a proposed equivalent planar method which links the insight obtained using a more sophisticated non-planar crack growth analysis to the planar crack growth analysis presented in earlier chapters of this dissertation.

## 5.2 Existing Non-Planar Crack Growth Criterion

For the case of mixed mode I + II loading and non-planar crack growth modeling, the most commonly used criterion for tensile crack propagation is the maximum tangential stress (MTS) criterion as proposed by Erdogan and Sih (1963) [149]. The tangential stress, $\sigma_\theta$, near the tip of a crack subjected to mixed I+II mode is expressed by

$$\sigma_\theta = \frac{1}{\sqrt{2\pi r}} \cos\left(\frac{\theta}{2}\right)\left\{K_I \cos^2\left(\frac{\theta}{2}\right) - \left(\frac{3}{2}\right) K_{II} \sin(\theta)\right\} \qquad (37)$$

where the crack deflection angle, $\theta_{\sigma,}$ can be obtained from solving the equations

$$\frac{\partial \sigma_\theta}{\partial \theta}|_{\theta=\theta_0} = 0 \quad \text{and} \quad \frac{\partial^2 \sigma_\theta}{\partial \theta^2}|_{\theta=\theta_0} < 0 \tag{38}$$

which yields the angle, $\theta_\sigma$, at the maximum $\sigma_\theta$ that is obtained from the expression

$$K_I \sin(\theta_\sigma) + K_{II}(3\cos(\theta_\sigma) - 1) = 0 \tag{39}$$

The equivalent SIF for mode I, $\Delta K_{Ieqv}$, for mixed mode cracks is then given by the expression

$$\Delta K_{I,eqv} = \Delta K_I \cos^3(\frac{\theta_\sigma}{2}) - 3\Delta K_{II} \cos^2(\frac{\theta_\sigma}{2}) \sin(\frac{\theta_\sigma}{2}) \tag{40}$$

where $\Delta K_I$, $\Delta K_{II}$ are the mode I and mode II stress intensity factors for the initial crack, and $\theta$ is the crack propagation angle.

Richard [150] later approximated the $\Delta K_{Ieqv}$ expression given by Erdogan and Sih for Mode I+II as

$$\Delta K_{I,eqv} = \frac{\Delta K_I}{2} + \frac{1}{2}\sqrt{\Delta K_I{}^2 + 4(\alpha \Delta K_{II})^2} \approx \frac{\Delta K_I}{2} + \frac{1}{2}\sqrt{\Delta K_I{}^2 + 6\Delta K_{II}{}^2} \tag{41}$$

and also approximated the crack deflection angle by

$$\theta_\sigma = \pm\left[155.5^o \frac{|K_{II}|}{|K_I| + |K_{II}|}\right] - 83.4^o \left[\frac{|K_{II}|}{|K_I| + |K_{II}|}\right]^2 \tag{42}$$

which has been proven to be a good approximation by a large number of experiments [151]. Richard later extended previous approximation functions to be used for crack growth prediction under the general mixed mode I+II+III loading case. The function in Eqn. (42) has been extended to the three dimensional case as follows

$$\theta_\sigma = \pm\left[A\frac{|K_{II}|}{K_I + |K_{II}| + |K_{III}|}\right] - B\left[\frac{|K_{II}|}{K_I + |K_{II}| + |K_{III}|}\right]^2 \tag{43}$$

where $\theta_o<0^o$ for $K_{II}>0$ and $\theta_o>0^o$ for $K_{II}<0$ and $K_I \geq 0$. The equivalent stress intensity factor is then suggested to take the form of

$$K_{eqv} = \frac{K_I}{2} + \frac{1}{2}\sqrt{K_I^2 + 4(\alpha_1 K_{II})^2 + 4(\alpha_2 K_{III})^2} \qquad (44)$$

With $\alpha_1=K_{IC}/K_{IIC}=1.155$ and $\alpha_2=K_{IC}/K_{IIIC}=1.0$, excellent agreement has been observed with that obtained from the $\sigma_1'$ criterion (given in Eqn. (61) ).

Pook [141] made another approximation to the original MTS criterion with the expression

$$\Delta K_{eqv} = \frac{0.83\Delta K_I + \sqrt{0.4489\Delta K_I{}^2 + 3\Delta K_{II}{}^2}}{1.5} \qquad (45)$$

And Yan [152] suggested another functional form for mixed mode I+II loading given by

$$\Delta K_{eqv} = \frac{1}{2}\cos(\frac{\theta_\sigma}{2})\left[\Delta K_I(1+\cos\theta_\sigma) - 3\Delta K_{II}\sin\theta_\sigma\right] \qquad (46)$$

where $\theta_\sigma$ is the crack growth direction obtained from the maximum tangential stress criterion determined through Eqn. (38).

Tanaka [153] proposed the parameter

$$\Delta K_{eqv} = \left[\Delta K_I{}^4 + 8\Delta K_{II}{}^4\right]^{1/4} \qquad (47)$$

which can be extended to the Mode I+II+III case as follows

$$\Delta K_{eqv} = \left[\Delta K_I{}^4 + 8\Delta K_{II}{}^4 + \frac{8\Delta K_{III}{}^4}{(1-\upsilon)}\right]^{1/4} \qquad (48)$$

or, based on the energy release rate criterion for mixed mode I+II,

$$\Delta K_{eqv} = \left[\Delta K_I{}^2 + \Delta K_{II}{}^2\right]^{1/2} \qquad (49)$$

and for the extended to the Mode I+II+III case as

$$\Delta K_{eqv} = \left[\Delta K_I{}^2 + \Delta K_{II}{}^2 + (1+\upsilon)\Delta K_{III}{}^2\right]^{1/2} \qquad (50)$$

The rate of mixed mode crack propagation using any of these criteria is higher than that predicted from $\Delta K_I$ only, and the inclusion of mode II and III stress intensity range is necessary in the crack propagation law [156].

Another criterion that has been used for the tensile crack growth direction is the Local Symmetry (LS) criterion proposed by Kitagawa [154]. The LS criterion assumes that a crack propagates in the direction where the mode II stress intensity factor of a kinked crack is zero, and the stress field is symmetrical with respect to the mode I crack. Additionally, the maximum strain energy release rate criterion proposed by Palaniswamy and Knauss [155] assumes that the crack grows in the direction where the strain energy release rate is the maximum and that the maximum value is a material constant. The crack growth directions predicted by the LS criterion and the maximum strain energy release criterion are generally very close to the direction predicted by the MTS criterion [156].

For shear mode fatigue crack growth, the maximum shear stress (MSS) criterion proposed by Otsuka [157] has been used. The shear stress, $t_{r\theta}$, near the crack tip is given by

$$t_{r\theta} = \frac{1}{\sqrt{2\pi r}}\cos\left(\frac{\theta}{2}\right)\left\{\left(\frac{1}{2}\right)K_I \sin\theta + \left(\frac{1}{2}\right)K_{II}(3\cos\theta - 1)\right\} \qquad (51)$$

where the angle, $\theta_r$, for the maximum shear stress, $t_{r\theta}$, is

$$(3\cos\theta_t - 1)K_I - 2\tan\left(\frac{\theta_t}{2}\right)(3\cos\theta_t + 1)K_{II} = 0 \qquad (52)$$

For fatigue crack propagation, the range of the SIFs is substituted in the above equation, and the equivalent SIF for Mode II, $\Delta K_{IIeqv}$, for mixed mode cracks is given by

$$\Delta K_{IIeqv} = \cos\left(\frac{\theta_t}{2}\right)\left\{\left(\frac{1}{2}\right)\Delta K_I \sin\theta_t + \left(\frac{1}{2}\right)\Delta K_{II}(3\cos\theta_t - 1)\right\} \qquad (53)$$

Pook [158] later approximated the above expression to the simpler form of

$$\frac{\Delta K_{II}}{\Delta K_{IIeqv}} = \left[1 - \left(\frac{\Delta K_I}{2.6\Delta K_{IIeqv}}\right)^2\right]^{1/2} \qquad (54)$$

At low stress levels, the shear growth of fatigue cracks is not stable, and in most cases cracks propagate in the direction predicted by MTS or LS criteria where the propagation mode quickly kinks to make $\Delta K_{II}$=0. At high stresses, however, aluminum alloys show shear-mode crack growth under mode II loading [159]. The rate of shear propagation of fatigue cracks in self-similar manner can be expressed by the equivalent SIF, $\Delta K_{eqv}$, which is a combination of $\Delta K_I$ and $\Delta K_{II}$.

For the mixed mode I+II+III case, Sih [160,161] proposed a popular mixed mode model known as the strain energy density criterion, which is based on the strain energy density around the crack tip. The strain energy density factor, $S$, is given by the expression:

$$S = a_{11}K_I^{\,2} + 2a_{12}K_I K_{II} + a_{22}K_{II}^{\,2} + a_{33}K_{III}^{\,2} \qquad (55)$$

where the coefficients under plane strain are

$$a_{11} = \left(\frac{1}{16\pi\mu\cos\psi}\right)\left[(3 - 4\upsilon - \cos\theta)(1 + \cos\theta)\right] \qquad (56\text{ a.})$$

$$a_{12} = \left(\frac{1}{8\pi\mu\cos\psi}\right)\left[(\sin\theta\{\cos\theta - 1 + 2\upsilon)\}\right] \qquad (56\text{ b.})$$

$$a_{22} = \left(\frac{1+\upsilon}{\pi 8E}\right)\left[4(1-\upsilon)(1-\cos\theta) + (1+\cos\theta)(3\cos\theta - 1)\right] \qquad (56\text{ c.})$$

$$a_{33} = \left(\frac{1}{4\pi\mu\cos\psi}\right) \qquad (56\text{ d.})$$

where $\mu$ is the shear modulus of elasticity and $\upsilon$ is Poisson's ratio. The crack angles, $\theta$ and $\psi$ are derived by minimizing $S$

$$\left.\frac{\partial S}{\partial\theta}\right|_{\theta=\theta o} = 0 \quad \text{and} \quad \left.\frac{\partial S}{\partial\psi}\right|_{\psi=\psi o} = 0 \qquad (57)$$

Crack extension occurs when the strain energy density factor reaches a critical value in a direction defined by $\theta_o$, which corresponds to the direction of minimum strain energy density. For cyclic loading, a cyclic strain energy density factor is defined by

$$\Delta S = 2\left[a_{11}(\theta_o)K_I^{\,mean}\Delta K_I + 2a_{12}(\theta_o)(K_{II}^{\,mean}\Delta K_I + K_I^{\,mean}\Delta K_{II}) + a_{22}(\theta_o)K_{II}^{\,mean}\Delta K_{II} + a_{33}(\theta_o)K_{III}^{\,mean}\Delta K_{III}\right]$$

(58)

which includes both the stress range and the mean stress, and can be used after determining the direction of crack growth from *Eqn.* (57). The crack growth rate is directly related to $\Delta S$ through the expression

$$\frac{da}{dN} = C_s(\Delta S)^{m/2} \qquad (59)$$

where

$$C_s = C\left(\frac{2\pi E}{(1-2\upsilon)(1+\upsilon)}\right)^{m/2} \qquad (60)$$

Schollmann [162] proposed the $\sigma_1'$ crack growth criterion that also can be applied to the three dimensional case. The criterion is based on the assumption that crack growth develops perpendicularly to the direction of $\sigma_1'$, which is a special maximum principal stress. $\sigma_1'$ can be defined by the near-field stresses $\sigma_\theta$, $\sigma_z$, and $\tau_{\theta,z}$ as follows

$$\sigma_1^{'} = \frac{\sigma_\theta + \sigma_z}{2} + \frac{1}{2}\sqrt{(\sigma_\theta + \sigma_z)^2 + 4\tau_{\theta z}^2} \qquad (61)$$

Due to the assumption that the crack growth direction is perpendicular to $\sigma_1'$, the crack deflection angle, $\theta_o$, can be calculated by

$$\left.\frac{\partial \sigma_1^{'}}{\partial \theta}\right|_{\theta=\theta_o} = 0 \quad \text{and} \quad \left.\frac{\partial^2 \sigma_1^{'}}{\partial \theta^2}\right|_{\theta=\theta_o} > 0 \qquad (62)$$

After substituting the near-field stress solutions and differentiating partially with respect to $\theta$, the following formulation can be found

$$\begin{aligned} &-6K_I \tan\left(\frac{\theta}{2}\right) - K_{II}\left(6 - 12\tan^2\left(\frac{\theta}{2}\right)\right) \\ &+\left\{\left[4K_I - 12K_{II}\tan\left(\frac{\theta}{2}\right)\right] x \left[-6K_I \tan\left(\frac{\theta}{2}\right) - K_{II}\left(6 - 12\tan^2\left(\frac{\theta}{2}\right)\right)\right] - 32{K_{III}}^2 \tan\left(\frac{\theta}{2}\right)\left(1 + \tan^2\left(\frac{\theta}{2}\right)\right)^2\right\} \\ &x\left\{\left[4K_I - 12K_{II}\tan\left(\frac{\theta}{2}\right)\right]^2 + 64K_{III}^2\left(1 + \tan^2\left(\frac{\theta}{2}\right)\right)^2\right\}^{1/2} \end{aligned} \qquad (63)$$

The equivalent stress intensity factor can then be calculated as

$$K_{eqv} = \frac{1}{2}\cos\left(\frac{\theta_o}{2}\right)\left\{K_I \cos^2\left(\frac{\theta_o}{2}\right) - \frac{3}{2}K_{II}\sin\left(\frac{\theta_o}{2}\right) + \sqrt{\left[K_I \cos^2\left(\frac{\theta_o}{2}\right) - \frac{3}{2}K_{II}\sin\left(\frac{\theta_o}{2}\right)\right]^2 + 4K_{III}^2}\right\} \qquad (64)$$

As evident from the lengthy discussion above, numerous criteria have been developed to approximate the crack kinking phenomenon that has been observed under mixed mode loading conditions for both the crack kinking direction and equivalent stress intensity factor solutions. For mixed I+II+III mode loading conditions a good literature review can be found in Richard [163], Tanaka [156], and Marquis and Socie [164]. Additionally, the work by Liu [165] provides a thorough review of both *S-N* based multiaxial fatigue models as well as mixed mode fatigue crack growth models.

While various theoretical models to predict non-planar crack kinking behavior have been proposed, none has been widely accepted as a universal theory. Each of the above criterions is different from the others, but it is not clear exactly how much difference will be observed in the fatigue life prediction resulting from each criterion. Some criteria may predict similar crack trajectories and only slight differences will exist, while others may result in significantly different crack paths and fatigue life predictions.

In addition to the mathematical representation of the fatigue crack path prediction provided by the equations above, it is also necessary to be able to incorporate the crack direction modeling approach within the current finite element model. There needs to exist a method to update crack shapes and sizes within the finite element model for accurate determination of the local stresses at the crack tip for various cracked configurations. For the three-dimensional fatigue crack problem, where surface cracks can grow in a non-planar fashion with different kink angles along the entire crack front, creating robust crack extension and local remeshing algorithms for all of the criteria mentioned above is not a trivial task. It is impractical to try to evaluate all of the candidate non planar fatigue crack growth models as a result of the high computational

expense and implementation time necessary to do so. Therefore, for the purposes of this research, only a few of the most common models are evaluated.

## 5.3 Component Stress Analysis and Non-Planar Crack Modeling

The software Fracture Analysis Code in 3-Dimensions/Next Generation (FRANC3D/NG) is used for its crack insertion and local remeshing algorithms which help to simplify the modeling complexities that exist in modeling the non-planar fatigue crack growth problem using finite element software. FRANC3D/NG is a newer version of the original FRANC3D crack growth simulation software package developed by the Cornell Fracture Group and the Fracture Analysis Consultants [166]. In addition to other improved features, FRANC3D/NG uses finite element software instead of the boundary element method for component stress analysis and incorporates both stress analysis and crack propagation capabilities within its construct. FRANC3D/NG has the capability to adaptively insert and extend cracks and/or voids in pre-existing finite element meshes, and has been developed to work in conjunction with commercial finite element software packages such as ANSYS, ABAQUS, and NASTRAN.

For the non-planar crack growth framework within this study, stress analysis is performed using the ANSYS version 11.0 commercial software package, same as in Chapter 3 for planar cracks. Initial crack insertion within the finite element model is performed within the FRANC3D/NG software and local remeshing at the crack location is performed using crack tunnel and singular elements at the crack front as presented in Section 3.3. Once a crack is inserted into a finite element model, the commercial finite

element software ANSYS is used to solve the stress analysis of the cracked component. Stress intensity factors can be calculated using the displacement correlation or M-integral (interaction integral) method and can be used for subsequent crack growth modeling. To ensure that a significant additional model form error was not introduced into the problem by the choice in methods to calculate the stress intensity factors, solution comparisons were performed using the two different methods. Typical results obtained using the two methods are included within *Figure 46*. As can be seen in the figure, the two methods had good agreement along the entire crack front. Therefore, an additional model form error term was not necessary for this analysis and the stress intensity factors extracted from the finite element analysis were treated as deterministic values.

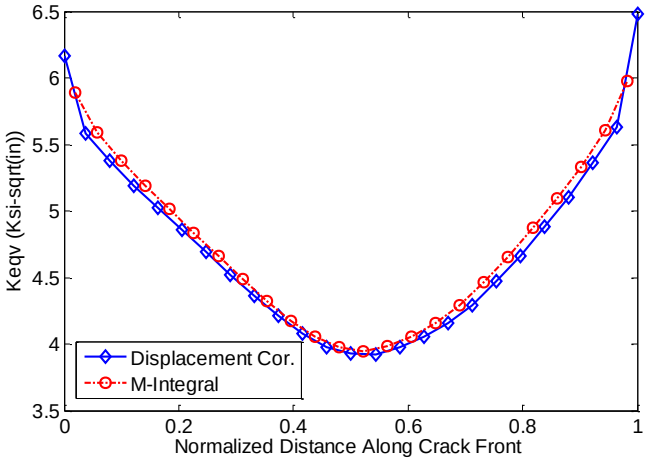


***Figure 46:*** Typical *stress intensity factor calculations along crack front obtained using displacement correlation and M-integral methods.*

*Figure 47* presents a schematic of the workflow and individual steps that are performed within the ANSYS and the FRANC3D/NG software codes.

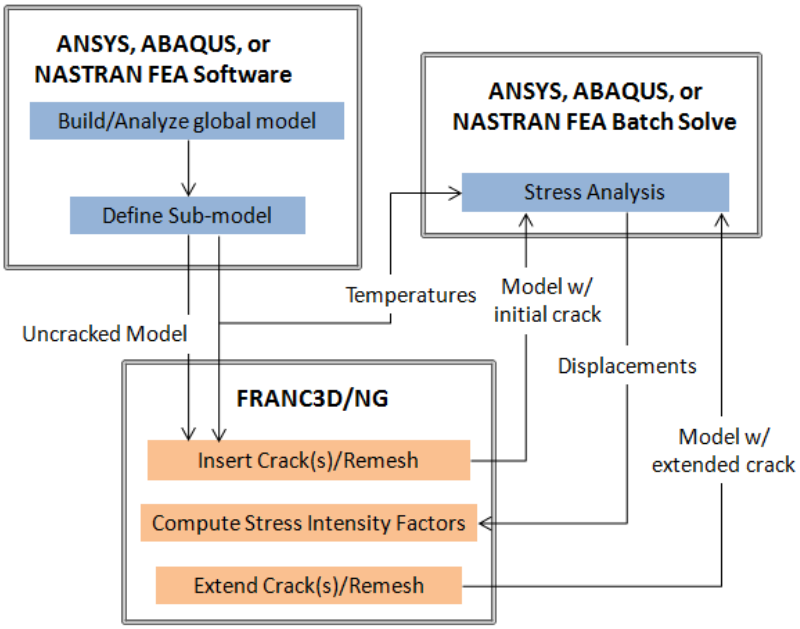


***Figure 47:*** *Work flow chart of FRANC3D/NG and finite element software for non-planar fatigue crack modeling*

At the present time, no universally accepted non-planar three-dimensional crack extension criteria currently exists, however, many two-dimensional models have been presented in the literature. The current state of the art for three-dimensional crack extension modeling is to evaluate the crack propagation direction at several discrete points along the crack front using two-dimensional plane strain equations. Plane strain equations are applied in the plane normal to the crack front tangent to determine the direction of propagation using one of several available crack propagation criteria. This technique effectively reduces the three-dimensional crack growth problem to a series of two-dimensional problems, evaluated at discrete points along the crack front.

The application of this method results in the relative extension of each node along the crack front based on local stress conditions at that specific location. The result of this

approach is a theoretical new crack front shape and location, based on a finite number of nodes. In order to maintain suitable finite element meshes at the crack front location, a best fit polynomial function is used to represent the updated crack front location. In doing so, a necessary approximation is made to the predicted crack front location leading to a smoother crack front representation than was initial predicted by the theoretical models. However, the suitability of this approximation can be monitored throughout the crack growth simulation to ensure that a reasonable crack front representation is maintained. *Figure 48 a.)* shows an example of a non-planar crack growth analysis where a theoretical crack front location is indicated by the green nodal positions and the best fit location is shown by the blue nodal locations and the "crack tunnel". Additionally, this relationship can also be shown through simple plots such as that one shown in *Figure 48 b.)*, which depicts the theoretically predicted nodal extensions by the individual dots and the best fit polynomial by the solid line (with good correspondence shown here for a $3^{rd}$ order polynomial).

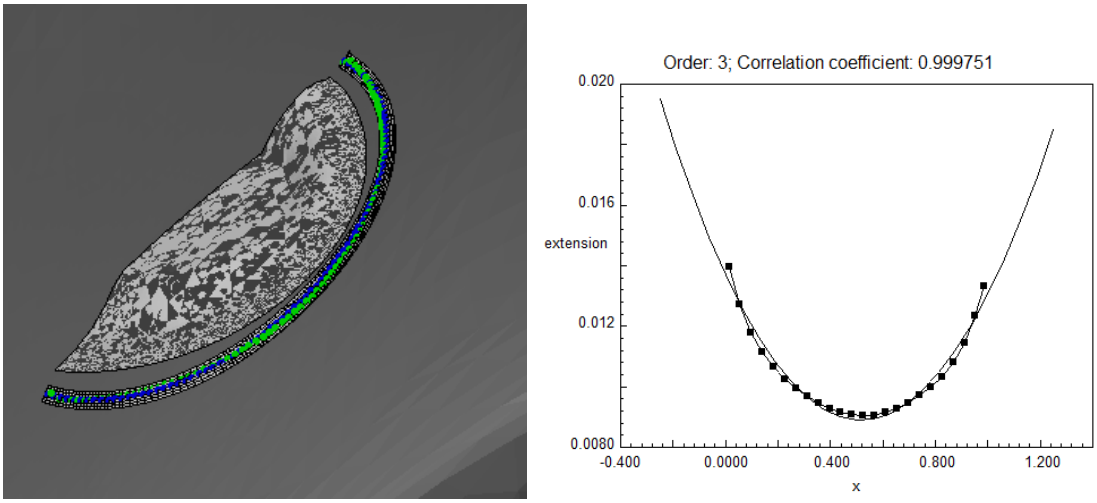


*(a.)* *(b.)*

***Figure 48:*** *Non-planar crack growth analysis showing crack surface as well as predicted and 'best fit' crack extension locations*

For the purpose of this work, two common crack direction modeling criteria will be evaluated within the non-planar crack growth framework; the maximum tangential stress (MTS) criterion, and the modified strain energy release rate criterion. These criteria are chosen based on the fact that they have already been incorporated within the FRANC3D/NG code, as well as for the familiarity of the fatigue research community with their functional forms.

For the general mixed mode I+II+III condition, the maximum tangential stress criterion identifies the crack kinking angle, $\theta$, as given in Eqn. (65)

$$\theta_{Kink} = \theta \quad \text{such that}$$

$$MAX\left(\sigma_{\theta\theta}(\theta)\right) \tag{65}$$

and a transition to the maximum shear stress criterion can be incorporated by including shear terms, which results in the expression

$$MAX\left(\sigma_{\theta\theta}(\theta)|_{\max}, \sqrt{\left(\frac{K_{IC}}{K_{IIC}}\right)^2[\sigma_{r\theta}(\theta)]^2 + \left(\frac{K_{IC}}{K_{IIIC}}\right)^2[\sigma_{\theta z}(\theta)]^2}\,|_{\max}\right) \qquad (66)$$

where $K_{IC}$ , $K_{IIC}$ ,and $K_{IIIC}$ are the mode I, mode II, and mode III fracture toughness values. The modified strain energy release rate criterion identifies the crack kinking angle, $\theta$, as given in Eqn. (67)

$$\theta_{Kink} = \theta \quad \text{such that}$$

$$\sigma_{\theta\theta}(\theta)|_{\max} \quad \text{and} \quad \sqrt{[\sigma_{\theta\theta}(\theta)]^2 + \left(\frac{K_{IC}}{K_{IIC}}\right)^2[\sigma_{r\theta}(\theta)]^2}\,|_{\max} \qquad (67)$$

For crack growth modeling, stress analysis is performed on the cracked component, and the local stress conditions are used within either the maximum tangential or the modified strain energy release rate models to determine crack extension *directions* at discretized points along the crack front. Stress intensity factors are evaluated from the local stress results and the relative advance at each point along the crack front can be evaluated using a crack growth law.

Several options exist for modeling crack extension magnitude, including cycle-by-cycle, incremental block-type, and median extension based approaches. For the cycle-by-cycle crack growth, crack extensions are performed for each and every load cycle using traditional fatigue crack growth laws, such as those presented in *Table 1*. Although the cycle-by-cycle approach is considered to be the most accurate of the above crack growth modeling approaches, it also presents significant computational challenges during numerical evaluation. For the high cycle fatigue problem, much of the crack growth occurs in the near threshold and the lower portion of the Paris/linear region of the

fatigue crack growth curve (shown schematically in *Figure 3*). Cycle-by-cycle crack extension within these regions is of the order of $10^{-10}$ - $10^{-8}$ in/cycle, meaning hundreds of thousands of individual stress analyses, crack extensions, and local remeshing functions are needed to double the size of an initial crack of 0.01 inch.

In addition to the substantial computational expense that the cycle-by-cycle approach demands, other limitations exist in the forms of mesh size and crack shape representations. In theory, the minimum element size contained within the mesh must be able to capture the crack profile. Therefore, to accurately represent cyclic crack extension within the near threshold region, the mesh size must be of the order of the crack extension, that is $\sim 10^{-10}$ inches, resulting in an unacceptably large number of elements contained within the finite element model. For non-planar crack propagation, not only is the extension magnitude calculated for each analysis, but also the direction of crack growth is necessary. For the cycle-by-cycle case, each individual crack growth step may have different propagation directions, leading to a highly complex, small scale zigzag type crack path. Again, this type of crack profile across the entire crack front presents problems for accurately and efficiently remeshing the crack front. From a computational time and numerical stability standpoint, a more reasonable crack propagation approach must be adopted.

An alternative to the cycle-by-cycle approach is to adopt a block-type crack growth extension method. This approach is similar to that of the cycle-by-cycle approach, with the exception that crack extension and direction modeling is held constant over a user-defined number of cycles. The block-type extension technique is based on the idea

of extending points along the crack front by a multiple of the crack growth increment determined for a single load cycle. Mathematically, this can be represented as

$$\Delta a_{update} = N_{user} * \frac{da}{dN_i} = N_{user} * \Delta a_i \qquad (68)$$

where $\Delta a_{update}$ is the total crack growth applied to the current crack, $N_{user}$ is the user defined block increment, and $\frac{da}{dN_i}$ is the crack growth magnitude for the current load cycle. This method allows for cyclic based crack extension, without requiring crack updating and remeshing for *every* load cycle, and is well suited to represent block-type loading conditions where the load history is composed of many sub-blocks of constant amplitude loading.

The median extension crack growth approach can also be used to overcome both the efficiency and stability issues that are inherent in the cycle-by-cycle approach. The median extension technique is based on the idea of extending points along the crack front in some proportion to a user-defined extension length. The proportion of crack extension at a given location is determined from the ratio of the stress intensity at that location compared to the mean stress intensity factor found at any point along the entire crack front. Mathematically, this relationship can be represented as given in Eqn. (69).

$$\Delta a_{node\_i} = \Delta a_{user\_mean} * f\left(\frac{\Delta K_{node\_i}}{\Delta K_{mean}}\right) \qquad (69)$$

where $\Delta a_{user\_mean}$ is the user-defined allowable median crack length extension. Using this formulation, the stress intensity factor at each crack front node is evaluated , $\Delta K_{node\_i}$, and crack extension is evaluated by comparing the stress intensity factor at that location to the mean stress intensity factor obtained along the entire crack front, $\Delta K_{mean}$. The parameter *f*

can be related to standard crack growth laws such as the Paris power law or the NASGRO/FNK growth equation, and represents the proportionality constant which is used for relative crack extension along the crack front. Although the median extension method is a departure from the classic cycle-by-cycle approach in which crack growth is evaluated for each and every load cycle, it presents a convenient way to update the crack size only after a minimum crack extension is determined while retaining relevant information pertaining to the relative stress concentrations along the crack front.

It is clear that each of these methods will result in a different crack length after a given number of crack growth increments, resulting in model prediction uncertainty due to simplifying assumptions. For the high cycle fatigue problem, the cycle-by-cycle approach does not present a computationally practical method as a result of the overwhelming number of small crack growth increments that would be required. The incremental block-type approach improves upon this limitation by updating the crack size only after a set number of load cycles. However, practical and numerical limitations remain on the acceptable values for the user-defined parameter $N_{user}$ in Eqn. (68). This is because minimum element sizes must be maintained within the FEA mesh to avoid excessively large models. However, if the updating increments can be set such that crack extension is possible, then the cyclic crack growth values can be retained within model simulations. Ultimately, the crack growth rate curve should be used on a cyclic basis so that the crack extension can be directly related to the number of applied load cycles, allowing for fatigue life assessment of a cracked component in terms of number of load cycles which can easily be related to flight hours. The median extension method departs altogether from the cycle-based crack growth approach, as crack extension along the

crack front is dictated by user input as opposed to number of applied load cycles. This approach arbitrarily imposes crack extensions in an attempt to ensure numerical stability and to better manage the relative extensions of the crack front at each load step.

Depending on the characteristics of the applied load history as well as the overall goal of the numerical simulation, either the incremental or the median extension method might be more appropriate.

## 5.4 Surrogate Model Development

Response surface methodology can be used in place of expensive finite element models for iterative fatigue analysis to reduce the computational effort needed to calculate the stress intensity factor at the crack tip. This is particularly useful in uncertainty analysis where multiple simulations of cycle-by-cycle crack growth analysis have to be executed. In Chapter 3, a response surface approximation was developed to approximately capture the relationship between the input variables (crack length, shape, and load value) and the output variable (mixed mode stress intensity factor) within the planar fatigue crack growth modeling framework. The finite element model was used to "train" a Gaussian process surrogate model to an acceptable degree of accuracy by evaluating the FEA at selected points within the design space identified by using the greedy point algorithm. The use of a surrogate model drastically improves the computational effort needed to perform crack growth analysis by eliminating the need for repeated evaluation of the full finite element model for each load cycle and crack configuration.

A surrogate modeling approach would provide extremely useful within the non-planar fatigue crack growth modeling framework for similar reasons. However, construction of a meaningful and useful surrogate model for the non-planar crack growth case is a significant challenge for several reasons. The first major obstacle in constructing a surrogate model is how to precisely define the three-dimensional complex crack shape. The crack shape for a non-planar three-dimension crack depends on the surface crack length, crack depth, and the individual kink angles along the crack front for each previous crack growth evaluation. As opposed to the planar crack shape, which could be well characterized by a few simple parameters, the non-planar crack shape is most fully suited to characterization by a three-dimensional, undulating surface. Therefore, crack characterization using basic parameters becomes a challenge. As a result, it is difficult to define the input parameters for crack characterization to be used to train the surrogate model.

A further challenge exists in the capability to generate complex crack configurations. Within the current non-planar modeling framework, a simple crack is introduced into the structural component and then is allowed to evolve into a non-planar crack due to the applied loading and crack extension criteria. As a result, complex crack shapes develop from simpler shapes over time, rather than being inputted directly. The capability to generate and evaluate any possible crack configuration are necessary and an accurate and efficient method to accomplish this is not currently available.

Another major complication in developing a surrogate model for general three-dimensional non-planar crack growth analysis is related to the form of the predicted model outputs. For this application, the nodal extension magnitude and directions are

needed to be predicted for each crack configuration. This means that the number of nodes along the crack front is known *a priori*, the surrogate model can identify and appropriately handle physical model boundaries, and that the surrogate modeling method itself is capable of predicting multiple output values in vector form.

Currently, these limitations present a significant challenge for easy extension of the surrogate modeling approach developed in Chapter 3 to the non-planar crack growth framework investigated in this chapter. Further research is needed to expand the current modeling approach in this application.

## 5.5 Equivalent Planar Method

An equivalent planar approximation is presented within this section as a method which may be valuable for reducing the computational expense of performing non-planar fatigue crack analysis within a probabilistic framework. The method creates a link between the non-planar crack growth analysis methods presented within this chapter, and the simpler planar crack growth analysis method described in Chapter 3. The method aims to retain valuable information obtained through initial non-planar crack propagation analyses for use within the planar analysis.

The basic idea behind the modeling approach is to try to use the results from the non-planar fatigue crack growth analyses to identify crack characteristics that can be transferred to a simpler planar crack configuration. A simplified initial crack can then be based on the characteristics of the non-planar fatigue crack, and can be grown in a planar fashion using the probabilistic planar crack growth analysis method developed in

Chapters 2, 3, and 4 to determine the statistics of the component fatigue life prediction. If a planar crack (with a defined initial orientation) can be used to reasonably represent a more complex non-planar crack within the FEA, then the computational expense can be reduced and crack representation can be simplified without significantly sacrificing accuracy in the model prediction.

Initially, a full fatigue crack growth analysis is necessary in which the initial crack is modeled such that it is allowed to grow in a non-planar fashion. The load history is applied to the component and non-planar fatigue crack modeling is performed using the methods outlined in Section 5.3. Once the crack has reached a critical size, relevant crack characteristics can be extracted from the resulting final non-planar crack configuration. An "equivalent" planar representation can then be developed that captures the main features determined from the final non-planar crack analysis result. Such features may include, but are not limited to, flaw orientation/angle, surface crack edge length, and crack depth. Quantities such as crack length and depth can be measured directly using the total lengths along the various kinked surfaces, or approximated by simply using the tip to tip distance (ignoring crack kinking in between) which can be viewed to be essentially equivalent to a simple projection method. The flaw is introduced into the component with an initial orientation that matches that of the final kinked crack profile and planar crack growth analysis is performed on the new equivalent crack. The new crack is grown from an initial size until the previously identified critical non-planar size is reached using a planar extension rule.

It is necessary to evaluate the performance and accuracy of the equivalent planar crack growth modeling approach to results obtained using the non-planar kinked crack

approach. In order to make a fair comparison, the stress intensity factors obtained using the two different methods at the same crack size (length) and loading condition need to be compared. Additionally, plots of the resulting equivalent planar and non-planar crack fronts can be used to show differences that exist in the crack shapes resulting from the two different modeling strategies. A numerical evaluation comparing the two crack growth modeling approaches is presented in Section 6.5.

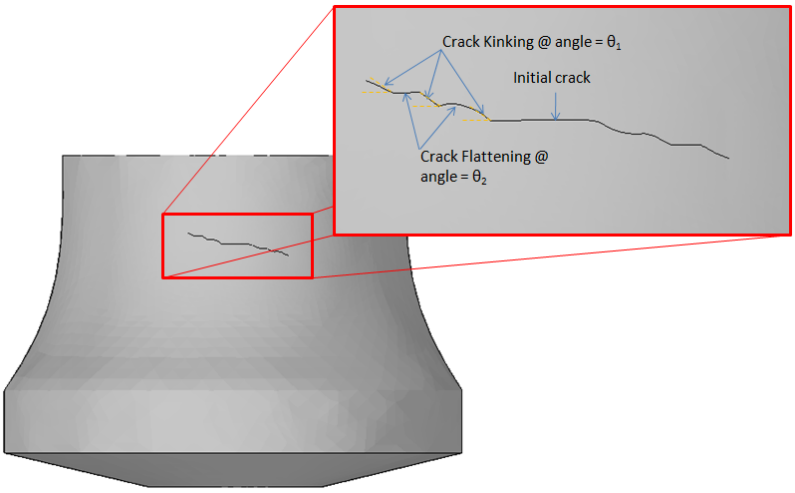


***Figure 49:*** *Final crack configuration (surface profile) of initial horizontal surface crack subjected to remote bending + torsion 2 block non-proportional loading. The crack is seen to kink towards two primary kink angles, $\theta_1$ and $\theta_2$ depending on applied loading*

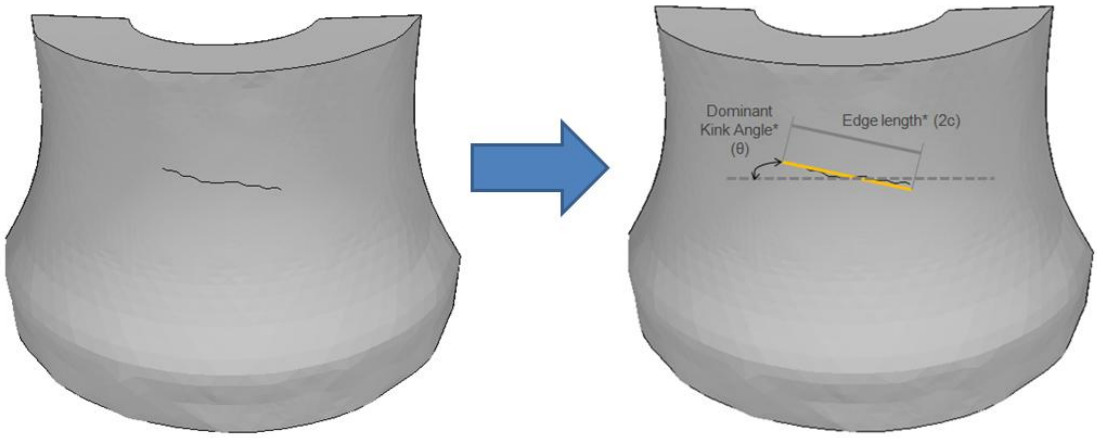


*a.)* *b.)*

***Figure 50:*** *a.) submodel showing final kinked crack shape after non-planar crack growth analysis; b.) submodel showing extraction of key flaw characteristics for use in equivalent planar crack analysis*

## 5.6 Summary

The crack growth modeling strategy adopted in this chapter allows for crack kinking and other non-planar propagation path behavior which may result from changes in loading conditions. Inclusion of crack path nonlinearities within the crack growth modeling framework is not a trivial task. When considering three dimension non-planar crack growth modeling, it is necessary to be able to predict and model both the crack extension magnitude and the crack path direction. In order to accomplish these objectives, advanced theoretical crack direction criteria which consider mixed mode stresses at the crack tip, as well as advanced crack tip extension and meshing algorithms are required.

Existing mixed mode crack growth models, which consider mixed mode stresses at the crack front can be used to determine relative crack kink direction and extension,

and a thorough review of several proposed methods has been presented in Section 5.2. The FRANC3D/NG commercial software code is used in this study to perform non-planar crack growth analysis using several different non planar crack kinking criteria and crack extension rules. The steps necessary for non-planar crack growth modeling in combination with finite element analysis are discussed in Section 5.3. An equivalent planar methodology is then presented in Section 5.4 in order to reduce the computational expense and facilitate probabilistic analysis.

Since non-planar crack growth modeling requires both crack extension and crack direction predictions, it is necessary to investigate the uncertainty in the crack shape and the component fatigue life predictions that results from the use of different non-planar crack growth criteria. Further uncertainty is introduced by the equivalent planar crack approach. The contribution of these sources of model uncertainty to the overall uncertainty in crack growth prediction will be addressed in Chapter 6.

# CHAPTER VI

# UNCERTAINTY QUANTIFICATION IN NON-PLANAR CRACK GROWTH ANALYSIS

## 6.1 Introduction

Fatigue crack growth modeling considering non-planar crack kinking behavior significantly increases the complexity of both the analytical models and the computational modeling demands. Crack growth under non-planar modeling approaches not only need to predict the crack extension per cycle, but also need to predict crack growth direction as well. As the dimensionality of the problem increases from the 2-dimensional case to the 3-dimensional case, additional complexities are introduced as the need to predict crack growth directions and extensions at multiple locations along the crack front arises. The result of non-planar, three dimensional crack growth modeling is a complex and potentially irregular crack configurations that no longer can be easily defined by a simple geometric shape. Rather, non-planar crack configurations may better be defined as fluctuating three dimensional surfaces with changing orientations at the crack front. Properly representing these complex crack configurations within theoretical fracture mechanics equations or within finite element meshes can prove to be a difficult task.

Non-planar crack growth is an incremental process where current crack configurations are dependent on previous crack growth applications. That is to say, the current crack shape is highly dependent on those stages of crack growth that preceded it.

Additionally, the current crack configuration directly affects the stress gradient at the crack tip, therefore affecting the subsequent crack direction and extension steps. In this way, the uncertainty associated with crack growth modeling at any previous step is contained within the current crack configuration, and will have some effect on the current model prediction.

It is clear from the lengthy discussion in Chapter 5, that many different crack propagation models for mixed-mode fatigue growth are available in the literature. Each presents a unique formulation, and therefore, a unique solution to the non-planar fatigue crack growth modeling analysis. This chapter focuses on uncertainties in crack shape development and model predictions resulting from the use of different non-planar crack propagation criteria.

A numerical evaluation of the uncertainty in model outputs resulting from the use of the different crack extension and direction criteria discussed in Chapter 5 is performed within this chapter. First, uncertainty resulting from different extension criteria will be examined. This section will focus on differences in crack shape and stress intensity factor solutions resulting from using different fatigue crack growth models; namely the Paris model [5] and the NASGRO (F-N-K) model [167]. The next section focuses on the differences in the crack shape development resulting from the use of different crack direction criteria. Crack shapes and stress intensity factor solutions obtained through numerical simulation will be compared for different methods. The third section investigates the uncertainties in non-planar crack shape development arising from uncertainty in load sequences. For this numerical investigation, crack growth modeling is performed under several different load sequences. The resulting crack shapes are used to

compare model predictions under different load sequences. Lastly, the uncertainties and modeling error resulting from replacing a non-planar analysis with an equivalent planar crack growth method is investigated. Detailed results corresponding to each of these topics is included within the following sections.

## 6.2 Uncertainty Resulting from Extension Criteria

In order to demonstrate the differences in crack shape that can develop as a result of different crack extension modeling approaches, two crack growth models of different sophistication will be examined. One of the earliest and most simple crack growth rate models is the Paris equation [5]. Here the predicted crack growth rate is modeled by the stress intensity factor raised to a power and multiplied by a constant, as given in Eqn. (2). This model assumes a linear relationship between the stress intensity factor and the crack growth rate when plotted in on a log-log scale. Another crack growth rate representation is the NASGRO (F-N-K) equation [167]. The NASGRO equation is substantially more complicated than the Paris model and conforms to the sigmoidial shape (in log-log scale) which is typical of fatigue crack growth rate data. The NASGRO equation is a full-range model that mathematically represents all three regions of the FCG curve with multiple empirically fitted constants and is given by:

$$\frac{da}{dN} = C\left[\frac{(1-f)}{1-R}\Delta K\right]\frac{\left(1-\frac{K_{th}}{\Delta K}\right)^{p}}{\left(1-\frac{K_{\max}}{K_{c}}\right)^{q}} \qquad (70)$$

where $C$ and $n$ are empirical parameters describing the linear region of the curve (similar to the Paris and Walker models) and $p$ and $q$ are empirical constants describing the curvature in the FCG data that occurs near threshold (Region I) and near instability (Region III), respectively. $\Delta Kth$ is the threshold stress intensity factor, $K_c$ is the critical stress intensity factor (related to the fracture toughness of the material), and the parameter $f$ corresponds to the crack opening function. Additional details of the model and associated parameters can be found in ref [167]. These two crack growth rate equations represent the extremes in terms of crack growth rate model sophistication. Numerical investigation into the differences observed in fatigue crack profiles and the corresponding stress intensity factor solutions at various crack growth stages using these two models is investigated below.

For the numerical study, the load history consisted of two block variable amplitude loading conditions where both bending and torsion were applied to the structure. The crack extension criterion was set to the mean extension criteria for both simulations. The initial flaw was set as a semi-circular surface flaw within the fillet radius region of the rotorcraft mast component. The initial flaw half length ($c$) and depth ($a$) were set to 0.05 inches. 12 individual crack growth increments with a median extension length of 0.01 inches were performed under alternating loading. Within the simulation, crack extension at each node along the crack front was evaluated for each growth increment using 2D plane strain approach outlined in Chapter 5. The results of the analysis can be seen in *Figure 51* and *Figure 52* the crack front profiles obtained using the Paris and NASGRO crack growth model are given. In order to improve the readability of the plots, only the initial crack front and the crack fronts obtained after 6

and 12 crack front extensions are plotted in the figures, however new crack front locations were calculated at each crack growth increment.

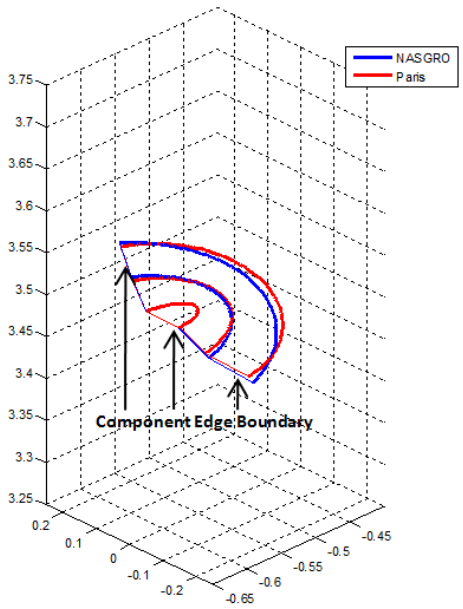


***Figure 51:*** *Isometric view of non-planar crack shape development showing initial crack, kinked crack profile after 6 growth increments, and kinked crack profile after 12 growth increments*

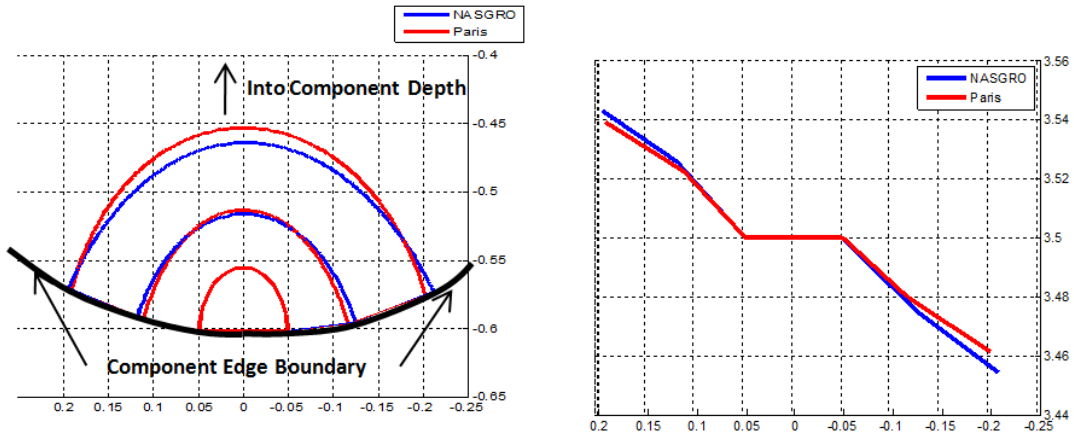


*a.)* *b.)*

***Figure 52:*** *a.) Plan and b.) Elevation view of non-planar crack shape development showing initial crack, kinked crack profile after 6 growth increments, and kinked crack profile after 12 growth increments (showing same crack profiles as Figure 51)*

It can be seen that the crack front profiles obtained from using the Paris and NASGRO crack growth models differs slightly. When compared, the Paris extension model appears to predict slightly larger crack growth in the crack depth position, and slightly less crack growth at the free surface of the cylinder. Additionally, at the free surface of the cylinder the crack edge predicted by the NASGRO equation appears to have a slightly larger kink angle after several crack growth steps have been made. The apparent difference in crack kink angle at the later stages of crack growth (clearly observable after the $6^{th}$ crack growth increment) can be attributed to the differences in crack length at the surface locations. Using the NASGRO extension method, the crack length at the free surface is seen to be larger than that predicted by the Paris model after the $6^{th}$ growth increment has been performed. This phenomenon can be seen within *Figure 52 b.)* where the crack length predicted by the Paris model is ~+/- 0.11 and by NASGRO is ~+/- 0.125 and the predicted crack kink angles have remained consistent for

both methods up to that point. As a result of the noticeable increase in crack length predicted by the NASGRO equation, the crack profiles predicted by each method at this crack growth stage are slightly different. The different crack profiles result in different stress gradients at the crack tip (during the subsequent load cycle), and the crack growth increment and direction prediction for the following crack growth stages will be different for each model.

This numerical simulation clearly shows how the use of different fatigue crack growth extension criterion can not only affect the predicted crack lengths, but also the predicted crack path. Different criterion will predict slightly different extensions at different points along the crack front, which will affect the stress gradient and SIF solution at the following load step, which will again affect the direction and extension predictions. As a result, it is clear that crack shape development under non-planar crack growth modeling is dependent on both the crack extension and crack direction criteria used.

### 6.3 Uncertainty Resulting from Direction Criteria

Several common crack direction modeling criteria are evaluated within the non-planar crack growth framework; these include the maximum tangential stress (MTS) criterion, maximum shear stress (MSS) criterion, and the modified strain energy release rate (MSERR) criterion. A transition from the maximum tangential stress criterion to the maximum shear stress (MSS) criterion can be performed by considering the mode I and mode II fracture toughness material properties. Each of these non-planar crack direction

criteria presents a unique solution to the non-planar fatigue crack growth modeling analysis. Therefore, this analysis produces three unique crack profiles that can be compared at each crack propagation step. These three direction criteria are chosen for numerical evaluation since they can be evaluated within the FRANC3D/NG code, as well as for the familiarity of the general fatigue community with their functional forms.

For the general mixed mode I+II+III condition, the maximum tangential stress criteria considering tensile only, and tensile + shear (MTS→MSS), is given by Eqn. (65), Eqn. (66), respectively and the modified strain energy release rate criterion is given by Eqn. (67). For the numerical study, the load history consisted of two block variable amplitude loading conditions wherein both bending and torsion were applied to the structure. The crack extension criterion was set to the mean extension criteria for all simulations. The results of the analysis can be seen in *Figure 53 a. & b*. where the crack front profiles obtained using the three different crack direction modeling criteria are compared. Additionally, since crack shape can have an effect on the stress gradient at the crack front, the stress intensity factors obtained at the same stage in the crack propagation analysis (same loading, same number of growth cycles) are compared within *Figure 54.* If significant differences can be seen in the resulting stress intensity factors, then different crack growth rates can be expected, and different component life predictions will be seen.

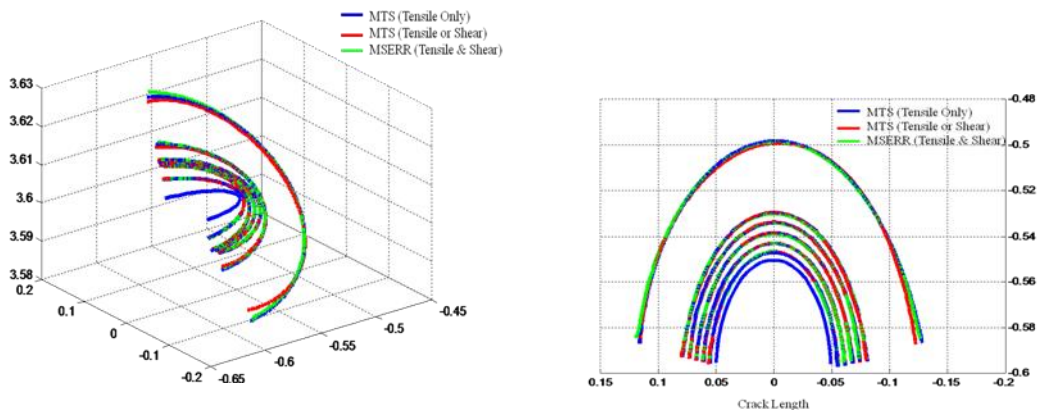


***Figure 53:*** *Simulated crack profiles using MTS (tensile only), MTS (tensile or shear) and MSERR criteria for crack kink direction modeling a.) isometric view; b.) plan view*

As can be seen within *Figure 53*, the predicted crack fronts for the three different methods do not appear to vary significantly from each other. As a result, it is also seen that the stress intensity factors for each of the simulated cracks also appear consistent. These results indicate that the crack direction is dominated by the tensile component of the stress, and that the shear component is not large enough for transition from tensile to shear dominated crack growth. In other words, the $\sigma_{\theta\theta}(\theta)$ component of Eqns. (65), (66) and (67) dominates the other terms for the loading conditions considered in this evaluation.

***Normalized Distance along crack front =0.1***

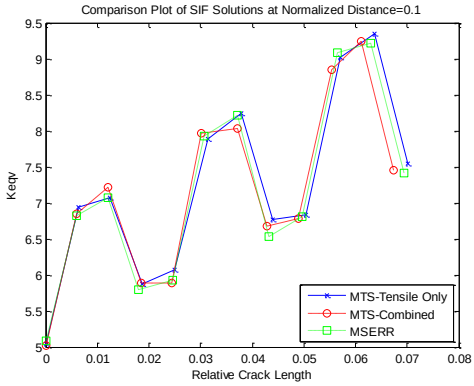


***Normalized Distance along crack front =0.5***

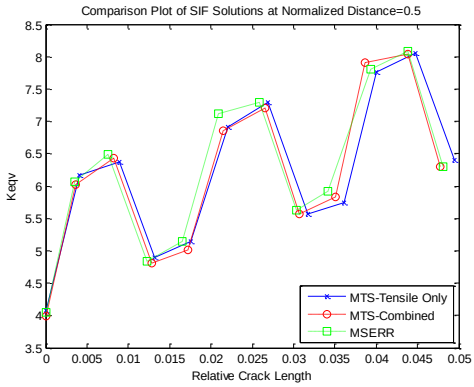


***Normalized Distance along crack front =0.9***

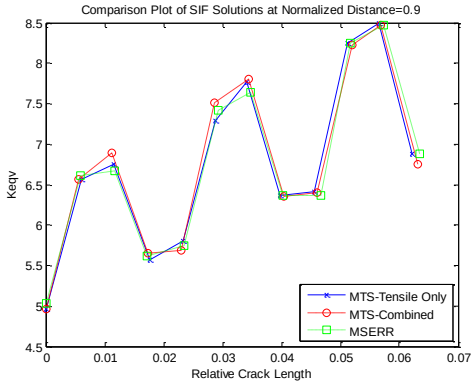


***Figure 54:*** *SIF solution comparisons at different stages of crack propagation for crack profiles obtained using different crack kink direction criteria. Comparisons shown at a.) 0.1 b.) 0.5 and c.) 0.9 of normalized distance along the crack front.*

The applied loading history was modified from that used within the previous analysis to one that contained more dominant shear loading component (increased torsion component while decreasing bending). The applied torsion load was increased by a factor of 2.5 while the bending load did not increase from its previous levels. A similar crack growth analysis was performed under the new, shear dominated loading conditions to determine if any significant difference could be observed in the crack shape development. It can be seen in *Figure 55* that under increased shear loading conditions, the maximum shear stress and the maximum normal stress criteria lead to different crack kinking angles and crack shape development. The increased torsion load on the component resulted in an overall increase in the mode III stress intensity factor, which experienced its largest value along the crack front in the depth direction (0.5 normalized distance along the crack front). The crack kinking angle predicted by the maximum shearing stress (MSS) criteria was determined to be smaller than the kink angle predicted by the maximum tangential stress (MTS) criteria. As evident within the figure, when shear loads cause the mode II and mode III stress intensity factors to be of the same order as the mode I stress intensity factor, the crack kinking angle predicted using the MTS and MSS criteria may be different. As a result, the crack shape development is expected to differ after several crack growth increments.

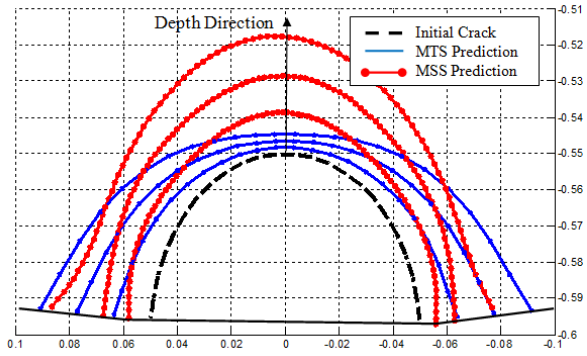


*(a.)*

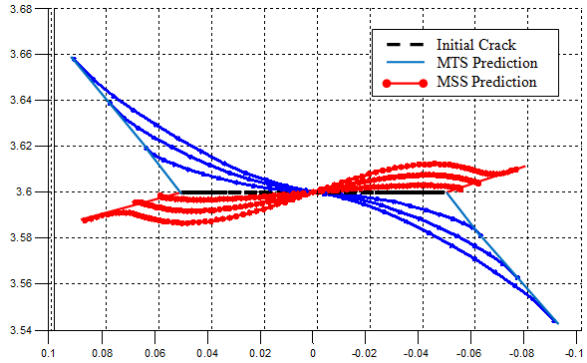


*(b.)*

***Figure 55:*** *Simulated crack profiles using MSS criteria for crack kink direction modeling a.) plan view; b.) elevation view*

## 6.4 Uncertainty Resulting from Load Sequence

Crack extension and direction predictions are based on the local stress gradient at the crack front location, which is directly related to the applied loading at the current load step. In addition to the influence that specific crack growth extension and direction criterion have on the crack shape development throughout the non-planar fatigue crack propagation (as discussed in previous sections within this chapter), the sequence of the applied loadings will also affect the crack shape development. This section investigates the role that load sequence has on crack shape development and crack tip orientation over

the course of a non-proportional multi-axial variable amplitude loading history. Numerical crack growth simulations are performed to determine differences in crack shapes and orientations at different stages of crack growth and comparisons are made at the final crack size. Included within this section are analyses which compare crack shape development for load histories with the same load values but different load sequence as well as for load histories which have different load sequences and load combinations. Details of each analysis are included below.

The first set of analyses focus on crack shape development and final flaw orientation for crack growth which is performed under load histories which contain the exact same load values (in number and magnitude) but which have unique load sequences. For the sake of this study, four block variable amplitude load histories which contain both applied bending and torsion are considered. Details of the different load cases contained in the load histories are given in *Table 7*.

***Table 7:*** *Details of load cases composing 4 block VAL histories*

| | Normalized | |
|---|---|---|
| Load # | Bending | Torsion |
| 1 | 0.75 | 0.25 |
| 2 | 0.5 | 0.5 |
| 3 | 0.5 | 1 |
| 4 | 0.25 | 1 |

FRANC3D/NG was used to simulate the non-planar fatigue crack propagation for a crack with an initial size until the crack reached a user-defined critical crack size. Each crack growth simulation was performed for a different load history that was composed of a specified combination of the four load cases given in the *Table 7* and was set to have a unique load sequence. Three individual crack growth profiles developed from numerical

simulation can be seen within *Figure 56*. Crack kinking behavior was predicted using the MTS criterion, and an initial horizontal oriented crack was allowed to grow in a non-planar fashion at each applied load step. It is seen that the crack shape development is dependent on the applied loading conditions and that each load sequence results in a unique crack shape and crack tip orientation at each stage of the crack growth analysis.

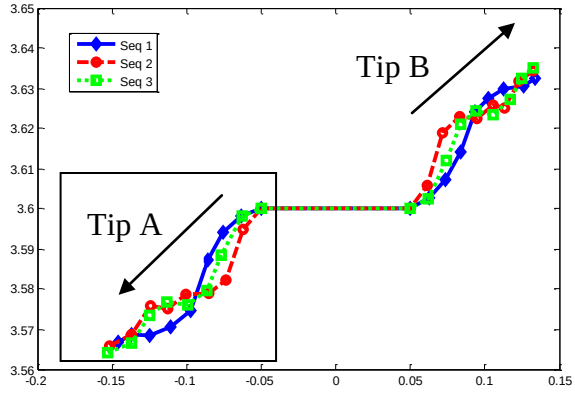


*(a.)*

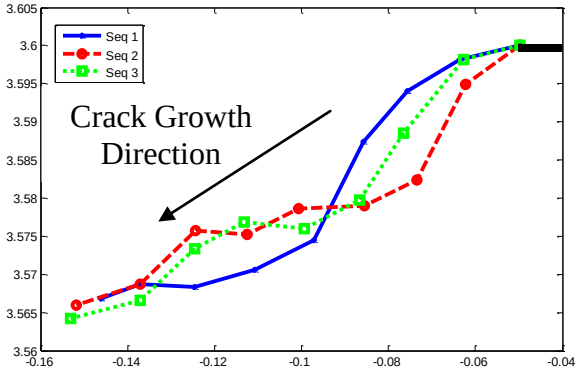


*(b.)*

***Figure 56:*** *a.) Full crack; b.) crack tip "A" surface profiles obtained from numerical simulation showing crack shape development for 3 distinct load sequences under 4 block variable amplitude loading conditions*

Although each individual load sequence was seen to cause a unique crack front orientation at each crack growth increment, it was found that the crack tip location after

application of all of the load steps was similar for all three of the numerical simulations. This result can be seen within *Figure 56* within the lower left hand side of the figure and indicates that although the individual crack orientations at each crack growth increment may be different, the combination of all of individual crack kinks result in a similar overall crack front location. This conclusion is dependent on the fact that each load history contained exactly the same number and magnitude of applied loading and is based on the simulation results obtained using the incremental crack growth methodology detailed in Chapter 5. Based on these results, it appears that the load sequence affects the crack shape development for interim crack growth stages, but ultimately will not significantly change the final crack tip location if the number and magnitude of applied loadings remains consistent from one history to another.

The next set of analyses focus on the differences in crack shape development under load histories which contain different combinations of the loads contained in *Table 7* and which also have which have unique load sequences. This numerical study differs from the previous case by allowing each load history to contain any combination and any sequence of the four load cases (whereas the previous study required the same combination of loads). Crack growth simulation was performed in a similar manner using the incremental crack growth method and MTS criterion where an initial horizontal crack was grown to a user-defined critical crack length for each unique load history.

Individual crack growth profiles developed from numerical simulations can be seen within *Figure 57* for this analysis. Similar to the results within the previous analysis, it is again seen that the crack shape development is dependent on the applied loading conditions and that each load sequence results in a unique crack shape and crack

tip orientation at different stages of the crack growth analysis. However, since each load history is composed of different combinations of the loading values given in *Table 7*, the crack tip locations at the conclusion of the analysis differ from one another. This is the result of some histories containing a larger number of loadings which are bending dominated (load case #1 in *Table 7*) which leads to a less severe crack kinking angle, and some histories containing a larger number of loading which are torsion dominated (load case #4 in *Table 7*) which leads to a more severe crack kinking angle.

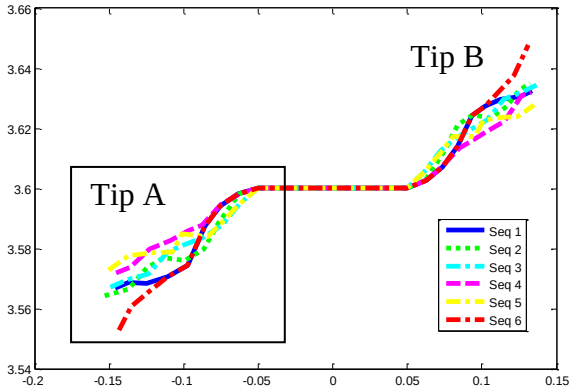


*(a.)*

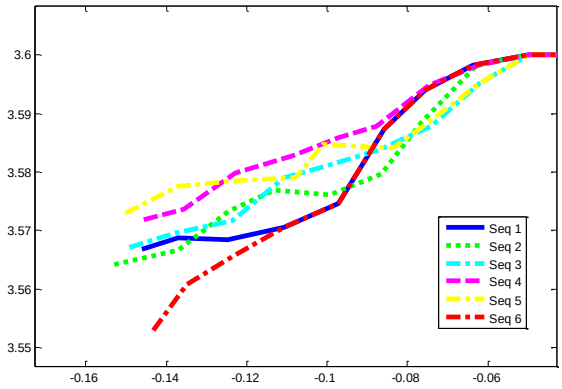


*(b.)*

***Figure 57:*** *a.) Full crack; b.) crack tip "A" surface profiles obtained from numerical simulation showing crack shape development for 3 distinct load histories with different loads and sequences under 4 block variable amplitude loading conditions*

It can be seen by comparing *Figure 56* and *Figure 57* that as the uncertainty in the applied loading is increased (completely known vs. any combination of specified load levels), the uncertainty in the resulting crack shape also increases. For the case where load histories are allowed to contain any combination of the specified loads (as was the case in the current analysis), it is possible to determine upper and lower bounds the crack front location by constructing histories that contain only the most extreme loading cases. For this example problem, these extremes are represented by load case #1 (bending dominated) and load case #4 (torsion dominated). Typical results for the crack shape development under these loading conditions are shown in *Figure 58*, where the solid black lines represent the bounds and all crack growth paths containing other combinations of the loading are expected to be within the two paths determined by performing crack growth under these extreme spectra. For comparison purposes, the other crack front profiles included in *Figure 57* are also included within *Figure 58*. The final tip to tip angles obtained for the crack fronts developed under the extreme load spectra were found to be $25.7^{o}$ for the upper bound and $4.7^{o}$ for the minimum bound. All crack fronts developed under different combinations of loading were found to have final tip to tip angles between the two extreme values.

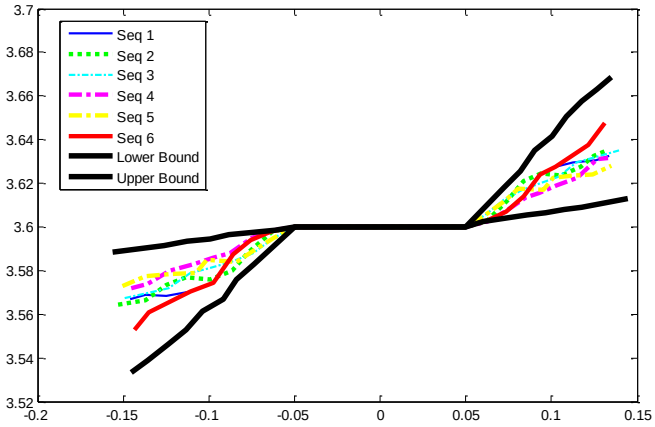


***Figure 58:*** *Upper and lower bounds on crack front paths determined by performing crack growth simulation under extreme load histories*

Through several numerical crack growth studies, it is shown that the sequence of the applied loadings can have a significant effect on the crack shape development over time. For the most general case, where possible load histories can only be characterized by the load levels (without any indication of how frequent each load level is or how often it is encountered), non-planar crack shapes may significantly deviate from one another depending on the combination of loads contained within each history. However, it is possible to determine the upper and lower bounds on the crack front location by identifying the loading cases which cause the most severe (largest and smallest) kink angles, and performing non-planar analysis using load histories containing only these values. As additional information is available on the expected frequency of each load level within the load history, less scatter is expected in the crack path predictions made under different load sequences. It was found that for the limiting case where each history is composed of loads which differ only in the sequence and not the magnitude or number/frequency of each applied load, the crack path differed during each crack growth

increment but converged to the same general location after all crack growth steps had been performed. Overall, it was determined that loading and load sequence can have a significant effect on the crack shape development when considering non-planar crack growth under variable amplitude, multi-axial loading conditions, and that uncertainty in the characterization of the applied loads results in increased uncertainty in the non-planar crack profile.

## 6.5 Non-Planar vs. Equivalent Planar Comparison

An equivalent planar crack growth modeling strategy has been presented in Chapter 5, which proposes the use of an equivalent planar crack, which can be characterized by various features extracted from the initial non-planar result, as an approximate representation of the more sophisticated non-planar approach. Errors will exist in the equivalent planar representation when compared to the original non-planar result as a result of these simplifications. These errors need to be quantified in order to be able to estimate the uncertainty in model predictions using the equivalent planar modeling approach.

This section will examine the crack growth modeling results for crack growth simulations using the equivalent planar method. The first investigation will use a simple constant amplitude loading condition (in both bending and torsion) to investigate the case where a single crack kink angle is expected. The second investigation will consider a two block loading condition where multiple crack kinking angles are expected. The final investigation will analyze the equivalent planar approximation under the four block load

history where load sequence effects are also considered. The initial crack size and location within the component remain the same as previous studies. The result of the analyses is included below.

The first comparison of the accuracy of the equivalent planar method in representing the non-planar crack growth modeling considered the simplest loading case, where only constant amplitude bending and torsion loading are applied. For this specific analysis, the applied loading was set to load level #3 in *Table 7*. *Figure 59 a) b)* and *c)* show comparison plots at different normalized distances around the crack front (0.1, 0.5, and 0.9 respectively) of the stress intensity factor results at various stages of crack growth for the non-planar and equivalent planar simulations under the constant amplitude bending + torsion loading conditions. For the constant amplitude load case only one primary kink angle is expected, resulting in the equivalent planar crack to be oriented directly at this kink angle. As seen in the plots, the planar representation is able to closely match those found using the non-planar crack methodology for this load case, as might be expected. The percent error between the equivalent planar and the non-planar analysis at any location along the crack front is found to be less than 15% at all stages of crack growth, and less than 6% for all stages after the initial crack growth increment, with an overall absolute mean error of 3.7%.

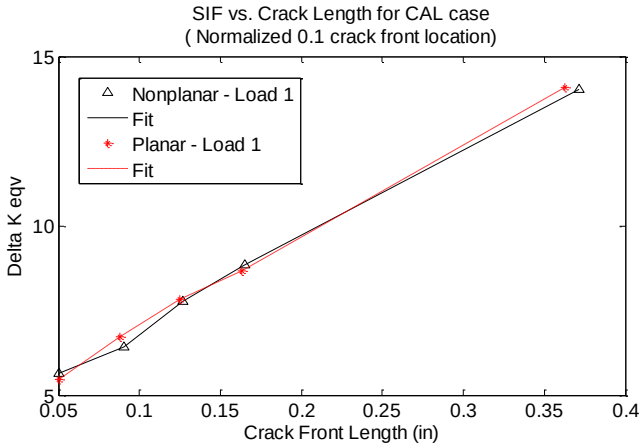


*(a.)*

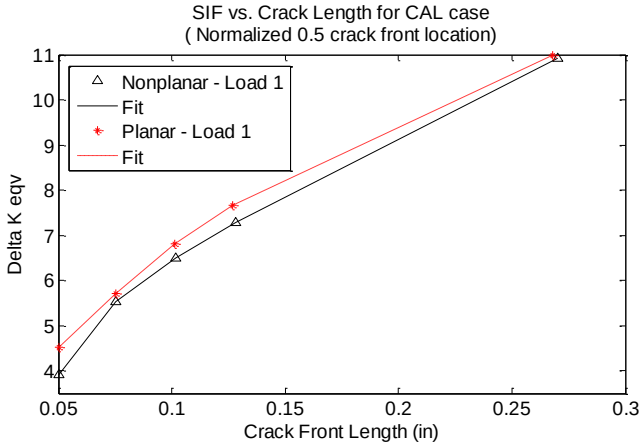


*(b.)*

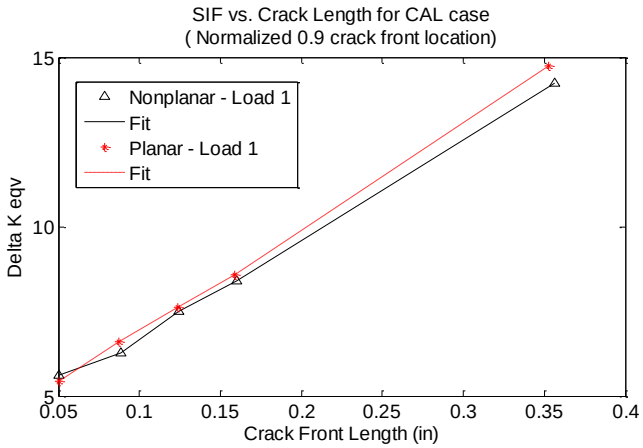


*(c.)*

***Figure 59:*** *Comparison plots of stress intensity factor solutions found using non-planar crack growth methodology and equivalent planar crack growth methodology for CAL load case. Plots show SIFs along the crack front at a.) 0.1 normalized distance (near surface); b.) 0.5 normalized distance (depth); c.) 0.9 normalized distance (near surface)*

The second comparison of the accuracy of the equivalent planar method in representing the non-planar crack growth modeling considered a two block variable amplitude loading case, where both bending and torsion loading are applied. For this specific analysis, the applied loading was restricted to load level #1 and load level #3 in *Table 7*. *Figure 60 a) b)* and *c)* show comparison plots at different normalized distances around the crack front (0.1, 0.5, and 0.9 respectively) of the stress intensity factor results at various stages of crack growth for the non-planar and equivalent planar simulations under the 2 block variable amplitude bending + torsion loading condition. Under the two-block loading case, two distinct kink angles are to be expected resulting in a zigzag type crack edge profile (as seen in *Figure 49*), and the resulting equivalent planar crack orientation essential becomes the average kink angle of the two loading conditions.

As seen from the plots, the planar representation is also able to closely match those found using the non-planar crack methodology for this 2 block load case. The largest discrepancy between the two results is seen during the first growth stage. At this point in the simulation, the two configurations are the most different as the crack has an initial orientation of $0^o$ for the non-planar crack growth before kinking, and ~$17^o$ in the case of planar crack growth. This large difference in orientation was found to effectively reduce the magnitude of both the mode II and III stress intensity factors for the planar analysis at the surface locations (as opposed to depth location), thus lowering the overall $\Delta K_{eqv}$ value for this crack size. However, after several crack growth steps, it is found that the planar approximation more closely matched that of the non-planar analysis. The percent error between the equivalent planar and the non-planar analysis are found to be

less than 18% at all stages of crack growth, and less than 7% for all stages after the initial crack growth increment, with an overall absolute mean error of 2.9%.

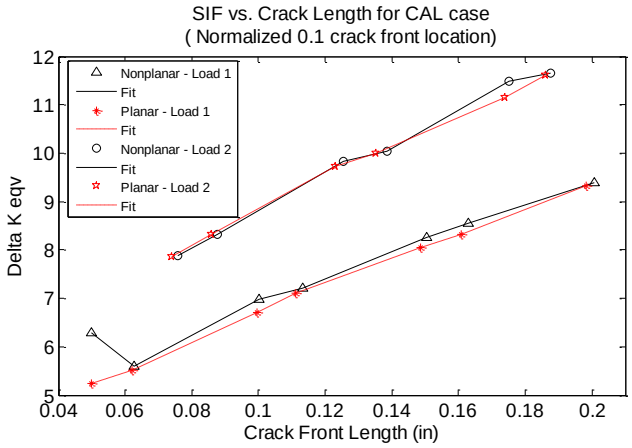


*(a.)*

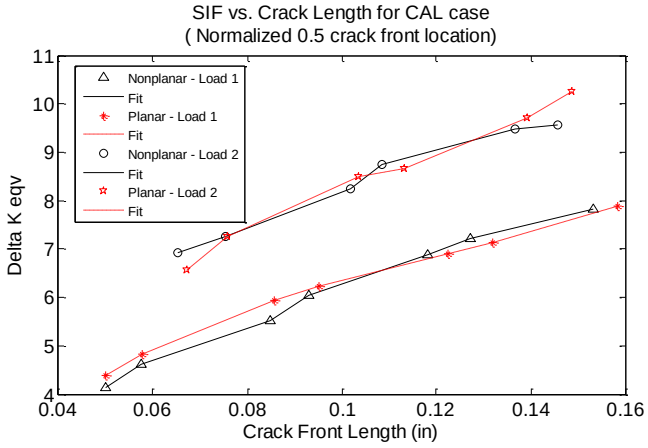


*(b.)*

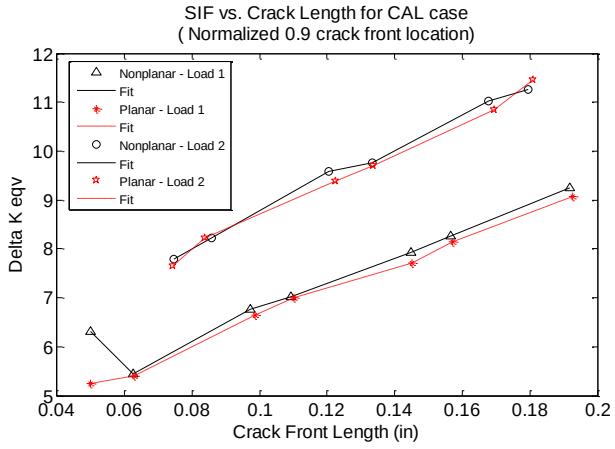


*(c.)*

***Figure 60:*** *Comparison plots of stress intensity factor solutions found using non-planar crack growth methodology and equivalent planar crack growth methodology for 2 block VAL load case. Plots show SIFs along the crack front at a.) 0.1 normalized distance (near surface); b.) 0.5 normalized distance (depth); c.) 0.9 normalized distance (near surface)*

The final analysis of the equivalent planar method considers the four block variable amplitude loading case wherein the load sequence is flexible. The three unique non-planar crack growth results obtained from previous analyses in Section 6.4 (and shown in *Figure 56*) are used to show how multiple non-planar crack growth results can be combined for a single equivalent planar crack analysis. Three different load histories (composed of the same loading values, but with different sequences) were used to perform non-planar crack growth simulations. The final angle of orientation between the crack tips at the surface locations was determined using the method detailed in Section 5.5 for each simulation result. For the three cracks shown in *Figure 56* corresponding to the three different load sequences, the angles of the equivalent flaw size were determined to be 13.18, 13.50, and 13.95 degrees. The orientation of the equivalent planar crack was set to be the average value obtained from the three individual results and planar crack growth analysis was performed and results compared. *Figure 61 a), b),* and *c)* show comparison plots at different normalized distances around the crack front (0.1, 0.5, and 0.9 respectively) of the stress intensity factor results at various stages of crack growth for the non-planar and average equivalent planar simulation for the 4 block variable amplitude history. Plots showing similar results are obtained when the stress intensity factors obtained from the average equivalent planar results are compared to those from the non-planar for other load histories.

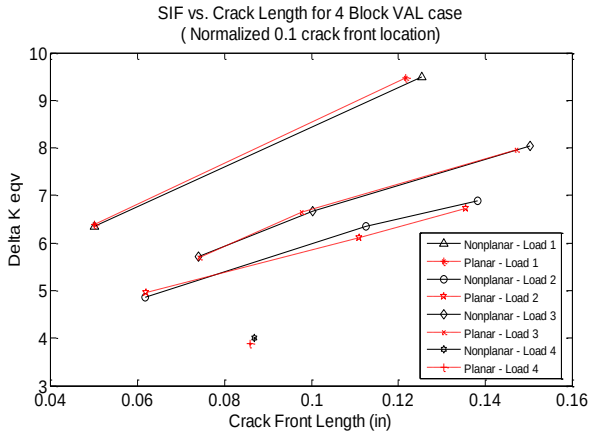


*(a.)*

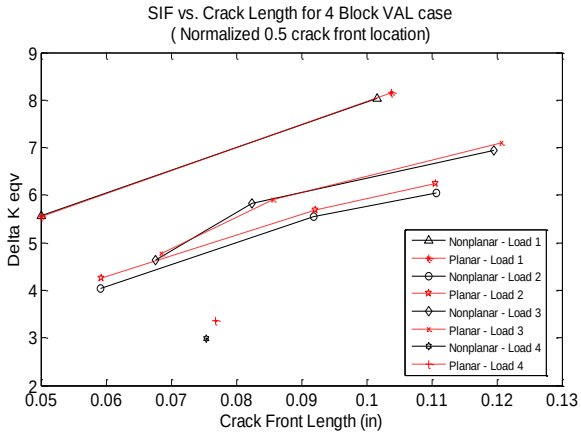


*(b.)*

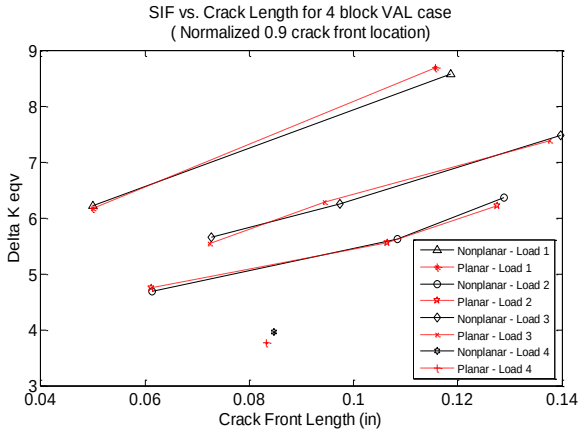


*(c.)*

***Figure 61:*** *Comparison plots of stress intensity factor solutions found using non-planar crack growth methodology and equivalent planar crack growth methodology for 2 block VAL load case. Plots show SIFs along the crack front at a.) 0.1 normalized distance (near surface); b.) 0.5 normalized distance (depth); c.) 0.9 normalized distance (near surface)*

For the more general load case where the exact combination of applied loadings contained within a load history is not precisely known, the orientation of the final non-planar crack has been shown to be dependent on both the applied load values and the sequence in which they are applied. This makes it difficult to accurately predict the final orientation of the fatigue crack without a full non-planar analysis for a specific load history. As a result, the need for an efficient and accurate method for non-planar crack shape development is desired to be able to predict the final crack orientation under unique load histories. This topic remains an open area of research and would enable a broader applicability to the current equivalent planar methodology by providing final flaw orientations without the expensive task of component stress and crack growth analysis.

Overall, the equivalent planar crack growth modeling approach appears to provide a reasonable approximation to the non-planar crack growth analysis. Comparative results are included for simple constant amplitude, two-block, and four-block variable amplitude load histories. Errors in the stress intensity factors at similar stages of crack growth resulting from the simplification to a planar crack representation were found to be anywhere from 5-20% for the cases considered. The equivalent planar method reduces the necessary computational effort and complex crack shape characterization by using the results from a non-planar analysis and effectively reducing them onto a single plane orientation. In doing so, this method reduces the complex non-planar crack growth problem to a planar type problem which can be effectively modeled using techniques developed in the previous chapters of this dissertation.

## 6.6 Summary

Non-planar crack kinking behavior significantly increases the complexity of both the analytical models and the computational modeling demands. Since non-planar crack growth modeling requires both crack extension and crack direction predictions and no universal theory exists, uncertainties are introduced into the model predictions resulting from the use of different non-planar crack growth criteria. The choice of crack extension and direction modeling criteria has an influence on crack shape, the stress gradient at the crack tip, and the overall predicted fatigue life. The use of different criteria may result in differences in fatigue crack growth model predictions and the differences between the various methods will be problem specific. It is important that crack growth model predictions to compare mode predictions to experimental and in-service physical specimens whenever possible.

Since non-planar crack growth is an incremental process where the crack shape development is dependent on previous crack growth predictions, the sequence and magnitude of applied loads may have an effect on the final crack size, shape, and orientation within the structural component. Uncertainty in the composition of loading values contained within a load history as well as loading sequence has been shown to have an effect on the crack shape development under multiaxial variable amplitude loading conditions. However, it is possible to determine upper and lower bounds on the crack tip orientation under different load combinations by performing non-planar analysis for extreme load spectra.

This chapter also investigated the uncertainty in stress intensity factor solutions and crack growth predictions using an equivalent planar crack growth modeling approach

in place of a more computationally demanding non-planar analysis. The equivalent planar method appears to provide reasonable approximations for most crack configurations and load combinations where a full non-planar analysis is possible and has been investigated under constant amplitude as well as variable amplitude block type loading conditions.

# CHAPTER VII

# SUMMARY & FUTURE WORK

## 7.1 Summary

The traditional damage tolerance (DT) approach to aircraft structures has assumed a deterministic damage accumulation process where deterministic crack growth curves, constant material properties, and specific initial flaw sizes are used. However, uncertainties exist at all levels of the fatigue damage tolerance modeling process, resulting in unknown confidence bounds on component life predictions made by engineers. In order to overcome this limitation, a systematic framework for stochastic fatigue crack growth modeling must be developed which accounts for different kinds and sources uncertainty that exist at all levels of the damage tolerance analysis. Each individual source of uncertainty, resulting from physical variability, data uncertainty, or modeling errors, needs to be identified and its statistical characteristics quantified in order to accurately assess the risk of failure of structural components. It is the goal of this dissertation to provide a methodical and practical framework for quantifying various sources of uncertainty and analyzing their effects on component reliability predictions over time.

The first several chapters of this work focus on uncertainty quantification, probabilistic fatigue crack growth modeling, and model error assessment for planar crack growth analysis. This research provides methods for uncertainty quantification of many fundamental material properties which are important to fatigue crack growth, such as the

threshold stress intensity factor and the fatigue limit, with particular attention focused on accurately representing the near threshold and linear (Paris) regions of the crack growth rate curve which are important to the high cycle fatigue problem. As each additional model within the fatigue crack growth analysis framework is used to represent the crack propagation, additional uncertainties are introduced into the model predictions as a result of model form errors. This research focuses on quantifying the statistical uncertainty in each model prediction to more accurately represent the overall uncertainty in component fatigue life predictions. Included in this area are topics ranging from uncertainty in fatigue crack growth rate model representation, finite element discretization errors, and uncertainty in surrogate model predictions. Each of these individual sources of modeling uncertainty needs to be represented in different ways, and this work provides a methodical approach for accurate quantification and inclusion within an overall probabilistic fatigue life assessment.

The latter half of this dissertation shifts focus to identify additional sources of uncertainty which are introduced when non-planar fatigue crack growth modeling is performed. When considering non-planar crack growth modeling, it is important to be able to predict and model both the crack extension magnitude and the crack path direction. This leads to an increase in the complexity of crack shape representation as well as computational modeling considerations. In order to try to capture the nonlinear crack extension behavior that has been seen in both experimental results and realistic applications, numerous crack growth direction and extension criteria have been proposed within the literature. However, to date no single criteria has been identified as a universally applicable model. This research investigates the differences in fatigue crack

shape development and fatigue life predictions which result from the use of different crack extension and direction modeling criteria. It is seen through numerical simulation results that the choices of both the extension and direction criteria can have an effect on the crack shape development of fatigue cracks growing under multiaxial variable amplitude loading conditions. Since crack growth analysis is an incremental process, where subsequent crack growth steps are directly dependent on previous crack growth steps (through the stress gradient at the crack tip), small differences in crack orientation and crack extension at each growth step can lead to different crack shape representations after a finite number of crack growth increments.

An equivalent planar crack representation method is developed within this work to try to utilize the information obtained about the crack shape development and final crack orientation from the more sophisticated non-planar analysis, while enabling the use of simpler crack representation and modeling approach afforded by the planar representation. The method proposes to utilize a finite number of non-planar crack growth analyses to characterize the non-planar crack shape development under multiaxial variable amplitude loading conditions. The orientation of the final crack shape is then used to determine a suitable angle of orientation of an initial crack within the component that can be used within a planar crack growth analysis procedure. The equivalent planar representation is an approximation to the more realistic non-planar crack growth method, but appears to provide reasonable results when compared to full non-planar analyses for constant amplitude and multiple block variable amplitude histories.

Overall, this dissertation systematically identifies, quantifies, and incorporates different types of uncertainties within an overall probabilistic life prediction modeling

approach. The uncertainty quantification (UQ) methodology is implemented with 3-dimensional planar and non-planar fatigue crack modeling, for structural components subjected to multi-axial, variable amplitude loading conditions. Included within the scope of this work are UQ methods for material properties and model parameters, as well as methods which focus on model error quantification – including FEA discretization error and surrogate modeling error. Additionally, the uncertainty quantification and propagation methodology is developed to be computationally efficient to enable the component reliability assessment to be performed within a Monte Carlo Scheme. Sensitivity analysis is presented to identify the contribution that each source of uncertainty has on the overall component life prediction.

Some of the key contributions contained within this work include:

- Extended stochastic field expansion technique to fatigue crack propagation modeling, which enables a more realistic representation of the correlation among the fatigue crack growth rate test data
- New framework for PFM enabling fatigue crack growth modeling under multi-axial, variable amplitude loading conditions incorporating FEA, characteristic plane, surrogate model, and cyclic crack growth modeling methods
- Developed new application of Gaussian Process surrogate modeling technique for mixed mode SIF evaluation under multi-axial loading for improved computational efficiency
- Implemented new technique for identifying critical input parameter combinations that help reduce uncertainty in the training point selection for the design of experiments (DOE) of the full model FEA

- Quantified and incorporated finite element discretization modeling errors within component fatigue life assessment framework
- Quantified and incorporated surrogate modeling (response surface) modeling errors within component fatigue life assessment framework
- Proposed an 'equivalent planar' fatigue crack growth modeling approach to reduce the computational expense of numerical simulations while retaining valuable features of a full scale non-planar crack growth analysis
- Quantified uncertainty in crack shape and stress intensity factor solutions resulting from use of different crack extension criteria for non-planar crack growth modeling
- Quantified uncertainty in crack shape and stress intensity factor solutions resulting from use of different crack direction criteria for non-planar crack growth modeling
- Evaluated model errors for an 'equivalent planar' fatigue crack growth modeling approach compared to traditional non-planar results

## 7.2 Future Research Needs

This study implemented fatigue crack growth analysis using both planar and non-planar fatigue crack growth modeling techniques. While the area of planar crack growth under constant amplitude and variable amplitude loading has been well documented within the fatigue research community, non-planar crack growth modeling, particularly in three dimensions, is a more recent area of interest. From a theoretical point of view,

continued research is necessary on developing a universal fatigue crack growth extension and direction criteria. Currently, many different criteria exist, and different researchers argue as to the appropriateness of each under different loading conditions and in reference to different experimental results. In order to develop a universal criteria that is widely applicable to different load conditions, it is necessary to increase the current physical understanding of fatigue crack growth mechanisms under multiaxial loads. Efforts are underway to increase experimental testing under multi-axial loads for different materials, where only simple uniaxial tensile load cases have previously been performed. However, one current limitation which makes direct comparison and data transfer possible difficult is the lack of a standardized and detailed multiaxial testing procedure and standard test specimen. As a result, results obtained from different sources and researchers tend to use different testing procedures on a wide range of test specimen which raises the question of whether differences seen in the results for mixed mode fatigue crack growth properties are the result of natural variability or whether they are simply the product of different testing methods. Further research in this area is necessary before a meaningful and thorough database of mixed mode material properties can be built.

Surrogate modeling techniques were implemented within the planar fatigue crack growth analysis to efficiently capture the relationship between the crack shape, size, and current loading conditions and the stress intensity factors along the crack tip. Within the non-planar crack growth analysis procedure, the development of a similar method is much more involved as a result of the complexity in crack shape representation and the interdependence between the previous loads and the crack shape development. A

promising area of future research exists in developing an efficient and accurate method for three dimensional non-planar crack shape predictions. New methods must be developed which address the issue of how to best represent the complex, non-planar three dimensional crack surface. Any surrogate modeling technique must also be able to capture the direct relationship that exists between the previous applied load sequence and the current crack shape representation. Once developed, these methods will still rely on accurate non-planar crack growth analysis for training data under multiaxial load histories. As a result, continued effort and resources should be focused on improved finite element models, remeshing algorithms, increased computational efficiency, and more robust crack growth modeling capabilities.

Overall, many advanced topics in the fields of fatigue and fracture mechanics for multiaxial crack growth still exist and are worth pursuing. As new theoretical and computational methods are developed and proposed, it is necessary that a sufficient amount of meaningful and representative experimental results are available to compare, verify, and validate the proposed methods against those which have been previously developed.

## REFERENCES


[1] R.P. Reed, J.H. Smith, and B.W. Christ, "The economic effects of fracture in the United States," SP647-1,NBS, March 1983, 3.

[2] A.F. Grandt, Jr., Fundamentals of structural integrity: damage tolerant design and nondestructive evaluation, John Wiley & Sons, Inc., 2004.

[3] Y.C. Tong, Literature review on structural Risk and reliability analysis. Aeronautical and Maritime Research Laboratory. report DSTO-TR-1110, Melbourne, Australia, Feb. 2001.

[4] FAA, Rotorcraft Damage Tolerance (RCDT) R&D Roadmap for metallic materials. Airworthiness Assurance Team, FAA, 2006.

[5] P.C. Paris, M.P. Gomez, W.E. Anderson, A rational analytic theory of fatigue, The trend in engineering. University of Washington, 13(1), 1961, pg. 9-14.

[6] R. G. Forman, V. E. Kearney, R. M. Engle, Numerical analysis of crack propagation in cyclic-loaded structures. Journal of Basic Engineering, Trans, ASME, Vol. 89, pp. 459-464, 1967.

[7] K. Walker, The effect of stress ratio during crack propagation and fatigue for 2024-T3 and 7075-T6 Aluminum, ASTM STP 462, American Society for Testing and Materials (Philadelphia), p. 1, 1970.

[8] F. Erdogan,M. Ratwani, Fatigue and fracture of cylindrical shells containing a circumferential crack. International Journal of Fracture Mechanics, 6, 379-392.

[9] T.L. Anderson, Flaw Characterization, Comprehensive structural integrity Volumes 1-10, Edited by: I. Milne, R.O. Ritchie, B. Karihaloo, Elsevier, 2003.

[10] A.F. Grandt, Jr. Fundamentals of Structural Integrity: Damage tolerant design and nondestructive evaluation, John Wiley & Sons, Inc., New Jersey, 2004.

[11] J.P. Gallagher, F.J. Glessler, A.P. Berens, USAF Damage Tolerant Design Handbook: guidelines for the analysis and design of damage tolerant aircraft structures, AFWAL-TR-82-3073, 1984.

[12] X.B. Lin, R.A. Smith, An improved numerical technique for simulating the growth of planar fatigue cracks, Fatigue Fracture Engineering Materials & Structures, Vol. 20, No. 10, pg 1363-1373, 1997.

[13] Y. Liu, S. Mahadevan, Analysis of subsurface crack propagation under rolling contact loading in railroad wheels using FEM, Engineering Fracture Mechanics, Vol. 74, pg 2659-2674, 2007.

[14] X.B. Lin, R.A. Smith, Fatigue growth simulation for cracks in notched and unnotched round bars, International Journal of Mechanical Sciences, Vol. 40, No. 5, pg 405-419,1998.

[15] P.M. Besuner, Probabilistic fracture mechanics, In: Probabilistic fracture mechanics and reliability, Ed: J.W. Provan, Martinus Nijhoff Publishers, 1987.

[16] S. Rahman, B.N. Rao, Probabilistic fracture mechanics by Galerkin meshless methods – part II: reliability analysis, Computational Mechanics, Vol. 28, No. 5, May, 2002.

[17] C.A. Rau, Jr. P.M. Besuner. Probabilistic fracture mechanics, Product Engineer, Vol. 50, pg 41-47, 1979.

[18] M. Shinozuka, J.N. Yang, Optimum structural design based on reliability and proof load test, Annals of Assurance Science Proceedings of the Reliability and Maintainability Conference, Vol. 8, July, 1969.

[19] J.N. Yang, W.J. Trapp, Reliability analysis of aircraft structures under random loading and periodic inspection, AIAA Journal, Vol. 12, pg 1623-1639, 1974.

[20] H. Alawi, Designing reliably for fatigue crack growth under random loading, Engineering Fracture Mechanics, Vol. 37, No. 1, pg 75-85, 1990.

[21] D.O. Harris, E.Y. Lim, D.D. Dedhia, Probability of pipe fracture in the primary coolant loop of a PWR plant, Vol. 5, Probabilistic Fracture Mechanics, U.S. Nuclear Regulatory Commission Report NUREG/CR-2189, 5, Washington D.C., 1981.

[22] S.C. Forth, M.A. James, W.M. Johnston, J.C. Newman Jr., Anomalous fatigue crack growth phenomena in high strength steel, In: Proceedings international congress on fracture, Italy, 2007.

[23] U.H. Tiong, R. Jones, Damage tolerance analysis of a helicopter component, International Journal of Fatigue, Vol. 31, pg. 1046-1053, 2009

[24] B. Ayyub, Uncertainty modeling and analysis in civil engineering, CRC Press LLC, 1998.

[25] N.R. Moor, D.H. Ebbeler, and M. Creager, Probabilistic service life assessment, AD-Vol. 28, Reliability Technology, ASME 1992

[26] M.E. Melis, E.V. Zaretsky. Probabilistic analysis of aircraft gas turbine disc life and reliability, NASA/TM-1999-107436.

[27] R.V. Lust, Y.T.J. Wu, Probabilistic structural analysis – an introduction, Experimental Techniques, September/October 1998.

[28] Y. Xiaoming, H.C. Kuang, K.C. Kyung. Probabilistic structural durability prediction, AIAA Journal, Vol. 36, No. 4, April 1998.

[29] T. Svensson, Prediction uncertainties at variable amplitude fatigue. International Journal of Fatigue, 17, pg 295-302, 1997.

[30] R. Bullough, V.R. Green, B. Tomkins, R. Wilson, J.B. Wintle, A review of methods and applications of reliability analysis for structural integrity assessment of UK nuclear plant. International Journal of Pressure Vessel Piping, Vol. 76, pg 909-919, 1999.

[31] P. Dillström, F. Nilsson, B. Brickstad, and M. Bergman, Probabilistic fracture mechanics analysis of a nuclear pressure vessel for allocation of in-service inspection. International Journal of Pressure Vessel Piping, Vol. 54, pg 435-463, 1993.

[32] O. Ditlevsen and H.O. Madsen, Structural reliability methods, Wiley, Baffins Lane, Chichester, pg 372, 1996.

[33] F.M. Burdekin, W. Hamour. SINTAP contribution to Task 3.5, Safety factors and risk, UMIST, pg. 25, 1998.

[34] British Energy, Assessment of the integrity of structures containing defects, British energy generation report R6, revision 4, Gloucester, UK, 2001.

[35] L.P. Pook, Metal Fatigue: what it is, why it matters. Springer, 2007.

[36] L.P. Pook, The role of crack growth in metal fatigue. Metals Society, London, 1983.

[37] J. Backlund, A.F. Blom, C.J. Beevers, Fatigue threshold, fundamentals and engineering applications, in Proceedings of the International Conference held in Stockholm, June 1981.

[38] M. Klesnil, P. Lukas, Effect of stress cycle asymmetry on fatigue crack growth, Material Science Engineering, Vol. 9, pg 231-240, 1972.

[39] J.M. Barsom, Fatigue behavior of pressure vessels steel, WRC Bulletin 194, Welding Research Council, New York, May 1964.

[40] B. Farahmand, Fatigue and Fracture Mechanics of High Risk Parts, Chapman & Hall, New York, 1997.

[41] A. Haldar, S. Mahadevan, Probability, reliability, and statistical methods in engineering design, John Wiley & Sons, 2000.

[42] F.P. Beer, E.R. Johnston Jr., Mechanics of Materials (2nd Edition). McGraw-Hill, Inc. 1992.

[43] R.C. Rice, J.L. Jackson, J. Bakuckas, S. Thompson. Metallic materials properties development and standardization (MMPDS), DOT/FAA/AR-MMPDS-01, January 2003.

[44] M. McDonald, K. Zaman, and S. Mahadevan, Representation and First-Order Approximations for Propagation of Aleatory and Distribution Parameter Uncertainty. In the Proceedings of 50th AIAA/ASME/ASCE/AHS/ASC

Structures, Structural Dynamics, and Materials Conference, 4 - 7 May 2009, Palm Springs, California.

[45] B. Efron, R. Tibshirani. An Introduction to the Bootstrap. New York: McGraw-Hill, 1993.

[46] B. Efron, Bootstrap methods: another look at the jackknife, Annals of Statistics, Vol. 7, No. 1, pg. 1-26, 1979.

[47] P. Dillstrom, F. Nilsson, Probabilistic fracture mechanics, In: Comprehensive Structural Integrity, ED: l Milne, R.O. Ritchie, B. Karihaloo, Elsevier, 2003.

[48] J.N. Yang, G.C. Salivar, C.G. Annis Jr., Statistical modeling of fatigue crack growth in nickel-base superalloy, Engineering Fracture Mechanics, Vol. 18, No. 2, pg. 257-270, 1983

[49] J.W. Provan, Probabilistic Fracture Mechanics and Reliability, Martinus Nijhoff, Dordrecht, 1987.

[50] N.R. Moore, D.H. Ebbeler, S. Sutharshana, M. Creager, Probabilistic failure risk assessment for structural fatigue, Jet Propulsion Laboratory, 1992.

[51] T.A. Cruse, S. Mahadevan, R.G. Tryon, Fatigue reliability of gas turbine engine structures, NASA/CR-97-206215, Lewis Research Center, 1997.

[52] Y. Liu, S. Mahadevan, Stochastic fatigue damage modeling under variable amplitude loading. International Journal of Fatigue, Vol. 29, pg 1149-1161, 2007.

[53] J.N. Yang, S.D. Manning, "A simple second order approximation for stochastic crack growth analysis", Engineering Fracture Mechanics, Volume 53, Issue 5, pp. 677-686, 1996.

[54] Z. Zhao, A. Haldar, Bridge fatigue damage evaluation and updating using non-destructive inspections. Engineering fracture mechanics, Vol. 53, No. 5, Pg 775-788, 1996.

[55] R. Zheng, S. Mahadevan, Model uncertainty and bayesian updating in reliability-based inspection. Structural Safety Vol. 22, pg 145-160, 2000.

[56] T.D. Righiniotis, Simplified calculations involving the maximum load on bridge fatigue details under inpection. Part II: Fatigue. Journal of Constructional Steel Research, Vol. 50, pg 825-839, 2004.

[57] M. S. Cheung, W.C. Li, "Probabilistic fatigue and fracture analyses of steel bridges", Structural Safety, Vol. 25, Issue. 3, pp. 245–62, 2003.

[58] L. Min, Y. Qing-Xiong, A probabilistic model for fatigue crack growth, Engineering Fracture Mechanics, Vol. 43, No. 4, pg 651-655, 1992.

[59] J. N. Yang, S.D. Manning, A simple second order approximation for stochastic crack growth analysis, Engineering Fracture Mechanics, Volume 53, Issue 5, pp. 677-686, 1996.

[60] M. Loeve. Probability Theory 4th Ed., New York, Springer, 1977.

[61] K. K. Phoon, S. P. Huang, S.T. Quek. Simulation of non-gausssian processes using Karhunen-Loeve expansion. Computers and Structures, Vol. 80, pg. 1049-1060, 2002.

[62] D. F. Socie, M.A. Pompetzki, Modeling variability in service loading spectra, Journal of ASTM International, Vol. 1, No. 2, 2004.

[63] J. B. de Jonge, The analysis of load-time histories by means of counting methods. *NLR MP 82039U*, National Aerospace Laboratory, The Netherlands, 1982.

[64]L. D. Lutes, S. Sarkani, Stochastic analysis of structural and mechanical vibrations. New Jersey: Prentice-Hall, 1997.

[65] B. Zuccarello, N. F. Adragna, A novel frequency domain method for predicting fatigue crack growth under wide band random loading. International Journal of Fatigue, 29,1065-1079,2007.

[66] P. Heuler, H. Klatschke, Generation and use of standardized load spectra and load-time histories. Internationals Journal of Fatigue, 27, 974-990, 2005

[67] N. E. Frost, The current state of the art of fatigue: Its development and interaction with design, Journal of the Society of Environmental Engineering, Vol. 14, No. 2 pg 21-28, 1971.

[68] ASTM Standard 1049-85. Standard practices for cycle counting in fatigue analysis. 2005

[69] R. I. Stephens, A. Fatemi, H.O. Fuchs H.O. Metal fatigue in engineering, second edition. John Wiley & Sons, Inc. 2001.

[70] R. Tovo, On the fatigue reliability evaluation of structural components under service loading. International Journal of Fatigue 23, pg 587-598, 2001.

[71] M. Matsuishi, T. Endo, Fatigue of metals subjected to varying stress, paper presented to the Japan Society of Mechanical Engineers, Fukuoka, Japan, March 1968.

[72] G. E. Lesse, G. Socie editors, Multiaxial Fatigue: Analysis and Experiments AE-14. SAE Fatigue Design and Evaluation Committee. 1989.

[73] C. Amzallag, J. P. Gerey, J. L. Robert, J. Bahuaud, Standardization of the rainflow counting method for fatigue analysis. International Journal of Fatigue 1994, 16:pg 287-293.

[74]A. Haldar, S. Mahadevan, Probability, Reliability and Statistical Methods in Engineering Design. John Wiley & Sons, Inc. 2000.

[75] S. Karlin, A First Course in Stochastic Processes, 1 ed., New York, NY, Academic Press, 1966.

[76] USAF., 1974, **"**Airplane damage tolerance requirements". Military Specification. Washington, DC. (MIL-A-83444).

[77] Joint service specification guide aircraft structures, JSSG-2006. United States of America: Department of Defense; 1998.

[78] J. P. Gallagher, A.P. Berens, and R.M. Engle Jr. (1984). USAF damage tolerant design handbook: guidelines for the analysis and design of damage tolerant aircraft structures. Final report. 1984.

[79] A. Merati, and G. Eastaugh. (2007). Determination of fatigue related discontinuity state of 7000 series of aerospace aluminum alloys. Eng Failure Anal2007; 14(4):673–85.

[80] J. N. Yang. (1980). Distribution of equivalent initial flaw size. In: Proceedings of the annual reliability and maintainability symposium. San Francisco (CA): 1980.

[81] P. M. G. P. Moreira, P.F.P. de Matos, and P.M.S.T. de Castro, Fatigue striation spacing and equivalent initial flaw size in Al 2024-T3 riveted specimens. Theory of Applied Fracture Mechanics 2005; 43(1):89–99.

[82] S.A. Fawaz, Equivalent initial flaw size testing and analysis of transport aircraft skin splices, Fatigue and Fracture of Engineering Materials & Structures, Vol. 26, 3, pg 279-290, 2003.

[83] P. White, L. Molent, and S. Barter, Interpreting fatigue test results using a probabilistic fracture approach. International Journal Fatigue 2005; 27(7): 752–67.

[84] L. Molent, Q. Sun, and A. Green, Characterization of equivalent initial flaw sizes in 7050 aluminum alloy. Fatigue & Fracture Engineering Materials & Structures, 2006; 29:916–37.

[85] Y. Liu and S. Mahadevan, Probabilistic fatigue life prediction using an equivalent initial flaw size distribution, International Journal of Fatigue, Volume 31, Issue 3, March 2009, Pages 476-487, 2008

[86] H. Kitagawa, and S. Takahashi, Applicability of fracture mechanics to vary small cracks or cracks in early stage. In: Proceedings of the 2nd international conference on mechanical behavior of materials. USA (OH): ASM International; 1976.

[87] M. H. El Haddad, T. H. Topper, and K. N. Smith. (1979) Prediction of nonpropagating cracks. Engineering Fracture Mechanics 1979;11:573–84.

[88] H. Tada, P. Paris, G. Irwin, The stress analysis of cracks handbook, 3rd edition. American Society of Mechanical Engineers, New York, NY, 2000.

[89] ANSYS. (2007). ANSYS theory reference, release 11.0. ANSYS Inc., 2007.

[90] Y. Liu, L. Liu, and S. Mahadevan. (2007). Analysis of subsurface crack propagation under rolling contact loading in railroad wheels using FEM. Engineering Fracture Mechanics, Vol. 74, pgs 2659-2674, 2007.

[91] R. D. Henshell, K. G. Shaw, Crack tip finite elements are unnecessary. International Journal of Numerical Methods in Engineering. 9, 495-507.

[92] R. S. Barsoum, On the use of isoparametric finite elements in linear fracture mechanics. International Journal of Numerical Methods in Engineering. 10, 25-37.

[93] A. S. Beranger, A fatigue life assessment methodology for automotive components, in European Structural Integrity Society. 1997, Elsevier. p. 17-25.

[94] P. M. Toor, A unified engineering approach to the prediction of multiaxial fatigue fracture of aircraft structures. Engineering Fracture Mechanics, 1975. 7(4): p. 731-741.

[95] J. Qian, and A. Fatemi, Mixed mode fatigue crack growth: A literature survey. Engineering Fracture Mechanics, 1996. 55(6): p. 969-990.

[96] A. Carpinteri, R. Brighenti, Circumferential surface flaws in pipes under cyclic axial loading. Engineering Fracture Mechanics, 1998, 60(4), 383-396.

[97] A. Carpinteri, R. Brighenti, A. Spagnoli, Fatigue growth simulation of part through flaws in thick walled pipes under rotary bending, International Journal of Fatigue, 2000, 22, 1-9.

[98] M. Fonte, E. Gomes, M. Freitas, Stress intensity factors for semi-elliptical surface cracks in round bars under bending and torsion. International Journal of Fatigue, 1999; 21:457-463.

[99] Fatigue Crack Growth Computer Program "NASA/FLAGRO", developed by R.G. Forman, V. Shivakumar, and J.C. Newman. JSC-22267A, January 1993.

[100] Y. Liu, S. Mahadevan, Multiaxial high-cycle fatigue criterion and life prediction for metals. International Journal of Fatigue, 2005. 27(7): p. 790-800

[101] Y. Liu, S. Mahadevan, Threshold stress intensity factor and crack growth rate prediction under mixed mod loading, Engineering Fracture Mechanics, Vol. 74, pg 332-345, 2007.

[102] C. B. Storlie, L. P. Swiler, J. C. Helton, C. J. Sallaberry, Nonparametric regression procedures for sensitivity analysis of computationally demanding models. Sandia report, SAND2008-6570, 2008.

[103] T. W. Simpson, J. D. Peplinski, P. N. Koch, J. K.. Allen, Metamodels for computer-based engineering design. Engineering with Computers: An international journal for simulation-based engineering. Vol. 17, pg 129-150. 2001.

[104] C. Rasmussen. *Evaluation of Gaussian processes and other methods for non-linear regression*. PhD thesis, University of Toronto, 1996.

[105] T. J. Santner, B. J. Williams, and W. I. Noltz. *The Design and Analysis of Computer Experiments*. Springer-Verlag, New York, 2003.

[106]J. McFarland, Uncertainty analysis for computer simulations through validation and calibration. Ph D. Dissertation, Vanderbilt University, 2008.

[107] D. R. Jones, M. Schonlau, and W. J. Welch. Efficient global optimization of expensive blackbox functions. Journal of Global Optimization, 13(4):455–492, 1998.

[108] B. J. Bichon, M. S. Eldred, L. P. Swiler, S. Mahadevan, and J. M. McFarland. Efficient global reliability analysis for nonlinear implicit performance functions. AIAA Journal, Vol. 46, No. 10, October 2008.

[109] M. Janssen, J. Zuidema, R.J.H. Wanhill, Fracture Mechanics. second edition. VSSD. 2002.

[110] J. T. Pinho de Castro, Automation of the fatigue design under complex loading. Society of automotive engineers, inc. 2000.

[111] J. D. Clothiaux, N. E. Dowling, Verification of rain-flow reconstructions of a variable amplitude load history. M.S. Thesis. Virginia Polytechnic Inst. and State Univ., Blacksburg. 1992.

[112] A. K. Khosrovaneh, N. E. Dowling, Fatigue loading history reconstruction based on the rainflow technique. NASA contract report 181942, 1989.

[113] K. Dreβler, M. Hack, W. Kruger, Stochastic reconstruction of Loading Histories from a rainflow matrix. Zeitschrift für Angewandte Mathematik und Mechanik 77 3 (1997), pp. 217–226.

[114] A. K. Khosrovaneh, N.E. Dowling, A.P. Berens, J.P. Gallagher, Fatigue life estimates for helicopter loading spectra, NASA contractor report 181941, 1989.

[115] O. E. Wheeler, Spectrum loading and crack growth, Journal of Basic Engineering, Vol. 94, pg 181-186, March 1972.

[116] J. Willenborg, R.M. Engle, H. A. Wood, A crack growth retardation model using an effective stress concept, Technical report AFFDL-TR-71-1, Air Force Flight Dynamics Laboratory, Wright-Patterson AFB, Ohio, January 1971.

[117] B. C. Sheu, P. S. Song, and S. Hwang. Shaping exponent in wheeler model under a single overload. Engineering Fracture Mechanics 1995;51(1): 135–43.

[118] P. S. Song, B.C. Sheu, and L. Chang. A modified wheeler model to improve predictions of crack growth following a single overload. JSME Int J Series A 2001;44(1):117–22.

[119] .K. C. Yuen, and F. Taheri. Proposed modifications to the Wheeler retardation model for multiple overloading fatigue life prediction, International Journal of Fatigue, Volume 28, Issue 12, December 2006, Pages 1803-1819, 2005.

[120] R. Rebba, S. Mahadevan, S. Huang, Validation and error estimation of computational models. Reliability Engineering and System Safety. Vol. 91, pg 1390-1397, 2006.

[121] S. Mahadevan, R. Rebba, Inclusion of model errors in reliability-based optimization. ASME Vol. 128., pg 936-944, 2006.

[122] N. C. Barford, Experimental Measurements: Precision, error, and truth. Wiley, New York, 1985.

[123] J. A. Hoeting, D. Madigan, A. Raferty, C.T. Volinsky, Bayesian model averaging: A tutorial (with discussion). Statlist Sci,14(4), pg 382-417, 1999.

[124]C. Chen, D. Le, "Stress-Intensity Factor and Fatigue Crack Growth Analyses For Rotorcraft Using AGILE", The 7th Joint DoD/FAA/NASA Conference on Aging Aircraft, New Orleans, Louisiana, September 8 - 11, 2003.

[125] C. T. Chen, Z. Han, D. Le, Cuervas E. Stress-intensity factor and fatigue crack growth analyses for rotorcraft using AGILE. The 7th Joint DoD/FAA/NASA conference on aging aircraft, September 2003.

[126] Y. Liu, S. Mahadevan, Subsurface fatigue crack propagation under rolling contact loading, Fatigue & Fracture of Engineering Materials & Structures, 2006(c). (under review)

[127] S. A. Richards, Completed richardson extrapolation in space and time. Commun. Numerical Methods Eng., Vol. 13, pg 573-585, 1997.

[128] P. J. Roache, Verification and Validation in Computational Science and Engineering, Hermosa, Albuquerque, NM. 1998.

[129] P. W.M John, Statistical design and analysis of experiments, The Macmillan Company, New York, 1971.

[130] V. Hombal, S. Mahadevan, Gaussian process surrogate modeling with bias minimizing training point selection, Int. Journal of Numerical Methods in Engineering (under review), 2010.

[131] S. Suresh, Crack deflection: Implications for the growth of long and short fatigue cracks. Metallurgical and Materials Transactions, Vol. 14, Num 11, 1983.

[132] K. Tanaka, Fatigue crack propagation. Comprehensive Structural Integrity, Edited by: Karihaloo, Milne, Ritchie.

[133] L. P. Pook, The role of crack growth in metal fatigue. Metals Society, London. 1983.

[134] L. P. Pook, Metal Fatigue: What it is, Why it matters. Springer, Netherlands. 2007.

[135] L. P Pook, The significance of Mode I branch cracks for mixed mode fatigue crack growth threshold behavior. In: Brown, M.W., Miller K.J. (Eds) Biaxial and Multiaxial Fatigue. EGF 3. Mechanical Engineering Publications, London, pg 247-263, 1989.

[136] K. B. Broberg, On crack paths. Engineering Fracture Mechanics, Vol. 28, pg 663-679, 1987.

[137] B. Cotterell, Notes on the paths and stability of cracks. International Journal of Fracture Mechanics, Vol. 2, pg 526 -533, 1966.

[138] W. G. Knauss, An observation of crack propagation in anti-plane shear. International Journal of Fracture Mechanics. Vol. 6, pg 183-187, 1970.

[139] K. Minoshima, Suezaki, K. Komai, Genetic algorithms for high precision reconstruction of three dimensional topographies using stereo fractographs. Fatigue Fracture Engineering Material Structures. Vol. 23, pg 435-443, 2000.

[140] Z. V. Parton, Fracture mechanics: from theory to practice. Gordon and Breach Science Publishers, Philadelphia, PA. 1992.

[141] L. P. Pook, Linear elastic fracture mechanics for engineers: theory and applications. WIT Press, Southampton. 2000.

[142] J. Vinas-Pich, J. C. P. Kam, W. D. Dover, Variable amplitude corrosion fatigue of medium strength steel tubular welded joints. In: Dover W.D., Dharmavasan, S. Brennan F.P. Marsh K.J. (eds) Fatigue crack growth in offshores structures. Engineering Materials Advisory Services, Solihull, pg 147-178. 1996.

[143] P. J. E. Forsyth, A two stage process of fatigue crack growth. In: Proc. Crack Propagation Symposium, The College of Aeronautics, Cranfield, Vol. 1, pg 76-94. 1961.

[144] J. Cervenka, V.E. Saouma. Numerical evaluation of 3-D SIF for arbitrary finite element meshes, Engineering Fracture Mechanics, Vol. 57, pg 541-563, 1997.

[145] I.S. Raju, J.C. Newman. Three-dimensional finite element analysis of finite thickness fracture specimen. NASA TN D-8414, 1977.

[146] L.F. Martha, P.A. Wawrzynek, A.R. Infraffea. Arbitrary crack representation using solid modeling. Engineering with Computers, Vol. 9, pg 63-82, 1993.

[147] P. Krysl, T. Belytschko. The element free Galerkin method for dynamic propagation of arbitrary 3-D cracks. International Journal for Numerical Methods in Engineering, Vol. 44, pg 767-800, 1997.

[148] B. J. Carter, P. A. Wawrzynek, A. R. Ingraffea, Automated 3-D crack growth simulation, International Journal for Numerical Methods in Engineering, 47, pg 229-253,2000.

[149] F. Erdogan, G.C. Shi, On the crack extension in plates under plane loading and transverse shear. Trans. ASME, Journal Basic Engineering. Vol. 86, pg 519-527, 1963.

[150] H. A. Richard, W. Linnig, K. Henn, Fatigue crack propagation under combined loading. Journal of Forensic Engineering, Vol. 3, pg 99-109, 1991.

[151] H. A. Richard, In: CD-Rom Proceedings of ICF10, Honolulu, HI, USA, 2001.

[152] X. Yan, S. Du, Z. Zhang, Mixed mode fatigue crack growth prediction in biaxially stretched sheets. Engineering Fracture Mechanics, Vol. 43, pg 471-475, 1992.

[153] K. Tanaka, Fatigue crack propagation from a crack inclined to the cyclic tensile axis. Engineering Fracture Mechanics, Vol. 6, pg 493-507, 1974.

[154] H. Kitagawa, R. Yuuki, Stress intensity factor of branched cracks in two dimensional stresses. Trans. Japan Society of Mechanical Engineering. Vol. 41, pg 1641-1649, 1975.

[155] K. Palaniswamy, W. G. Knauss, On the problem of crack extension in brittle solids under general loading. In: Mechanics Today, ed. S. Nemat-Nasser, Pergamon, New York, Vol. 4, pg 87-148, 1978.

[156] K. Tanaka, Fatigue crack propagation. Comprehensive Structural Integrity, Edited by: Karihaloo, Milne, Ritchie.

[157] A. Otsuka, K. Mori, and T. Miyata, The condition of fatigue crack growth in mixed mode condition. Engineering Fracture Mechanics, Vol. 7, pg 429-499, 1975.

[158] L. P. Pook, Crack Paths. WIT Press, Southampton, 2002.

[159] A. Otsuka, K. Mori, T. Oshima, S. Tsuyama, Fatigue crack growth of steel and aluminum alloy specimens under mode II loading. Journal of Soc. Material Science, Japan, Vol. 29, pg 1042-1048, 1980.

[160] G. C. Sih, International Journal of Fracture, Vol. 10, pg 305-321, 1974.

[161] G. C. Sih, Mechanics of Fracture Initiation and Propagation. Kluwer Academic Publishers, Dodrecht, Netherlands, 1990.

[162] M. Schollman, H. A. Richard, A. Kullmer, and M. Fulland, International Journal of Fracture. Vol. 117, pg 129-141, 2002.

[163] H. A. Richard, M. Fulland, M. Sander, Theoretical crack path prediction. Fatigue Fracture Engineering Mater. Structures, Vol. 28, pg 3-12, 2005.

[164] G. B. Marquis, D. F. Socie, Multiaxial Fatigue. In: Comprehensive Structural Integrity. Elsevier, 2003

[165] L. Liu, Modeling of mixed-mode fatigue crack propagation, Ph D. Dissertation, Vanderbilt University, 2008.

[166] P. A. Wawrzynek, B. J. Carter, A. R. Ingraffea, Advances in simulation of arbitrary 3D crack growth using FRANC3D/NG, under AFRL/RXLMN contract numbers FA6650-04-C-5213 and FA8650-07-C-5216.

[167] NASGRO Fracture Mechanics and Fatigue Crack Growth Analysis Software," v5.0, NASA-JSC and Southwest Research Institute, July 2006.